

ISTANBUL TECHNICAL UNIVERSITY ★ GRADUATE SCHOOL OF SCIENCE
ENGINEERING AND TECHNOLOGY

**INTEGRATION OF SPATIAL PROCEDURES TO COMBAT THE
DESERTIFICATION IN NINEVEH GOVERNORATE, IRAQ**



Ph. D. THESIS

Bashar Muneer YAHYA

Department of Geomatics Engineering
Geomatics Engineering Programme

NOVEMBER 2019

ISTANBUL TECHNICAL UNIVERSITY ★ GRADUATE SCHOOL OF SCIENCE
ENGINEERING AND TECHNOLOGY

**INTEGRATION OF SPATIAL PROCEDURES TO COMBAT THE
DESERTIFICATION IN NINEVEH GOVERNORATE, IRAQ**



Ph.D.THESIS

**Bashar Muneer YAHYA
(501142603)**

Department of Geomatics Engineering

Geomatics Engineering Programme

Thesis Advisor: Prof. Dr. Dursun Zafer SEKER

NOVEMBER 2019

İSTANBUL TEKNİK ÜNİVERSİTESİ ★ FEN BİLİMLERİ ENSTİTÜSÜ

**İRAK'IN NİNEVEH VİLAYETİNDE ÇÖLLEŞME İLE MÜCADELE İÇİN
MEKANSAL YÖNTEMLERİN ENTEGRASYONU**

DOKTORA TEZİ

**Bashar Muneer YAHYA
(501142603)**

Geomatik Mühendisliği Anabilim Dalı

Geomatik Mühendisliği Programı

Tez Danışmanı: Prof. Dr. Dursun Zafer ŞEKER

KASIM 2019

Bashar Muneer YAHYA, a Ph.D. student of ITU Graduate School of Science Engineering and Technology student ID 501142603, successfully defended the thesis/dissertation entitled “INTEGRATION OF SPATIAL PROCEDURES TO COMBAT THE DESERTIFICATION IN NINEVEH GOVERNORATE, IRAQ”, which he prepared after fulfilling the requirements specified in the associated legislations, before the jury whose signatures are below.

Thesis Advisor : **Prof. Dr. Dursun Zafer SEKER**
Istanbul Technical University

Jury Members : **Assoc. Prof. Dr. Oral YAGCI**
Istanbul Technical University

Assoc. Prof. Dr. Ozan ARSLAN
Kocaeli University

Prof. Dr. Cem GAZIOĞLU
Istanbul University

Prof. Dr. Hande DEMİREL
Istanbul Technical University

Date of Submission : 27 July 2019
Date of Defense : 22 November 2019





To my country, parents and my family



FOREWORD

My gratitude owed to my great country Iraq, represented by a wise government for giving me the opportunity to complete my higher education assisted with the Iraqi Ministry of Higher Education and Scientific Research. Also, extend my thanks and gratitude to the University of Mosul, especially the remote sensing center to provide technical and administrative support to facilitate the task of obtaining this scientific degree.

Full gratitude and appreciation to the Republic of Turkey through Istanbul Technical University, Civil Engineering and Geomatics Engineering Department for providing all the technical, administrative and using all university facilities from labs and libraries unconditionally.

My deepest appreciation goes to my supervisor Prof. Dr. Dursun Zafer SEKER, for his advice, commitment, encouragement, mentorship and his friendship. I am thankful for his valuable experience that he share it with me to draw my paths to be an independent scientist.

I am very grateful to all the professors whom I met during the period of my study at Istanbul Technical University, where I gained great knowledge and science experience in different fields. My special gratitude to Prof. Dr. Abdulsalam ALTINKAYNAK, Assoc. Prof. Dr. Oral YAGCI and Assoc. Prof. Dr. Ozan ARSLAN for sharing me their knowledge and experience in many scientific fields.

Gratitude owed to many individuals who have helped me in one way or another over the study years, often without knowing they were doing so. Moreover, I extend my gratitude to my brother and my sisters and all my friends who supported me in several forms. Especially my sister Hiba YAHYA and her husband Dr. Ubi RAMEZ, who they managed my finances issues throughout the study period, and they deserve much more than a simple ‘thank you’.

Finally yet importantly, to my wife and daughters Sama and Sana, I say thank you for all your sacrifices and your unlimited support and encouragement, love you all.

November 2019

Bashar Muneer YAHYA

TABLE OF CONTENTS

| | <u>Page</u> |
|--|--------------|
| FOREWORD | ix |
| TABLE OF CONTENTS | xi |
| ABBREVIATIONS | xiii |
| LIST OF TABLES | xv |
| LIST OF FIGURES | xix |
| SUMMARY | xxi |
| ÖZET | xxiii |
| 1. INTRODUCTION | 1 |
| 1.1 Problem Statement and Study Rationale | 3 |
| 1.2 Aims and Objectives..... | 5 |
| 1.3 Background Reviews..... | 6 |
| 1.4 Study Phases | 11 |
| 2. DESERTIFICATION CONCEPTS | 13 |
| 2.1 Desertification in Iraq-Historical Facts..... | 14 |
| 2.2 Study Area Description | 19 |
| 2.2.1 Meteorology and hydrology..... | 20 |
| 2.2.2 Geology | 24 |
| 2.2.3 Land cover | 25 |
| 2.2.4 Geomorphology..... | 26 |
| 2.2.5 Economy | 27 |
| 2.2.6 Agriculture | 27 |
| 3. DATA AND METHODOLOGIES | 29 |
| 3.1 Data Specifications and Used Softwares..... | 29 |
| 3.1.1 Meteorological data..... | 29 |
| 3.1.2 Remote Sensing data..... | 29 |
| 3.1.3 Digital maps..... | 30 |
| 3.1.4 Used softwares..... | 31 |
| 3.2 Remote Sensing..... | 32 |
| 3.2.1 Remote sensing methodologies..... | 32 |
| 3.2.1.1 Normalized difference vegetation index (NDVI)..... | 32 |
| 3.2.1.2 Image enhancement..... | 34 |
| 3.2.1.3 Supervised classification..... | 36 |
| 3.3 Geographic Information System (GIS)..... | 37 |
| 3.3.1 GIS methodologies..... | 38 |
| 3.3.1.1 Spatial analysis..... | 38 |
| 3.3.1.2 Tracking dust and sand storms events..... | 39 |
| 3.4 Computational Methods | 40 |
| 3.4.1 Standardized precipitation index..... | 40 |
| 3.4.2 The SCS-CN curve number method..... | 44 |
| 3.5 Artificial Intelligent (AI)..... | 46 |
| 3.5.1 Artificial neural network basic concepts..... | 47 |
| 3.5.2 Artificial neural network biological design..... | 48 |

| | |
|---|------------|
| 3.5.3 Artificial neural network activation functions..... | 51 |
| 3.5.4 Artificial neural network training algorithms..... | 51 |
| 3.5.5 Artificial neural network design procedures..... | 51 |
| 3.6 Designing ANNs Models..... | 53 |
| 3.6.1 Model description..... | 53 |
| 3.7 Fuzzy Logic..... | 66 |
| 3.7.1 Fuzzy logic theory basics and concepts..... | 67 |
| 3.7.2 Adaptive neuro fuzzy inference system (ANFIS) | 77 |
| 3.8 Development Neuro-Fuzzy Inference System (ANFIS)..... | 79 |
| 3.8.1 Model description..... | 79 |
| 4. RESULTS AND DISCUSSIONS..... | 87 |
| 4.1 Remote Sensing Techniques..... | 88 |
| 4.2 Geographic Information System (GIS)..... | 100 |
| 4.3 Artificial Intelligent (AI)..... | 107 |
| 4.4 Computational Methods..... | 111 |
| 4.5 Statistical Analysis..... | 119 |
| 5. CONCLUSIONS AND RECOMMENDATIONS | 123 |
| REFERENCES | 129 |
| APPENDICES | 141 |
| CURRICULUM VITAE..... | 147 |

ABBREVIATIONS

| | |
|---------------|---|
| AI | : Artificial Intelligent |
| ANN | : Artificial Neural Network |
| ARIMA | : Linear Autoregressive Integrated Moving Average |
| BPNN | : Back Propagation Neural Network |
| CBPN | : Cascade-Forward Back Propagation Neural Network |
| COG | : Center of Gravity Method |
| DEM | : Digital Elevation Model |
| ERTS | : Earth Resources Technology Satellite |
| FAO | : Food and Agriculture Organization |
| FL | : Fuzzy Logic |
| FLCS | : Fuzzy Logic Controller System |
| FCM | : Fuzzy C-Mean Clustering Technique |
| GIS | : Geographic Information System |
| IOM | : Iraqi Organization for Meteorological Information |
| IAMN | : Iraqi Agricultural Meteorological Network |
| MF | : Membership Functions |
| MLP | : Multilayer Perceptron |
| NARX | : Nonlinear Autoregressive Exogenous |
| NDVI | : Normalized Difference Vegetation Index |
| NESDIS | : National Environmental Satellite, Data, and Information Service |
| RBF | : Radial Basis Function |
| RDI | : Reconnaissance Drought Index |
| RGB | : Red-Green-Blue |
| RMSE | : Root Mean Square Error |
| RS | : Remote sensing |
| SPI | : Standardized Precipitation Index |
| UN | : United Nation |
| UNEP | : United Nations Environment Program |
| UNISDR | : United Nation Office for Disaster and Risk Reduction |
| WMO | : World Meteorological Organization |



LIST OF TABLES

| | <u>Page</u> |
|---|-------------|
| Table 2.1 : The geomorphologic landscapes | 26 |
| Table 3.1 : Type of remote sensing data and their uses..... | 30 |
| Table 3.2 : Different vegetation indices techniques..... | 33 |
| Table 3.3 : Different band combinations False Colors Compositions images..... | 35 |
| Table 3.4 : Classification of the Standardized Precipitation Index (SPI) values..... | 42 |
| Table 3.5 : Seasonal rainfall limits for three antecedent moisture conditions..... | 45 |
| Table 3.6 : Different soil group classifications | 46 |
| Table 3.7 : MATLAB script codes for design ANN structure.. | 58 |
| Table 3.8 : Architectures design of develop ANNs sub- models | 60 |
| Table 3.9 : Training process analysis of designed sub-models | 64 |
| Table 3.10 : Testing process analysis of designed sub-models | 64 |
| Table 3.11 : Predicted period with irrational results after collapsing stage | 65 |
| Table 3.12 : A decision matrix representation | 72 |
| Table 3.13 : Some of the fuzzy rules covering extremely dry drought scenario ... | 82 |
| Table 4.1 : Error matrix of ground training samples for image dated 1992 | 91 |
| Table 4.2 : Error matrix of ground training samples for image dated 2016 | 92 |
| Table 4.3 : Gradient analysis and the area between the contours intervals | 96 |
| Table 4.4 : Expected rainwater harvested volume | 98 |
| Table 4.5 : Comparing rainfall results (actual and predicted) | 109 |
| Table 4.6 : Drought assessment in two studied periods | 111 |
| Table 4.7 : Drought results according to rainfall records (actual and predicted)... | 112 |
| Table 4.8 : Predicted SPI-3 classification for the period (2017-2026). | 115 |
| Table 4.9 : Predicted SPI-12 classification for the period (2017-2026) | 115 |
| Table 4.10 : Curve number for three antecedent moisture conditions | 116 |
| Table 4.11 : Calculated runoff (mm) and water volume (m3) per year | 117 |
| Table 4.12 : Runoff estimated results from predicted rainfall values | 118 |
| Table 4.13 : Data standardization using excel | 120 |
| Table B.1 : Formatted SPI equations in Excel format. | 147 |



LIST OF FIGURES

| | <u>Page</u> |
|--|-------------|
| Figure 1.1: Thesis progress flow chart | 12 |
| Figure 2.1: Crop lands effected due to desertification in Iraq..... | 15 |
| Figure 2.2: Iraqi water resources sources..... | 16 |
| Figure 2.3: Impact of dust and sand storms in several places in Iraq..... | 18 |
| Figure 2.4: Types of dust and sand storms in Iraq..... | 19 |
| Figure 2.5: The study area..... | 20 |
| Figure 2.6: Meteorological parameters in Iraq (modified after IOM, 2000).... | 21 |
| Figure 2.7: Water bodies within Nineveh boarder..... | 23 |
| Figure 2.8: Ground water depth (modified after Al-Jiburi and Al-Basrawi 2015). .. | 24 |
| Figure 2.9: Tectonic divisions of Nineveh | 25 |
| Figure 2.10: Land cover | 25 |
| Figure 2.11: Agriculture zones in Nineveh | 27 |
| Figure 3.1: The distribution of meteorological stations in the study area. | 30 |
| Figure 3.2: FCC combination (modified after Rees and Pellika 2010)..... | 35 |
| Figure 3.3: Dividing the storm into small parts..... | 39 |
| Figure 3.4: SPI analysis for precipitation records..... | 43 |
| Figure 3.5: Biological neurons versus artificial neural network..... | 49 |
| Figure 3.6: Different artificial neural networks types | 50 |
| Figure 3.7: Designed Flowchart structure of the developed model..... | 54 |
| Figure 3.8: RBFNN design structure..... | 58 |
| Figure 3.9: The designed interface window for the develop model..... | 59 |
| Figure 3.10: The perfect selected number of hidden nodes..... | 61 |
| Figure 3.11: RBF-R sub-model training results..... | 62 |
| Figure 3.12: NARX-R sub-model training results..... | 63 |
| Figure 3.13: FCM-R sub-model training results..... | 64 |
| Figure 3.14: The fuzzy logic theory in simple words..... | 66 |
| Figure 3.15: Fuzzy Logic Control system FLC categories..... | 67 |
| Figure 3.16: A membership function definition..... | 69 |
| Figure 3.17: A Membership Function parts..... | 69 |
| Figure 3.18: Membership functions for linguistic variable (rainfall) | 71 |
| Figure 3.19: Fuzzy sets operations..... | 71 |
| Figure 3.20: Center gravity method (modified after Ross, 2005)..... | 74 |
| Figure 3.21: Mamdani method inference example (Url-3)..... | 75 |
| Figure 3.22: Basic mathematics of ANFIS model (modified after Jang,1993)... .. | 76 |
| Figure 3.23: A typical architectures of ANFS model (modified after Jang 993)... .. | 77 |
| Figure 3.24 Designed flowchart structure of the developed ANFIS..... | 79 |
| Figure 3.25: Correlation relationship between the input variables and actualSPI... .. | 80 |
| Figure 3.26: Designed membership functions for inputs dataset..... | 81 |
| Figure 3.27: Designed membership functions for drought..... | 81 |
| Figure 3.28: Mamdani fuzzy inference system..... | 83 |

| | |
|--|------------|
| Figure 3.29: Developed ANFIS model..... | 85 |
| Figure 3.30: Comparing actual and predicted SPI values..... | 86 |
| Figure 4.1: Landsat TM FCC 4,3,2 of the study area with different date..... | 89 |
| Figure 4.2: NDVI analysis for a part of the study area..... | 89 |
| Figure 4.3: NDVI density slicing maps..... | 90 |
| Figure 4.4: Supervised classification analysis using ERDAS imagine v.13..... | 91 |
| Figure 4.5: Vegetation health index VHI maps | 92 |
| Figure 4.6: Drought expansion maps..... | 93 |
| Figure 4.7: Surface drainage network map..... | 94 |
| Figure 4.8: Deriving the contour map using (Global map v.13)..... | 95 |
| Figure 4.9: Gradients and contours intervals classification..... | 96 |
| Figure 4.7: Surface drainage network map..... | 94 |
| Figure 4.8: Deriving the contour map using (Global map v.13)..... | 95 |
| Figure 4.9: Gradients and contours intervals classification..... | 96 |
| Figure 4.10: Cross section sites for selected dams..... | 97 |
| Figure 4.11: Simulation procedure for createing rainwater storage lake (L3).... | 98 |
| Figure 4.12: The default artificial lakes that are formed behind the dams.... | 99 |
| Figure 4.13: Final 3D vision for the study area..... | 99 |
| Figure 4.14: Dust and sand sources effective regions..... | 101 |
| Figure 4.15: Storms events classification according to their detected sources | 102 |
| Figure 4.16: Wind regime analysis | 103 |
| Figure 4.17: The movement paths of the last dust and sand storm..... | 104 |
| Figure 4.18: Spatial distribution of long term SPI-12 in the study area..... | 104 |
| Figure 4.19: Al Murr basin analyze by Arc Map v.10.2..... | 105 |
| Figure 4.20: Short term predicted analysis..... | 106 |
| Figure 4.21: Long term predicted analysis..... | 106 |
| Figure 4.22: Runoff distribution for actual and predicted time period..... | 107 |
| Figure 4.23: Runoff spatial distribution for the period (1956-2050)..... | 107 |
| Figure 4.24: The scatter plot between actual and predicted rainfall..... | 109 |
| Figure 4.25: The predicted time series of rainfall from 2018 to 2050..... | 110 |
| Figure 4.26: Predicted average drought intensity for the period (2017-2026)..... | 112 |
| Figure 4.27: Different timescales SPI charts for Mosul station..... | 113 |
| Figure 4.28: Average drought with different SPI timescales..... | 114 |
| Figure 4.29: The relationship between the rainfall-runoff in AL Murr basin..... | 118 |
| Figure 4.30: Rainfall, temperature and storms temporal variation analysis..... | 120 |
| Figure 4.31: Temporal variation analysis of runoff, drought and storm events..... | 121 |
| Figure 4.32: Temporal variation analysis of rainfall and temperature..... | 122 |
| Figure A.1: MODIS on NASA's Terra satellite taken between 2005 to 2006 | 143 |
| Figure A.2: MODIS on NASA's Terra satellite taken between 2007 to 2009 | 143 |
| Figure A.3: MODIS on NASA's Terra satellite taken between 2010 to 2012 | 144 |
| Figure A.4: MODIS on NASA's Terra satellite taken between 2013 to 2015 | 144 |
| Figure A.5: MODIS on NASA's Terra satellite taken between 2016 to 2018 | 145 |

INTEGRATION OF SPATIAL PROCEDURES TO COMBAT THE DESERTIFICATION IN NINEVEH GOVERNORATE, IRAQ

SUMMARY

Desertification has played a significant role in human history, contributing to the collapse of several large empires, such as Carthage, Greece, and the Roman Empire, as well as causing displacement of local populations. Historical evidence shows that the serious and extensive land deterioration occurring several centuries ago in arid regions had three epicentres: the Mediterranean, the Mesopotamian Valley, and the loessial plateau of China, where the population was dense. Climate change, human activities, successive wars and lack of optimal solutions have aggravated desertification in Nineveh governorate northwestern Iraq. Drought expansion and increasing of dust and sandstorm events have had major social, economic and environmental impacts in this area.

Much type of data used in this study divided into two groups. First, described as “observed data”, taken from official sources that include all meteorological data (Atmospheric oscillations data not considered or used in this study) and remotely sensed images. Second, named “supplementary data”, includes all estimated data where the Curve Number (SCS-CV) method used to estimate the runoff values, and the Standardized Precipitation Index (SPI) method used to find drought levels.

This study evaluates many techniques where remote sensing, geographic information systems are used to assess the drought and finding a suitable location for constructing theoretical reservoir seasonal lakes as a solution based on rainwater harvesting techniques. Farther more, Artificial Intelligent used to monitor, assess and predict weather variables and SPI to find solutions to reduce the risk of desertification. The applications of remote sensing and geographic information system techniques explored depending on different types of remote sensing data to monitor drought impacts and drought expansion in the study area.

Image enhancement, supervised classification and NDVI analysis used at the research stage. The results show massive changes in vegetation cover indicating increased drought levels in the study area. In addition, dust and sandstorm events are classified and their paths analyzed and effective dust and sand grain sources tracked. Different maps and figures types created at this stage of the research. Dust and sandstorms effective feeding-regions map show four feeding-sources areas were detected. The movement paths of the last dust and sand storm occurred on 24 March 2017.

Artificial Intelligent represented by neural network approaches and fuzzy logic were adopted in the research methodology. Software was designed to forecast the weather variables in the Nineveh Governorate based on Artificial Neural Networks (ANNs) consisting of Radial Basis Function (RPF), Fuzzy c-means (FCM) and a Nonlinear Autoregressive Network with Exogenous Inputs (NARX). Stistical error criterias such as Coefficient of Determination (R^2), Root Mean Square Error (RMSE), Nash-

Sutcliffe coefficient (CE) and Mean Absolute Percentage Error (MAPE) calculated to compare the ANN's performance. The software performance accuracy, shows the designed ANN sub-models have performance accuracy range fluctuated as 67.9% to 84.2% represented by performance Criteria. Comparatively.

On the other hand, a fuzzy-based model represented by an adaptive neuro-fuzzy inference system ANFIS model developed for drought forecasting depending on the correlation between the estimated standardized precipitation index with four selected climate variables (rainfall, temperature, wind speed, and evaporation). The results indicate that high flexibility and the capability to represent different scenarios are vital because of the wide range of simulated membership functions designed to predict SPI.

A kind of statistical analysis done using temporal variations analysis and spearman's rank correlation techniques. The results of these statistical analysis techniques show that from 1992 to 2017 remarkable behavior of the data series are evident. A reduction in runoff noticed in this period (only a small amount of runoff in 2016) and drought satiation fluctuated between moderate to extreme drought where all these events accompanied by an abnormal increase in the sandstorms frequency happened in the study area. The same remarkable behavior of rain, temperature, and sandstorm events has been monitored where the analysis for the same period from 1992 to 2017 shows increasing in sandstorm events with almost equal temperatures while the rain decreasing. Spearman's rank correlation technique has applied to summarize the strength (negative or positive) between the sandstorms frequency and rainfall, temperature, runoff and SPI.

This PhD research provides useful solutions that can help the decision-makers to develop optimal plans to address environmental changes and to raise the standards of environmental and agricultural plans, not only for the study area but also for Iraq as a whole.

IRAK'IN NINEVEH VİLAYETİNDE ÇÖLLEŞME İLE MÜCADELE İÇİN MEKANSAL YÖNTEMLERİN ENTEGRASYONU

ÖZET

Çölleşme insanlık tarihinde oldukça önemli bir rol oynamış, Kartaca, Yunanistan ve Roma İmparatorluğu gibi birçok büyük imparatorluğun çöküşüne sebep olmuş ve yerel nüfusun yerinden edilmesine neden olmuştur. Tarihsel kanıtlar, birkaç yüzyıl önce kurak bölgelerde meydana gelen ciddi ve yaygın arazi bozulmalarının üç merkez üssünün bulunduğunu göstermektedir. Bunlar; Akdeniz, Mezopotamya Vadisi ve nüfusun yoğun olduğu Çin'deki plato bölgesidir.

Çölleşmenin herkes tarafından birlikte yaşadığımız en karmaşık sorun ve çevresel bir tehdit olarak algılanması gerekmektedir. Zaman içerisinde, iklim değişikliği, insan aktiviteleri, devam eden savaşlar ve uygun çözümlerin eksikliği Kuzeybatı Irak'taki Nineveh Valiliğinde yaşanan çölleşme sorununu daha da artırmıştır. Kuraklığın yayılması ve kum ve toz fırtınalarının artması bölgede büyük çaplı sosyal, ekonomik ve çevresel etkilere sebep olmuştur.

Bu çalışmada çok çeşitli veri kullanılmış olmasına karşın genel anlamda bunlar iki gruba bölünebilirler. Bunlarda ilki “gözlemlenebilir veri” olarak tanımlanmaktadır ve bütün meteorolojik verileri ve uzaktan algılama görüntüleri kapsamaktadır. İkincisi “tamamlayıcı veriler” olarak isimlendirilmektedir ve akış değerlerinin ve çölleşme seviyesini tahmin etmekte kullanılan yöntemleri içerir.

Bu çalışmada çölleşmenin belirlenmesi amacıyla uzaktan algılama ve coğrafi bilgi sistemleri gibi birçok farklı teknik kullanılmıştır. Bu teknikler ayrıca, yağmur suyunun biriktirilmesine yönelik olarak teorik rezervuarların yerlerinin belirlenmesinde de kullanılmıştır. Yapay zeka, çölleşme tehlikesinin azaltılmasına yönelik olarak iklimsel değişimlerin izlenmesi, değerlendirilmesi ve tahmini için kullanılmıştır. Çalışma bölgesindeki kuraklık etkilerini ve kuraklık dağılımını izleyebilmek için farklı türdeki uzaktan algılama verilerine bağlı olarak uzaktan algılama ve coğrafi bilgi sistemleri tekniklerinin birlikte uygulanabilirliği de araştırılmıştır.

Araştırma aşamasında, görüntü zanginleştirme, denetimli sınıflandırma NDVI analizi, dilimleme yöntemi ve mekânsal geoistatistik analizler kullanılmışlardır. Çalışmanın sonuçları, çalışma alanındaki bitki örtüsü seviyesinde artan kuraklık seviyelerini gösteren büyük değişiklikler olduğunu göstermektedir. Gerçek ve öngörülen değişkenler arasındaki ilişkiyi bulmak için zamansal varyasyon analizi ve Spearman'ın rank korelasyonu ile temsil edilen istatistiksel analizler uygulanmıştır.

Buna ek olarak, toz ve kum fırtınası olayları sınıflandırılmış ve izleri analiz edilerek etkin toz ve kum tanelrinin kaynakları izlenmiştir. Araştırmanın bu aşamasında değişik haritalar ve şekiller oluşturulmuştur. Bunlar arasındaki toz ve kum fırtınası ile etkili besleme bölgeleri haritası, dört besleme kaynağı alanı tespit edildiğini göstermiştir. Sınıflandırılmış tüm toz ve kum fırtınası dizilim sıklığını irdelenerek yerel, yabancı veya karışık toz ve kum tanecikği gibi potansiyel kaynakları olan alanlar belirlenmiştir.

Çalışma alanında, bütün olası rüzgar olaylarının güneybatıdan kuzeydoğuya doğru olduğu durumlarda ortaya çıktığının da belirlendiği harita ve şekiller oluşturulmuştur. Bölgede 24 Mart 2017'de gerçekleşen son toz ve kum fırtınası da çalışmada ele alınmıştır.

Çalışmada yapay sinir ağı yaklaşımları ve bulanık mantık ile temsil edilen yapay zeka araştırma yönteminin kullanımı da yer verilmiştir. Nineveh Valiliği'ndeki hava durumu değişkenlerini tahmin edebilmek için, Radyal Bazlı Fonksiyonları (RPF), bulanık c-ortalamarı (FCM) ve doğrusal olmayan otoregresif ağlarla eksojen girdilerden (NARX) oluşan Yapay Sinir Ağları (YSA) temelli bir yazılım oluşturulmuştur. Her biri beş model olmak üzere onbeş model geliştirilmiştir. Tüm alt modeller eğitim ve test aşamalarında ayrı olarak, tahmin ve sunum aşamalarında ise birlikte çalıştırılmıştır. Belirleme katsayısı (R^2), En düşük kareler yöntemi (RMSE), Nash-Sutcliffe katsayısı (CE) ve Ortalama Mutlak Yüzde Hata (MAPE) gibi istatistiksel hata kriterleri YSA'ların performansını karşılaştırmak için hesaplanmıştır.

Yazılım performans doğruluğu, tasarlanan ANN alt modellerinin performans kriterlerinin %67,9 ile %84,2 arasında değişen performans doğruluk aralığına sahip olduğunu göstermektedir. Karşılaştırıldığında, NARX alt modellerinin ortalama doğruluğunun, diğer tasarlanmış alt modellerin ortalama doğruluğundan daha yüksek olduğu belirlenmiştir. Yazılım performansı kesinliği geliştirilen modellerin elli yıllık tahmin süreci içerisinde küçük istatistiksel hatalarla en yakın tahmin edilen sonuçları verdiğini göstermektedir ve bu noktadan sonra program sonuçları bozulmaya ve sonuçları irrasyonel olmaya başlamaktadır. Herhangi bir zorluk veya karışıklık ile karşılaşmadan bu yazılım ile çalışabilmek için bir arayüz tasarlanmıştır.

Tasarlanan arayüz kullanıcının tahmin edilen değişken tipini seçmesine izin vermekte ve tasarlanan öngörü fonksiyonunu seçmesine olanak sağlamaktadır. Tahmin edilen değerler istatistiksel olarak karşılaştırılabilen ve çizelgeler ve tablolar yardımıyla sonuçları dışarı aktarabilmektedir. Gelecekte, bu yazılım Irak'taki tüm meteoroloji istasyonlarının hava değişkenlerini tahmin etmek için kapsamlı bir yazılım haline getirerek geliştirebilir.

Diğer taraftan, seçilen dört iklim değişkeni (yağmur, sıcaklık, rüzgar hızı ve buharlaşma) için tahmin edilen standart yağış indeksi arasındaki korelasyona dayalı kuraklık tahmini için uyarlanabilir bir adaptif sinirsel bulanık çıkarım sistemi ANFIS tarafından temsil edilen bulanık mantık temelli bir model geliştirilmiştir. Sonuçlar yüksek esneklik ve farklı senaryoları temsil edebilme kapasitesinin SPI'yi (standart yağış indeksi) tahmin etmek için tasarlanan geniş çaplı simüle üyelik fonksiyonlarından dolayı önemli olduğunu göstermektedir. Geliştirilen ANFIS'in verim performansını belirlemek için, Belirleme Katsayısı $R^2 = 0.905$, Ortalama karesel ortalama hatası $RMSE = 0.935$, Nash-Sutcliffe katsayısı $CE = 0.83$ ve Ortalama Mutlak Yüzde $MAPE = \%17.39$, performans doğruluğunun $\%82.61$ olduğu, Bu çalışmada sistemi SPI tahmini için güvenilir ve verimli kıldığı değerlendirilmiştir.

Zamansal varyasyon analizi ve spearman'ın rank korelasyon teknikleri kullanılarak farklı bir istatistiksel analiz de gerçekleştirilmiştir. 1992'den 2017'ye kadar veri serisinin analiz edildiği bu istatistiksel analizler sonucuna, 2016 yılı verileri hariç su akışının azaldığını göstermektedir ve bu sonuç bölgedeki kuraklığın doyunluğunun orta ila aşırı kuraklık arasında değiştiğini göstermiştir. Yine çalışma bölgesinde toz ve kum fırtınası oluşumundaki sıklığın anormal biçimde artması da bu değişimlerin bir göstergesi olarak değerlendirilmiştir. Bölgede, yağmur, sıcaklık ve kum fırtınası olaylarının aynı dikkate değer davranışı izlenmiştir. Burada 1992 ile 2017 arasındaki

aynı döneme ait analizler, yağış miktarının azalmasına karşın ortalama sıcaklığın 28.3° yaklaşmaktır.

Kum fırtınası frekansı ile yağış, sıcaklık, yüzey akışı ve SPI arasındaki kuvveti (negatif ya da pozitif) özetlemek için Spearman sıra korelasyon tekniği uygulanmıştır. Sıra korelasyonu sonuçları, SPI ve sıcaklık arasında pozitif bir korelasyonun (+ 0.33) olduğunu göstermiştir. Ayrıca SPI ile yağış arasında negatif bir (- 0.65) korelasyonunu göstermektedir. Kum fırtınası frekansı ile sıcaklık ve SPI analiz sonuçları kum fırtınası frekansı ile sıcaklık ve SPI sonuçları arasında pozitif bir ilişki olduğunu ortaya koymuştur. Hesaplanan sonuçlara göre Kum fırtınasının sıcaklık ile korelasyonu + 0.45 ve SPI ile +0.16 olarak hesaplanmıştır.

Bu çalışmadan elde edilen sonuçlar irdelendiğinde, çalışma alanındaki çölleşme derecesine bağlı olarak, bu olayın etkileriyle mücadele etmek veya etkilerini tersine çevirebilmek için birçok öneri dikkate alınmalıdır. Bu önerilerden en önemlisinin, iklim değişikliği ile çölleşme arasındaki karmaşık durumu dikkatle incelemek için uzun vadeli stratejik planların oluşturulmasıdır. Bölgede, hızlı büyüyen ağaç türlerinin baskın yüzey rüzgârlarına karşılık gelen alanlarına dikilmesi bir başka öneri olarak değerlendirilmelidir.

Bölgede bu konuda yapılan ilk kapsamlı çalışma olarak ta ele alınması öngörülen bu doktora çalışmasının, çevresel değişiklikleri göz önünde bulundurarak, çevresel ve tarımsal planların standardını artırmak için en uygun planların geliştirilmesini isteyen karar verivilere, sadece çalışma alanı için değil Irak'ın tamamı için yardımda bulunacak yararlı araçlar sağladığı düşünülmektedir.



1. INTRODUCTION

Many countries in the Middle East suffer from drought problems, including Iraq, which has recently hit by a wave of drought events that have become apparent in many parts of the country. Iraq has classified in 2013 by the United Nation as the country of the most vulnerable to drought conditions in a comparable degree to its neighbouring countries Turkey, Iran, Kuwait, Saudi Arabia, Jordan and Syria. The problem is expected to exacerbate in the coming few years due to the acceleration of many factors that lead to desertification and drought expansion (UNEP, 2013; FAO, 2014). Dust and sandstorms are the most important environmental challenges facing Iraqi areas, where Iraq has witnessed a significant increase in the intensity and the frequency of these natural events in the past decade that can considered as one of the factors that effectively influence the increase of desertification in all Iraq. This situation prompted the United Nations Environment Program (UNEP) to predict that Iraq could witness 300 dust events in a year within 10 years, up from around 120 per year at now (UN, 2013). It has admitted that these natural events transcend boundaries and cannot handled effectively through national-level mediation alone (Kobler, 2013).

Most researchers in the field of desertification and drought expansion are convinced that several factors working in tandem to activate the negative role of this environmental phenomenon and these factors are divided into three parts (Tsismelis et al, 2019). The first part is represented by natural factors including the (global warming and climate change) effects which lead to a decrease in the amounts of precipitation and rain fluctuation negatively affecting the discharge of both the Tigris and Euphrates and resulting in lower water quotas allocated for agriculture especially for the agricultural land on the banks of the rivers. Dust and sandstorms, which have become a natural phenomenon, play another negative role through the encroachment of dunes that bury large patches of agricultural land, especially in the central and western regions of Iraq.

The second part of desertification factors is human factors represented by the absence of government's intervention in implementing promising plans to prevent the

increasing danger of desertification in Iraq and the neglect of the irrigation and agricultural sector from its agenda. The third part of the factors causing desertification in Iraq is the influence of neighboring countries exemplified by the role of Turkey in establishing several dams and reservoirs on the Tigris and Euphrates (Gleick, 1994; Al-Ansari, 2013). Which contribute to reducing the water share of Iraq in addition to the role of the Iranian and Syrian governments that are deliberately diverting the streams of small rivers that flow from their territory and prevent them from completing their natural course towards Iraqi territory. In particular, many techniques must assessed and used in such a way that they complement one another to emphasize finding solutions for combating desertification and drought expansion. Ideally, remote sensing, geographic information system, and Artificial Intelligent should play a major role in developing an operational capability for monitoring, assessing and predicting the magnitude of desertification with time in any selected area.

Several authors and readers do not differentiate between the terms (desertification and drought) due to their close meaning, which suggests that land is dry and infertile. The scientific difference between the concepts of both terms will be defined in this paragraph where the drought is a natural phenomenon that occurs because of the long period of dry weather, which means that rainfalls less than expected in a region in the long term. This phenomenon increases the speed of dry winds, causing a high evaporation rate and occurrence of local sandstorms, which deteriorate the soil layer in one way or another. These effects accompanied by developing high-pressure areas that prevent or limit the development of thunderstorm, therefore, reducing the chance of precipitation in these areas. There are several types of drought as Meteorological Drought, Agricultural Drought, Hydrological Drought and Ecological Drought where this study focused on Meteorological Drought in the study area.

Desertification from the other hand is the process of transformation of fertile agricultural land into less productive or unproductive land, this process of degradation becomes a complex process led by human activity represented by several wrong habits including (over-cultivation, irrigation and deforestation etc.) accompanied by a change in global climate. Through the definitions of drought and desertification, the scientific differences between them can reviewed.

To evaluate and limit the dimensions of this phenomenon in the study area, it is necessary to rely on modern methods and techniques to face this phenomenon. The

following scientific methods were used in this study that includes, Remote Sensing Technologies (RS), Geographical Information System (GIS), Artificial Intelligent (AI) and two computational methods represented by Standardized Precipitation Index (SPI) and The Soil Conservation Service (SCS-CN) in addition using some statistical analysis as effective tools in achieving the objective of the study.

1.1 Problem Statement and Study Rationale

Desertification is a natural phenomenon that negatively affects all components of life. However, this phenomenon is easy to monitor and proactive solutions can be set to prevent its harm when taking into account the nature changes in this phenomenon in the different regions that have different climate characteristics. Drought characterized by its severity, duration and spatial impact on a particular area and because of the different characteristics of the climate, it is difficult to determine the beginning of drought or when its negative impact becomes prominent in a particular area.

The impact of desertification on Iraq has become clear through several observations, including the decline of vegetation and agricultural land, which not long ago used to produce various economic crops such as wheat, barley and some vegetables like tomatoes. Studies and previous reports have shown that all parts of Iraq suffer from the phenomenon of desertification and related drought, which they reached advanced stages in some Iraqi parts.

Azooz and Talal, 2015, proved from analyzing climate data records for long periods that four Iraqi cities suffer from drought in advanced stages and it is affecting the ecological and living system of the inhabitants of these cities. Varoujan, et al. in 2013, noted that the increase in the frequency of sandstorms in Iraq is unprecedented in comparison to previous decades leading to severe effects on human health, economy, transportation and other social activities in Iraq.

Drought in Iraq investigated using remote sensing techniques and geographic information systems. The results showed that (14.4%) of Iraq are experiencing slight drought, (61.6%) experiencing moderate drought, (23.2%) experiencing severe

drought and (0.8%) of its areas are under extremely severe drought, with clear evidence that northern areas are more vulnerable to drought (Yaseen et al., 2012).

Hekmat S. and Basher M. 2012, noted that there are many factors play a prominent role in the advancing drought phenomenon in Nineveh province northwestern Iraq. These factors can lead to an increase in the speed of desertification and the speed encroachment of dunes that severely affect the vegetation cover in the region. Their study resulted in completing a geo-environmental classification map for Nineveh province. The main reason for increasing the regional dust storms is the drastic changes in annual rainfall and temperature, besides many other reasons, such as drought impacts, mismanagement of water and abandoning of agricultural lands (Varoujan K., et al. 2013).

To minimize the drought expansion situation in Iraq, the government should prudently manage the water resources. Non- conventional water resources like harvested water and processed wastewater should adopted as new suitable resources with suggested new methods for saving these sources. Accordingly, this study focused on some modern tools trying to propose multiple solutions to combating desertification in Nineveh governorate. More specifically, this study tries to address the following research questions and approaches:

- What is desertification, why this phenomenon occurs in Nineveh government (causes), how much the magnitude and levels of drought, which location suffering from this phenomenon?
- Can we use modern technologies such as RS, GIS and AI to find some realistic solutions related to desertification in Iraq and what are the results that can get from these procedures to combating desertification in Iraq?
- Design Artificial Intelligent models to predict weather variables, drought levels and runoff.

1.2 Aims and Objectives

The overall aim of this study is to propose suitable solutions using modern procedures to combating desertification by monitoring, assessing and predicting the meteorological drought in the study area and predict some weather variables that used to predict meteorological drought and runoff. The modern procedures can listed as

(Artificial Intelligent, remote sensing and geographic information system). The desired aims and objectives of this study are.

- Demonstrate the negative impact of desertification on the study area by monitoring and assess the vegetation cover using remote sensing data for two periods. Classification approaches such as supervised classification, band rationing and NDVI as remote sensing techniques adopted to achieve this stage of research.
- Many kinds of Artificial Intelligent approaches developed to solve the problems of non-linearity in different applied sciences, where finding the suitable one is a big task when the statistic errors and the performance of the model are taking into account. Using Artificial Intelligent procedures by adopted three kinds of artificial neural network (RBF, FCM and NARX) and ANFIS as a fuzzy logic system for developing models that can used as predicer tools for predicting weather variables, runoff and drought in the study area.
- There are many types of drought indices that depend on many variables where their estimation difficulties ranging between easy to difficult in some ways. Choosing the SPI index is a good choice for assessing drought levels because it depends only on one variable named rainfall. Besides the mathematics, procedure for SPI estimation easy solved by using traditional methods or by using relevant software. SPI index in this study assessed and a comparison made based on observed and predicted rainfall data.
- Using Geographic Information System (GIS) in analyzing and constructing databases with the possibility of representing the result in the form of maps with different purposes. Helped significantly the decision-makers to identify the magnitude of the problems (social and environmental etc.) that they face, making it easier for them to take the necessary decisions to resolve these problems that might happened with various levels of difficulty. GIS used to prepare different spatial distribution maps based on observable and predictable data. Dust and sandstorms effective feeding-regions map was prepared and by particle-tracking algorithm procedures using Playback Manager Tool, a realistic example analyzed to tracking a dust and sandstorm event that occurred on 24 March 2017 with a 36-hour duration.

1.3 Background Reviews

This study is multidisciplinary, thus selective literature reviews are required to cover all topics related to the structure of this study. These topics are RS, GIS, AI, SPI, SCS-CR and storms type. Special interest works are taken on forecasting weather variables but first, it is important to define the term forecast that can be defined as a dynamic filtering method in which future values are predicted based on the previous values of one or more time series (Tokar and Johnson 1999; Rohit, 2012; Deshpande 2012; Farajzadeh, et al, 2014). In this section, literature reviews were presented in sequence mater to serve the background of this study as.

Remote sensing techniques considered as advanced and effective means for studying soil, natural resources, water, and vegetation (Novara et al, 2018; Zhao et al, 2019). Remote sensing techniques are applied for monitoring and tracking environmental phenomena that effect on land use/land cover such as drought, soil degradation, desertification, soil erosion, salinity, and waterlogging (Fathizad et al, 2018; Gleason et al, 2018; Mariano et al, 2018).

Nowadays GIS has been combined with many modern technologies like Artificial Intelligent and remote sensing techniques for different drought studies as detected in many studies. GIS was able to translate the results of these modern technologies into clear formulas that enabled to classify the drought and its extension over time in many forms that are easy to understand (Belal et al, 2014; Hellwig et al, 2017). In this study, Feidas et al. 2007 were able to implement GIS in the development of an integrated automated operating system that assesses real-time rain forecasting as a solution to numerical weather prediction.

Runoff-rainfall prediction formula of annual stream flow was developed by Mustafa et al, 2017 for west Dar Fur state wadis system in Sudan, where GIS was proved to be successful and accurate integration procedure with rainfall and discharge data analysis. Different ANN structures have been applied by (Hsieh and Tang 1998) for predicting meteorology and oceanography data where they found that these procedures can analyze these kinds of data effectively and efficiently. Many advantages of ANN

procedures explained by (Liong and Shan 2010) include nonlinearity analysis, easy data preparation, ability to learn and high accuracy with low statistical errors.

Hung, et al, in 2009 set up a real-world case study in Bangkok, Thailand, using 4 years of hourly data from 75 rain gauge stations used to develop the ANN model. The results show a combination of meteorological parameters such as relative humidity, air pressure, wet bulb temperature, and cloudiness, along with rainfall data at the forecasting station and other surrounding stations, as an input for the model could significantly improve the forecast accuracy and efficiency.

Many hydrologists are trying to make predictions using the Artificial Neural Network (ANN) method in the field of hydrology like (Hsu, et al, 1995; Abhishek, 2012). Therefore, in order to produce efficient accurate results of prediction, (Mislán et al, 2015) applied an Artificial Neural Network (ANN) with the Backpropagation Neural Network (BPNN) algorithm. In this experiment, the rainfall data tested using two-hidden layers of BPNN architectures with three different epochs (BPNN) algorithm to predict rainfall data by studying and analyzing the patterns non-linear of the past data to obtain more accurate prediction results with a minimum error. In this experiment, the rainfall data tested using two-hidden layers of BPNN architectures with three different epochs. Many advantages of ANN procedures explained by (Liong and Shan 2010; Dou et al, 2018) include non-linearity analysis, easy data preparation, ability to learn and high accuracy with low statistical errors.

In this study, three famous ANNs as Radial Basis Function (RBF), Fuzzy C-Means (FCM) and Nonlinear Autoregressive Network with Exogenous (NARX) were chosen according to many scientific articles that prove their ability and efficiency to predict future weather data with high-performance accuracy. Radial Basis Functions RBF networks applied successfully in function approximation, curve fitting, time series prediction, control and classification problems etc. (Abrosimov and Brovko 2019).

NARX as an artificial neural network has proved its suitability for long-term prediction (Shen and Chang 2013; Arabeyyat et al. 2018). The NARX, artificial networks have proved its suitability for long-term prediction (Caswell 2014). To forecast daily rainfall

Devi et al, 2016, adopt different neural network models such as Cascade-forward Back Propagation Neural Network, Distributed Time-Delay Neural Network and NARX.

FCM is commonly used in a wide range of problems that can be solved using this technique like weather forecasting, agricultural engineering and remote-sensing image analysis etc. (Ding and Xian 2016). FCM can be classified under classical fuzzy clustering algorithms which are based on an idea of dividing a single data set or a time series into some groups which have specific attributes for each group (Maharaj et al, 2019; Naveen and Mohan 2019).

In 1965, Lotfi A. Zadeh presented the fuzzy logic term when he highlights his theory about the fuzzy set. During ten years until 1975, he continued to strengthen the foundation of fuzzy set theory to include many important axes like (decision-making, similarity relations, linguistic hedges etc.) (Tzimopoulos et al, 2008).

According to Kasabov's, 1996 book, there are many approaches in his compilation for solving different problems by combining different methods of Artificial Intelligent (Fuzzy Systems, and Neural Networks). To solve the decision problems, Bellman, and Zadeh, 1973 wrote an influential paper in fuzzy logic definition and strategy to build fuzzy logic inference system as a solution to address all problems related to fuzzy decision-making, control, optimization, etc. The starting point for accepting fuzzy logic as one of the solutions for various engineering applications was the explanation that made by Mamdani and Assilian 1975 for solving various engineering problems.

Bart Kosko, 1992 has written one of the most important books in the definition of fuzzy logic and its importance in many applications. The theory of fuzzy sets has been used in various fields of drought analysis. By using fuzzy logic Pesti et al, 1996 they were able to assess the drought according to its general patterns. A fuzzy rule developed by Pongracz et al, 1996 to predict regional drought depending on palmer index characterization. Ozger, et al, 2011 developed a combination model based on the principles of the wavelet and fuzzy logic for long term drought forecasting.

Mamdani method used in this work as one of fuzzy control system methodology that translates the fuzzy set theory based on human experiences. It was proposed in 1975 by Ebrahim Mamdani depended on his experience for controlling the steam engine and

boiler combination where his theory was built upon the efforts of Zadeh's 1973 studies on fuzzy logic (Mamdani, 1975; Jimoh et al, 2013).

Fuzzy Logic procedures has been applied to studying different activities. The rainfall-runoff relationship was studied using fuzzy logic in a small watershed in India (Pawar et al, 2004). Geographical information system (GIS) applications were adopted by many researchers (Hoang and Bui 2018; Faridi et al, 2018). Water management was assessment in many studies (Srinivas et al, 2018; Tabesh et al, 2018) etc.

Adaptive Neuro-fuzzy modelling ANFIS has designed to combine and applying various learning techniques developed in neural networks to the fuzzy logic theory in one system (Jang, 1993; Rahman et al. 2014). In many hydrological studies, ANFIS has adapted to be an efficient methodology for predicting rainfall and many hydrologic studies (Jung et al, 2018; Kuriqi and Ardiçlioğlu 2018). As found in many kinds of literature that several numbers of model efficiency criteria were used to evaluate the performance accuracy of various development models (Crochemore et al, 2015; Kasiviswanathan et al, 2019) were the best performance accuracy of a model is when the correlation is high and the errors are as small as possible.

Drought is a natural phenomenon that negatively affects all components of life. However, this phenomenon is easy to monitor where proactive solutions can be set to reduce its harm if its predicted values identified in the future. Drought characterized by its severity, duration, and spatial impact on a particular area, but because of different characteristics of the climate, it is difficult to determine when the drought begins and when or where it influences negatively on a specific area (Morid et al, 2007). There are four types of droughts, meteorological, agricultural, hydrological, and socio-economic were they classified according to many criteria where their direct or indirect impacts on the environment were including. The subject of this study is to predict and assess the meteorological drought. Sometimes meteorological drought called climatological drought that can be defined according to the magnitude and duration of a rainfall where any shortfall or anomalies of rainfall over time in a particular area leads to the emergence the effect of this type of drought on that area (Mohammad et al, 2018). Drought prediction is an essential procedure for many

disciplines related to water resource management, environmental studies, or the agricultural industry etc.

The Standardized Precipitation Index (SPI) is a statistical index that compares the total precipitation received by a given site during the rainy season in addition to long-term precipitation distribution at the same time at that site. The precipitation index SPI is calculated every month for a moving window (n) showing the period of precipitation accumulation in some rainy months, usually 1, 3, 6, 9, 12, 24 or 48 months. SPI index written in the form as (SPI-1, SPI-3, SPI-6, etc.) to indicate the values of SPI for a given number of rainy months (Ajay, 2016; Naumann et al, 2017). There are several ways to calculate the standardized precipitation index (SPI), which grouped into two methods (Daksh et al, 2018). The first method is calculated the SPI manually by applying several equations that can be solved using some supporting platforms like MATLAB workspace (Cancelliere et al, 2007). The second method is to rely on specialized software to calculate the values of this index such as SPI_SL_6, or DrinC (Tigkas et al, 2015).

Dust and sand storms are natural disasters that occur in areas classified under arid and semi-arid areas. These natural events cause many problems in terms of human health, society and the environment. Immigration, health problems, problems in air and land transport, soil erosion, desertification, destruction of crops and agricultural infrastructure etc. are some examples of the impact of these natural phenomena on different aspects of life (Goudie and Middleton 1992; Washington, 2003).

It has been admitted that these natural events transcend boundaries and cannot be handled effectively through national-level meditation. There are two types of dust and sandstorms in Iraq as confirmed by Furman in 2003 when he studied them according to their frequency in eight countries (Iraq, Syria, Jordan, Lebanon, Egypt, Sudan, Saudi Arabia and Iran). He found that the most frequent dust and sandstorms in north-eastern Iraq occur in summer, while the most frequent dust and sandstorms in western Iraq occur mainly in the spring. Also, Wilderson,1991, AFCC,1995 and UNISDR, 2009 refer to two different common types of dust and sandstorms in Iraq, Haboobs and Shamals.

The first one is Haboob that moves quickly in the form of a wall of dust turning daylight to total darkness in a few minutes. The sources of these storms are outside the

Iraqi border, especially from areas within Syria and Saudi Arabia. The second type is Shamal that's defined as a local sandstorm normally created in local Iraqi regions from the lower Tigris and Euphrates river valleys by northwest winds picking up dust in the atmosphere. The main difference between this type and the Haboob is that it can last much longer, with one event existing for four to five days alone (Kobler, 2013).

1.4 Study Phases

This study consisting of five chapters, each one represents a stage of the study, where each chapter discussed separately. The thesis structure illustrated as a flow chart shown in (Figure 1.1). Chapter one shows the necessary outlook represented by aims and objectives as well as the background review that covers all topics in order to illustrate the methodologies adopted in this study. In chapter two, the concepts of desertification clarified to give a clear view of the nature of this phenomenon from the environmental point of view. In addition, to reviewing the historical facts of the effects of this phenomenon on Iraq, also in this chapter, the study area defined according to several characteristics to get a clear picture of the importance of the study area.

Chapter three illustrate all the methodologies that adopted in the study where the basic concepts for each methodology have been clarified to give a basic definition for each methodology structure with the main steps that need to follow to obtain the desired results from these methodologies. In the fourth chapter, the obtained results were reviewed and discussed where most of these results were published in two research papers entitled "The Impact of Dust and Sandstorms in Increasing Drought Areas in Nineveh Province, North-western Iraq" and "Designing Weather Forecasting Model Using Computational Intelligent Tools". In addition, an artical entiled as "Integrated Fuzzy Logic for Long- Term Drought Prediction Northwestern of Iraq" was a accepted to published in International Journal of Computational Intelligent Systems.

The last chapter in this study is chapter five where a set of conclusions is explained in the form of points where each point explains the nature of the conclusion according to the results derived from each used methodology, as well as several recommendations, were set up to cover all the topics that needed to combat or even mitigating the desertification in the study area.

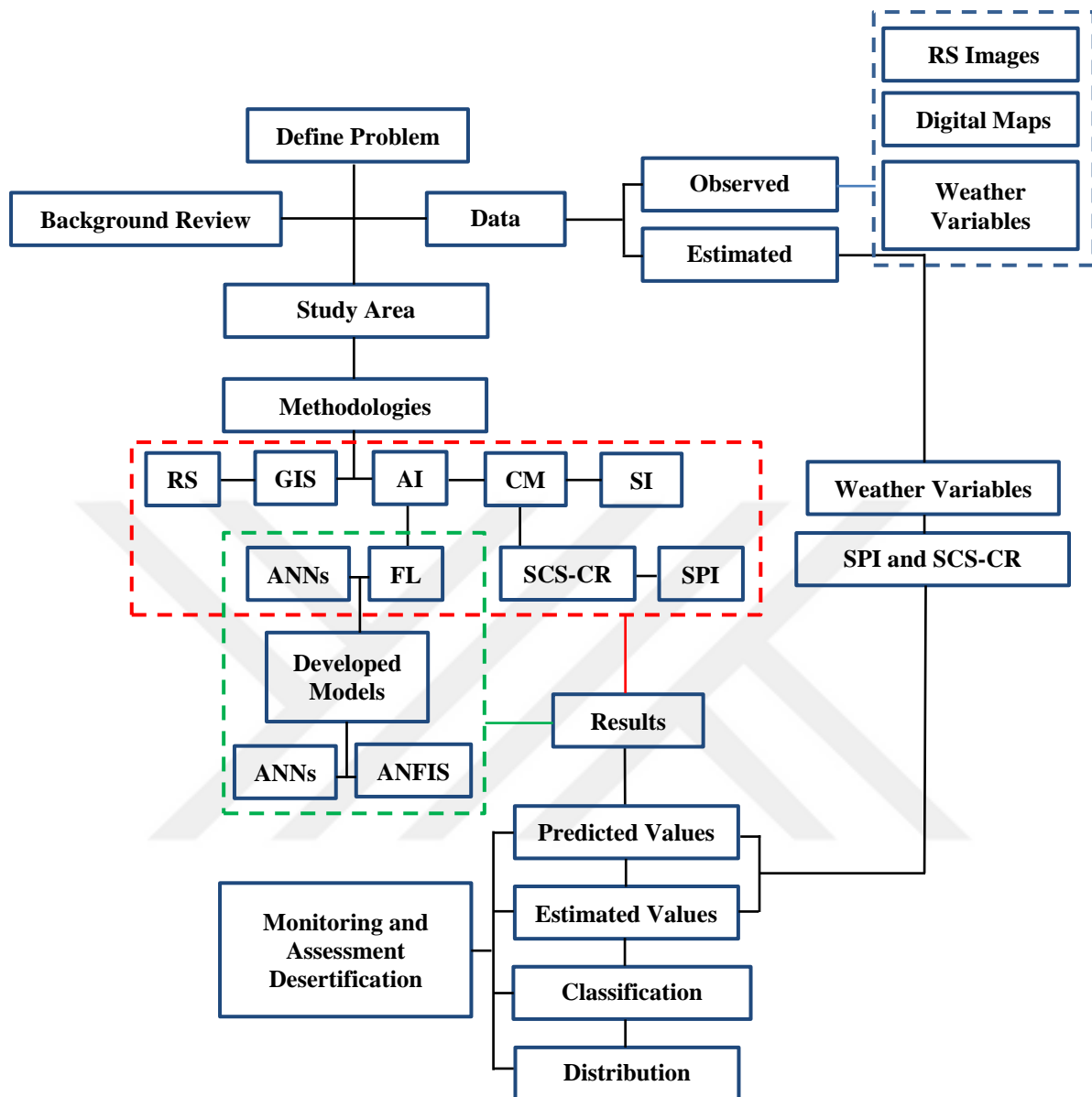


Figure 1.1 : Thesis progress flow chart.

2. DESERTIFICATION CONCEPTS

Desertification is the environmental event through which natural or agro-productive lands converted into unproductive land or completely degraded land in sometimes, especially when assessing their situation over time. In the past, it thought that, this phenomenon exacerbated only by the status of the local climate changes. Nevertheless, in the last two decades, it has noted that there several factors that are all contributing to the exacerbation of this phenomenon like global climate change and human activity through his role of transforming the natural lands for his purposes as examples. Desertification has a series of problems that effected on the ecosystems of any land where this phenomenon affects the productivity and biology of land, as well as the heterogeneity of the landscape. In other words, the ecosystems will not returned to the former state due to these problems. In this chapter, firstly the context of desertification was presented generally with it is related factors, secondly, the historical facts of desertification in Iraq were represented, then the study area was briefly introduced.

Many definitions of desertification, with many meaning concepts that used to coin this phenomenon according to its complex structure. All presented definitions agreed on one point. Desertification is an environmental phenomenon has catastrophic dangers to the local and global ecosystems. Its effect may not appear in the near future, but it was found by analyzing the properties of this phenomenon that their effects take a long time to failure lands resources balance in different ways without any indicator of quickly recovering (Li et al, 2018; Scoones, 2018).

In general, nature and human activity are two interactive elements that can perceived as the main factors that cause desertification. Human activities revolve around several wrong habits like natural resources over-exploitation through an increase in population leads to rising of human needs without taking into account the environmental system, which became more fragile with time. Waste of water resources, overgrazing, urbanization at the expense of vegetation cover, green housing emissions, wrong mining activity, random waste disposal, lack of respect the national and international laws regard to water sharing are the most factors lead in one way or another to

desertification. Climate change and drought situation have cited as nature factors that cause desertification. Climate change refers to statistical changes in natural climate regime with time where this factor is the primary cause of desertification, as well as the increasing of severing droughts probability for long periods can be considered as the second nature factor that causes desertification. It is difficult to control the natural factors, but several scientific ways used to understand how these factors changed with time where the development of prediction models is one of these scientific procedures.

2.1 Desertification in Iraq-Historical Facts

Iraq is located in the eastern part of the Middle East and North African countries (MENA) region that considered to be arid or semi-arid lands with average annual rainfall does not exceed 166 mm and classified as the most vulnerable in the world to the potential impacts of climate change. It is surrounded by Iran in the east, Turkey to the north, Syria and Jordan to the west, Saudi Arabia and Kuwait to the south and the Gulf to the southeast. The total area of Iraq is 438,320 km² of which 924 km² of inland water. Parry, 2007 expected that the (MENA) region will suffer from higher temperatures and intense heat waves affecting inhabitants and crop yields, and will also affect marine ecosystems and fisheries. Less but more intense rainfall, coupled with higher temperatures will likely cause more droughts and greater flooding, sea-level rise, more intense cyclones and new areas exposed to dengue, malaria, and other vector and waterborne diseases.

Like many other countries in the arid and semi-arid regions, Iraq exposed to desertification problems. According to the Iraqi Government, 92% of the total area of Iraq is at risk of desertification. Significant reductions in vegetation cover occurred all over the country. Between 2009 and 2012, the total area covered by vegetation decreased by 50% as presented in (Figure 2.1) (UNEP, 2013).

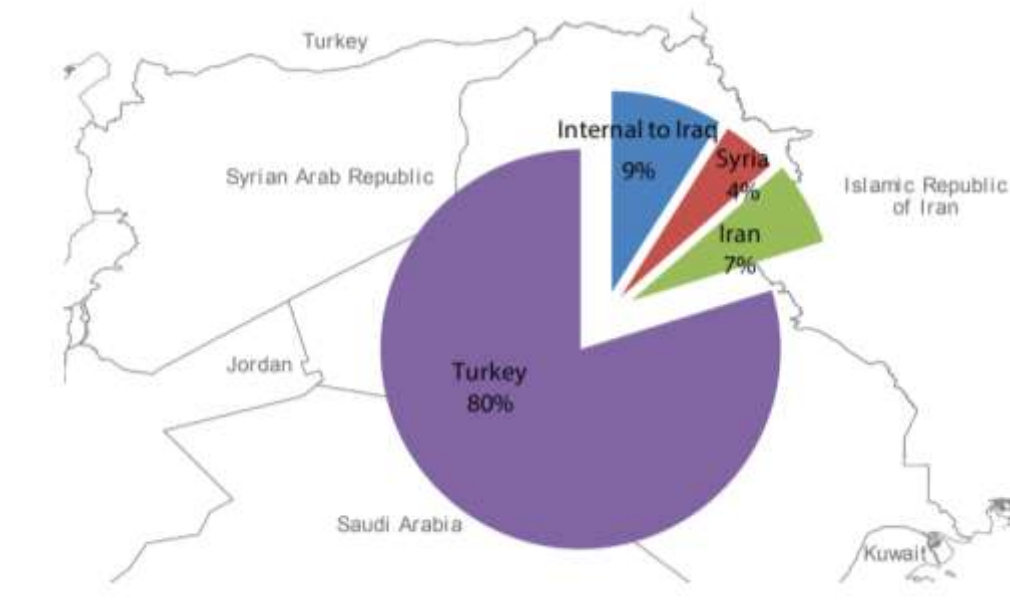


Figure 2.2 : Iraqi water resources sources.

1. The climate of Iraq. 90% of the area of Iraq is located within the dry and semi-dry climatic zone, where the hot and dry desert climate is located within the limits of the sedimentary plain and the western desert plateau. Global warming and climate change led to a decrease for rain and increased the level of drought in Iraq. High summer temperatures which sometimes reach more than 50° c, low rainfall rate, varying in size between 5-15 cm, is affected by the high evaporation rate, which is lower in most regions of Iraq. The rainfall rate in the south is 40 days and in the north 70 days with a lack of humidity that is very important in soil biological cycle and growth of Herbs. The prevailing winds in Iraq are the dry and hot Northwest winds, spreading local dust, and dry, long dry summers. This factor plays an important role in the occurrence of desertification in Iraq.

2. Human causes. The absence of the role of the current government to supporting the agricultural sector as result of non-nature conditions by its war with criminal gangs. Using the wrong agricultural practices, the bad exploitation of natural resources (overgrazing and depletion of groundwater resources and soil), increasing population and increasing development needs leads to over-consumption of water all these factors are leading to increased drought.

3. The effects of neighbouring countries. The dams that have built by Turkey and Syria on Tigris and Euphrates rivers, as well as Iran's water plans have put Iraqis at risk of harm. Where it built a series of dams and large water reservoirs on the course of water

flowing from its territory towards Iraq, causing the cutting of water, and the decline in the flow level reaches to zero.

Dust and sand storms are two of the most important environmental challenges facing Iraqi areas located within the semi-arid region where Iraq has witnessed a significant increase in the intensity and the frequency of these natural events in the past decade. This prompted the United Nations Environment Program (UNEP) to predict that Iraq could witness 300 dust events in a year within 10 years, up from around 120 per year now (UN, 2013). It has been admitted that these natural events transcend boundaries and cannot be handled effectively through national- level mediation alone (Kobler, 2013) as seen in (Figure 2.3).

There are two types of dust and sand storms in Iraq and this confirmed by Furman in 2003 when he studied these storms according to their frequency in eight countries (Iraq, Syria, Jordan, Lebanon, Egypt, Sudan, Saudi Arabia and Iran). Which found that the most frequent dust storms in northeastern Iraq occur in summer while the most frequent dust storms in western Iraq they occur mainly in the spring.



Figure 2.3 : Impact of dust and sand storms in several places of Iraq.

In addition, Wilderson, 1991 and AFCC, 1995 refers to two different common types of dust storms in Iraq, Haboobs and Shamals. The Haboob type moves quickly in the form of a wall of dust turning daylight to total darkness in a few minutes the sources of this storm is from outside the Iraqi border, especially from areas within both of Syria and Saudi Arabia as seen in (Figure 2.4-a). The other type is Shamal it is a local sand storm normally created from local dust regions exactly from lower Tigris and Euphrates river valleys by northwest winds picking up dust into the atmosphere. The main compared with Haboob it can last much longer actually from four to five days during one event (Figure 2.4-b).

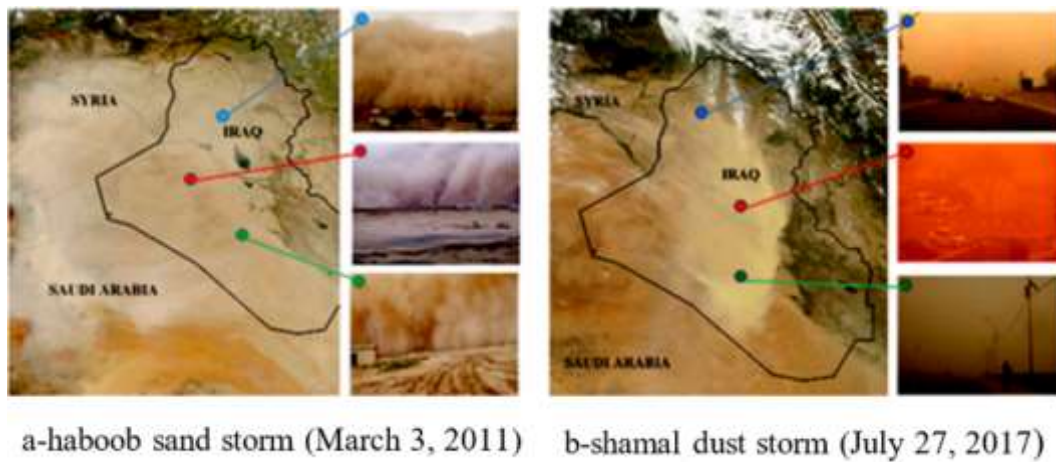


Figure 2.4 : Types of dust and sand storms in Iraq.

2.2 Study Area Description

In general, Iraq is located in the Middle East. Six countries Turkey, Iran, Kuwait, Saudi Arabia, Jordan and Syria have bordered with Iraq as well as a small stretch of the Arab Gulf and it has eighteen governorates. Nineveh as the third largest province of Iraq in terms of size selected as a study area where its total area is 37,323 km². Nineveh contained nine administrative districts as Tilkaif, Shikhan, Aqra, Al-hamdaniya, Mosul, Hadar, Al-baaji, Sinjar and Telafer. The provincial capital is the city of Mosul as given in (Figure 2.5) where located approximately 400 km north of Baghdad the capital of Iraq between located at 41° 30' – 44 ° 30' longitude and 35° 00' – 37 ° 00' latitude situated at elevation 228 meters above sea level. The Tigris River separated Nineveh in two parts as right bank and a left bank. It shares a border with Syria and several other Iraqi governorates. It has a population, ranges between 2 to 3 million people (IAU, 2010).

Two seasonal valleys selected within the study area where two case studies were completed based on the methodologies adopted in this study as described below.

a. Wadi AL-Mleh basin, the area of this basin investigated by 1000 square kilometres, which occupies 330.41 square kilometres. The larger area surrounding the basin chosen to give a comprehensive approach to analyze the deterioration of vegetation within the basin area and its surroundings. Wadi AL-Mleh which located in northern region of Nineveh governorate between the longitudes (43° 07' 00 ") and (43° 00' 00

) and between latitudes ($36^{\circ} 37' 00''$) and ($36^{\circ} 42' 30''$) and is about 33 kilometers from the Mosul city as shown in (Figure 2.5).

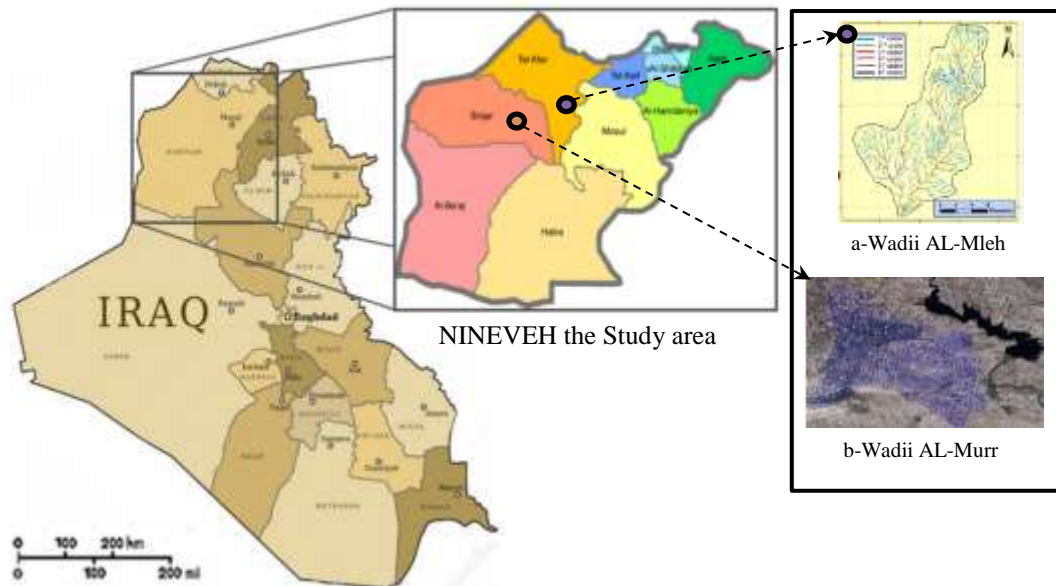


Figure 2.5 : The study area.

b. Wadi AL-Murr, this seasonal valley located in the west region of Nineveh, the area of this basin is 2460 square kilometres. The basin located between the longitudes ($42^{\circ} 00' 02''$), ($43^{\circ} 00' 13''$) and between latitudes ($36^{\circ} 17' 59''$), ($36^{\circ} 57' 05''$) is about 52 kilometres from the elimination of Mosul city within Nineveh Governorate border as seen in (Figure 2.5).

2.2.1 Meteorology and hydrology

The climate in Iraq is mainly of the continental, subtropical semi-arid type, with the north and northeastern mountainous regions having a Mediterranean climate. The desert climate dominates the center and south of Iraq with mild winters and extremely hot summers. The semi-desert climate dominates in the north, with relatively cold winters, while in the northern mountains, the climate is cold and rainy (or snowy) in winter, warm and sunny in summer, but with cooler nights due to the high altitude. Monthly average temperatures in Iraq range from higher than 48°C in July and August to below zero in January. The average annual rainfall estimated at 216 mm (FAO, 2003). Several attempts made by metrologists to classify the climates of the world. Cartographic and mathematical methods are some procedures of that classification,

these classifications done through the characteristics of temperature, rainfall and some secondary climatic variables as seen in (Figure 2.6).

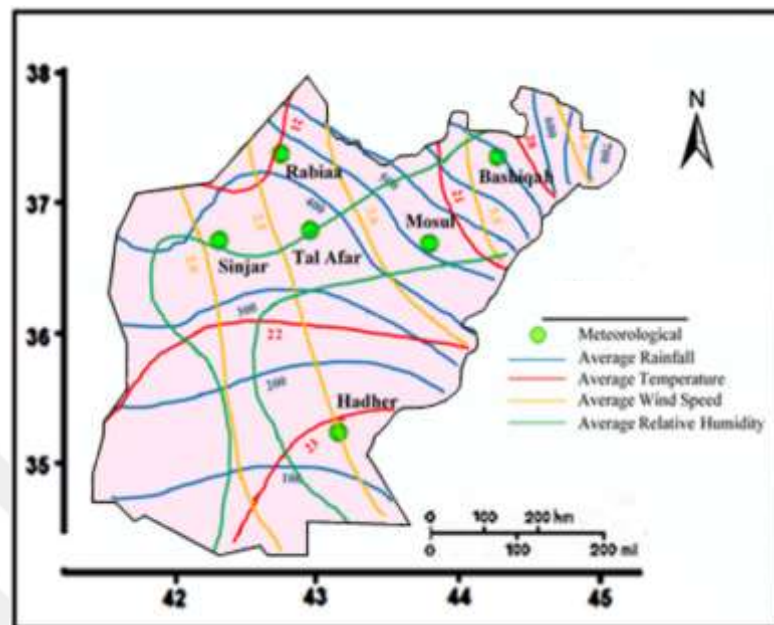


Figure 2.6 : Meteorological parameters in Iraq (modified after IOM, 2000).

Cobden's classification is the most common classification of the climate that classified Nineveh as a transitional climatic category or sometimes named the semi-dry climate. Winter in Nineveh is mild but not tropical; the average temperature in January is 7 c°. The summer in Nineveh is very hot and relentlessly sunny, with possible daytime temperatures of 43 c° in July and August; however, air humidity is low. The climate of Nineveh can be characterized as by Rainfall, Temperature and Humidity as weather variables as (Al-janabi 2010).

a. The rainfall in the in Nineveh varies in patterns, but most are either Cyclone rains or heavy rains. Cyclone rainfall is the predominant rain on most of the rain falling in the season. The rainforest of the year, though originating from the Mediterranean, is essentially hurricanes offerings formed in the northern sections of the Atlantic Ocean and pushed eastward to enter the area The Mediterranean is in winter from the Carcassonne Pass at the northern border of Spain. The second type of rainfalls on Nineveh is the heavy rains. Which is unique to Nineveh from the rest of Iraq and this rain pattern occurs exclusively in the spring when the ground temperature of the conductor increases due to the approaching separation summer, and at the same time

descend to the land of the city of Nineveh and neighboring cold air masses. It was stable on the plateau of Anatolia, and by the effect of thermal conductivity between the land areas. The density of the heavy rains decreases because of the thermal conductivity procedure. The average rainfall, in Nineveh, is 365 mm of rainfall the magnitude is not many concentrated between November and April, with very few rains in May and October, while between June and September it almost never rains.

b. The temperature in the study area indicated by the position of the angle of the solar radiation and varies astronomically throughout the year with the effect the virtual movement of the sun in the four seasons. Temperatures are highest in the summer months, with an average of July 34.4°C , and lowest in the winter months, especially on January 7.2°C where the average temperature for the year in Nineveh is 27.6°C .

c. Humidity is associated with the site for water bodies and the frequency of winds that blows on the city. Due to the distance of the city of Mosul from the maritime site, the air humidity was mainly associated with the rainy season of the year (winter). Relative humidity peaks in Nineveh in December and January where it is 80%, while in the summer shows relative humidity at their annual low, In July, it was only 24%. The relative humidity decrease in the hot season of the year because of the lack of rain in this season, as well as the high temperature of the air that makes its capacity and the acquisition of moisture is very high.

d. Nineveh, like many other parts of the world, exposed to wind movement. The wind is the horizontal movement of the air moving according to the variation in pressure values on the earth surface. Winds blowing towards the city of Mosul in different directions. Their frequency varies depending on the different pressure ranges at the same time. In Nineveh, the most continuous wind throughout the year is the northwest wind, because the location of Iraq between two opposing poles of atmospheric pressure, one north on the Anatolian plateau characterized by the semi-permanent high pressure and the other is the sub-tropical pressure that dominates the Arabian Sea and the Arabian Gulf region. This variation in the pressure bands makes the northern wind Western is the most common and continuous to Nineveh, and this does not prevent the wind from blowing different directions such as south-eastern, north-eastern, western, etc. Winds vary over the Nineveh during months because of seasonal variations. Where the eastern wind controls 45% of its trends in January, while western winds dominate 30% and north-west on 30% in April, while the ratio of control of the Northwest wind

to 20% and the Western To 40% in July, while the north-west wind is 30% and the eastern one is on 33% of its trends in October. The following steps can introduce the hydrological characteristics in the study area.

1. Surface water: Nineveh consist of several kind of water bodies that briefly discussed as follows.

- a. The Tigris River: From Taunus Mountains of Eastern Turkey, the Tigris River flows in a total length of 1850 km. Before entering Iraq, the river flows through Turkey about 400 km in length and when it enters the Iraqi border at Faish Khabur village the river flow at length equal 1418 km. The river feeds Iraq with five major tributaries from it's left bank that is Khabur, Greater Zab, lesser Zab, Uzaym and Diyala rivers as illustrated in (Figure 2.7). Tigris River reaches Mosul city with average discharge equal to $630 \text{ m}^3/\text{s}$ where the minimum discharge was detected in October 1935 equal $85 \text{ m}^3/\text{s}$ while the maximum discharge has been detected in May 1972 equal $7740 \text{ m}^3/\text{s}$.
- b. The Greater Zab: It is one of the eight tributaries that they feed Tigris River. It generates 13.18 km^3 as discharge at its confluence with the Tigris River. 62% of the total area of this river basin that equal $25,810 \text{ km}^2$ is in Iraq. Joining with the Tigris River south of Mosul about 60 km at Sharkat city.

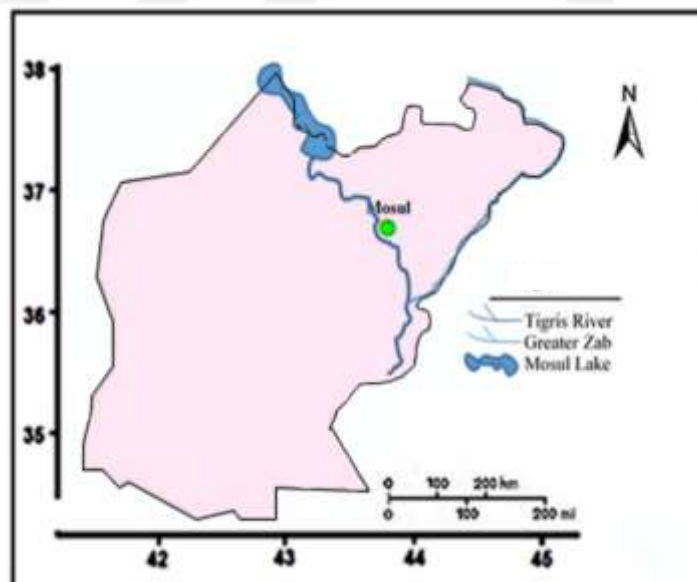


Figure 2.7 : Water bodies within Nineveh boarder.

- c. The Mosul Dam Lake: Mosul dam is the largest dam in Iraq. It is located on the Tigris River in the western governorate of Nineveh, 58 km upstream of the city of Mosul. Mosul Lake is the largest artificial water reservoirs in Iraq. This lake is the

main source of drinking water to most Iraqi cities that allocated southern of Nineveh. The surface area of the lake is 385 km² at the maximum operation level with a total storage volume of 11.13×10⁹ m³ and The dam drainage area is 50,200 km² (Khattab and Merkel, 2012).

2. Ground water: Recently the drilling of wells increased significantly and unwisely. This increasing because of several reasons, like, water interruption in many areas especially in the districts, lack of rainfall course decrease the normal recharging of wells and increasing the water demand for different purposes. The suitability of the groundwater in Nineveh for drinking, agricultural and many applied purposes were studied by many scientists like (Omran, 2012; Jassas and Merkel 2015) as seen in (Figure 2.8).

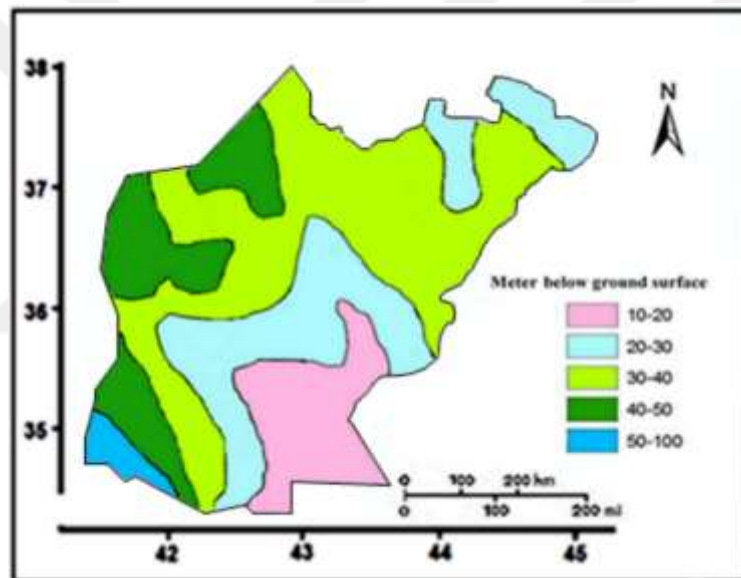


Figure 2.8 : Ground water depth (modified after Al-Jiburi and Al-Basrawi 2015).

2.2.2 Geology

The Arabian platform plate used as a reference to dividing Iraq into two first-order tectonic zones (Arabian Platform and Shalair Terrane). The Arabian Platform divided tectonically into six zones as Thrust Zones, Imbricated, High Folded, Low Folded, Mesopotamian and Western desert (Buday, 1980). The Nineveh tectonic map that modified from (Fouad, 2015) shows that Nineveh territory consists of four of the classified six tectonic zones as High Folded, Low Folded, Mesopotamian and complex zones as seen in (Figure 2.9).

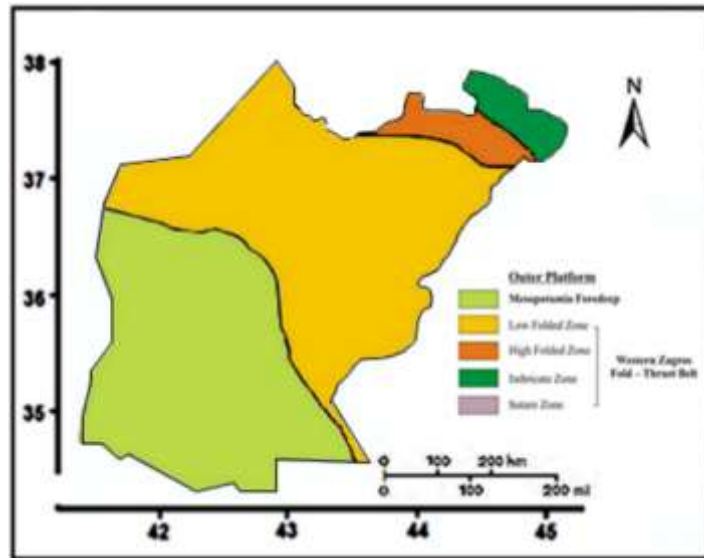


Figure 2.9 : Tectonic divisions of Nineveh (modified after Fouad, 2015).

2.2.3 Land cover

Climatic conditions, lithological escarpments, soil fertility can be considered as factors that causing variation of land cover in Nineveh. The basic land cover units were classified by many sciences like Jaradat 2003 and Al-Daghastani 2008 where (Figure 2.10) illustrate their results.

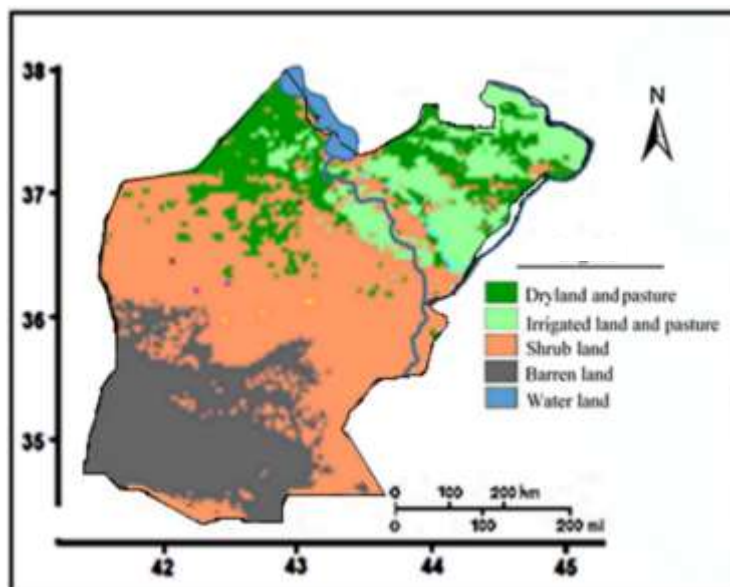


Figure 2.10 : Land cover (modified after Jaradat 2003 and Al-Daghastani, 2008).

2.2.4 Geomorphology

Nineveh characterized geomorphologically by many complex geomorphological landscapes. According to many researchers and specialists in this field, including Al-Daghastani, 2007, where he was able to distinguish these geomorphological landscapes using the satellite's imagery. The results of his study described in (Table 2.1).

Table 2.1 : Geomorphologic landscapes (modified after Al-Daghastani, 2007).

| Geomorphological Landscapes | | |
|--|---|--|
| Tectonic Origin | Fluvial Origin | Denotational Origin |
| Structurally controlled high folded topography | Tigris River valley and its tributaries | Stable accumulation glacis on sloping foothills surfaces |
| Structurally controlled low folded topography | Seasonal dry valleys | Mixed erosional glacis on sloping foothills surfaces |
| Structurally controlled denudational hills | Fluvial river terraces at low levels | Active erosional glacis on gently sloping surfaces |
| | Fluvial river terraces at high levels | Karstic landforms with sinkholes and subsurface valley |
| | Basin of Mosul dam lake | Aeolian sand deposits without distinct dune forms |
| | Depression salt areas and playa lakes | |

2.2.5 Economy

Nineveh considered as a prominent commercial center. It has many export products such as oil, agricultural, industrial products and mineral products. Several governmental factories established during the 1970s and 1980s. These factories support industrial sector in Iraq where these factories produce different important products such as pharmaceutical industry, medical equipment, particularly cement, precast concrete elements, textile, clothing, sugar, food processing industries and factories for processing wool, tanning and leather. In addition, it has many private factories that product wood, metal and aluminium furniture as well as many factories that produce different industrial food. Furthermore, there are cooperated factories between the government and private sectors like flour factories.

2.2.6 Agriculture

Nineveh governorate has most types of rites and climates (IAMN, 2019), which give it great agricultural flexibility, and high production capacity that benefits in improving income and exploitation of agricultural and natural resources. Six agriculture zones detected in Nineveh where these zones are suitable to cultivate several of economic crops. Perennial trees zone, large scale farming area zone, mechanized agriculture zone and marginal agriculture zone as seen in (Figure 2.11).

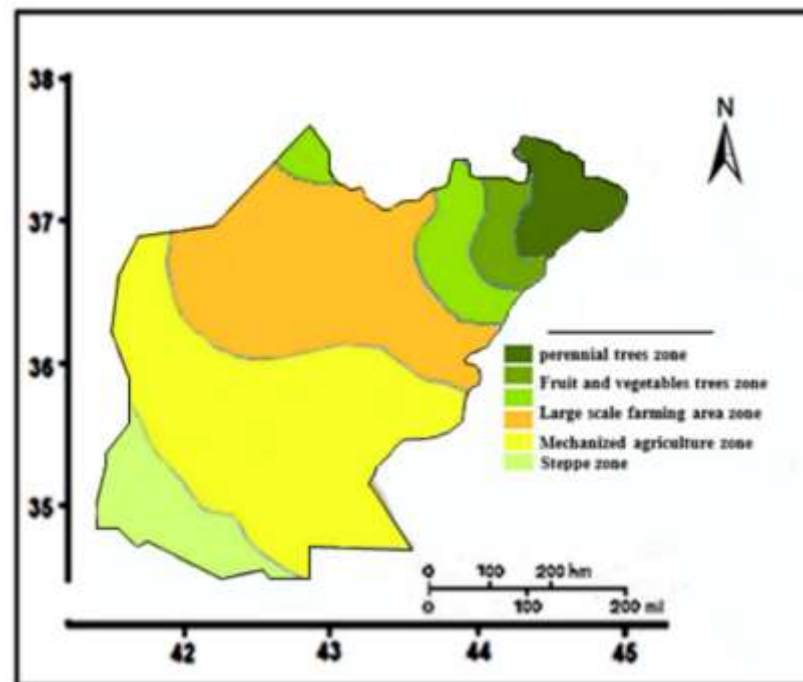


Figure 2.11 : Agriculture zones in Nineveh (Modified after IAMN, 2019).

Historically, Agriculture has been the main contributor to the economy in Nineveh where it known as the “breadbasket” of Iraq (USAID, 2006) due to the high proportion of arable land amounting to 46% of the total land suitable for agriculture in Iraq. Nineveh yielded annually about 45 % of wheat and barley production of Iraq's total annual production. Most of the wheat and barley production grown in the cities of Baaji and Hadar the two provinces that they located in west and south-west of Nineveh. Nineveh's average wheat production is 1.1 million tons and the average barley production is 0.5 tons annually, according to the statements of the Iraqi Ministry of Agriculture.



3. DATA AND METHODOLOGIES

This chapter includes the methodologies and data specifications used in thesis research strategy where several scientific activities should be performed to study the desertification phenomena. To satisfy the objectives of this study, Remote Sensing (RS), Geographical Information System (GIS), Standardized Precipitation Index, Soil Conservation Service (SCS-CN), Artificial Intelligent concepts and some statistical analysis were reviewed as scientific procedures used to complete the purpose of this study as in the following sections. The scientific procedures used in analyses suitable data, modelling and obtaining results that can play a role to combat desertification in critical environmentally sensitive areas like the study area.

3.1 Data Specifications and Used Software

Several types of data used in the study where their specifications illustrated below.

3.1.1 Meteorological data

Ideally, the analysis using ANNs need continues time-series data set (Zhang et al, 1998). Furthermore, it is logical to insert weather data records of all meteorological stations within a selected region when designing a weather forecasting model to ensure obtaining realistic results. The study area contains six meteorological stations (Mosul, Tal Afar, Sinjar, Hadher, Rabiaa and Ba'shiqah stations) as seen in (Figure 3.1) that separated within the study area (Iraqi Meteorological Network Data 2017).

3.1.2. Remote sensing data

Several kind of Remote Sensing data used in this study as illustrated in (Table 3.1) as follows:

1. Temporal satellite images from Landsat sensors used. Dataset path 170 row 35 on 25/4/1992 and 16/5/2016 taken by enhanced thematic mapper (ETM+) sensor board on Landsat7.

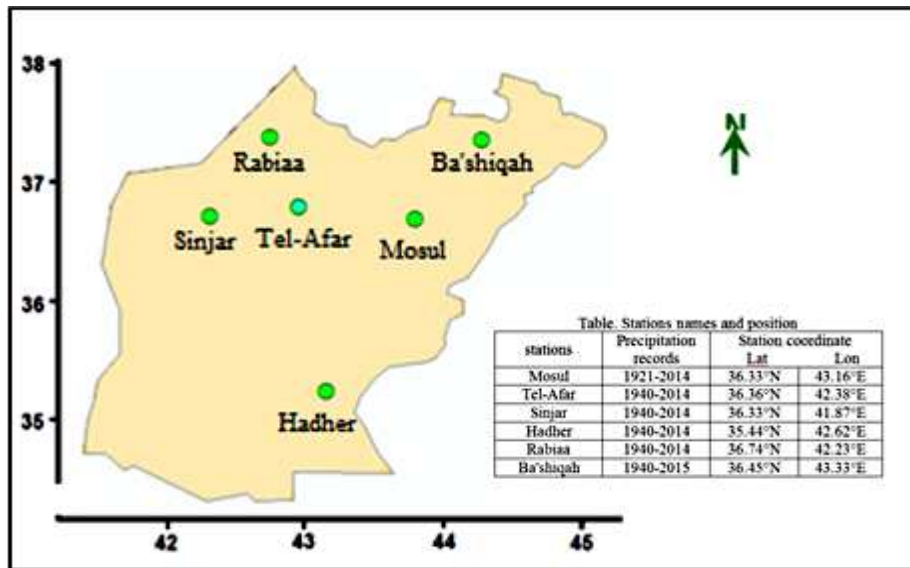


Figure 3.1: The distribution of meteorological stations in the study area.

Table 3.1: Type of remote sensing data and their uses.

| Data Type | Resolution | Function | Potential |
|-----------|------------|--|--|
| LANDSAT | 30 m | Used for interpretation and detect vegetation change | Map out and asses the classification procedures |
| MODIS | 500 m | Identified potential dust and sandstorm sources | Produce Dust and sand feeding areas map that affect the study area |

2. Forty (different time) true colour satellite images from 2003 to 2017 of dust and sandstorms captured by MODIS on the Aqua and Terra satellites operated by the National Aeronautics and Space Administration (NASA) (NESDIS, 2017; Url-1) and as seen in (APPENDIX A).

3.1.3 Digital maps

a. The map of dust loads in the Middle East produced by the World Meteorological Organization (WMO) (WMO, 2018) adopted in this study. This map produced from different numerical prediction models and represented at a common geographical domain. These models have very different characteristics like different resolutions, dust emission, dust assimilation, meteorological model, etc. (Nickovic et al., 2001).

b. Three maps of global vegetation health and three maps of drought change produced by the NOAA STAR center for Satellite Application and Research (Url-2) on three dates, 8 April 1992, 8 April 2010 and 8 April 2017, used in this study.

3.1.4 Used softwares

Three software's has used to complete the methodology stages they described as below.

a. Arc GIS v.10 is a geographic information system (GIS) software package working with maps and geographic information. It has multiple uses for creating and using maps and analyzing geospatial data. ArcGIS v.10 used for analyzing mapped information and managing geographic information in a database. Reliable results found when using geostatistical analysis and maps created.

b. ERDAS Imagine v. 14 is a remote sensing application with raster graphics editor abilities designed by ERDAS for geospatial applications. This software is used for geospatial raster data processing and allows users to prepare, display and enhance digital images for mapping use in geographic information system GIS and computer-aided design CAD software. It is a toolbox allowing the user to perform numerous operations on an image and generate an answer to specific geographical questions. Many extensions and functions were used for processing study areas imagery like indices, supervise classification and site location simulation.

The virtual GIS installed in ERDAS. It is a three dimensional (3D) visualization tool. In this extension, a virtual environment can be visualized through the ability of combined several layers of raster and vector images with real-time databases to create a 3D scene for the area under study (Ervin, 1993).

c. MATLAB v. R2017a is a multi-paradigm numerical computing environment and fourth-generation programming language MATLAB allows matrix manipulations, plotting of functions and data, implementation of algorithms, creation of user interfaces and interfacing with programs written in other languages including C, C++, Java, Fortran or Python etc.

d. Global Mapper v.11 is a geographic information system GIS software package currently developed by Blue Marble Geographic's BMG that runs on Microsoft Windows. The GIS software competes with ESRI, Geo-Media, Manifold System,

and MapInfo GIS products. Global Mapper handles both (vector, raster) and elevation data, and provides viewing, conversion, and other general (GIS) features.

3.2 Remote Sensing (RS)

Monitoring, assessment, modelling or predicting of any environmental phenomenon can be carried out easily using earth observation technologies, at different spatial and temporal levels. These technologies provide relevant strategies and support plans for all kinds of environmental management. Remote Sensing (RS) and Geographic Information System (GIS) are the best examples of these technologies.

based on the electromagnetic waves which enable it to detect all kinds of earth surface objects, in the other hand the detected objects, in turn, can interact with these electromagnetic waves. So according to this interaction vegetation, water bodies, or buildings as objects or a natural phenomenon like desertification, earthquakes environmental pollution etc. can be studied and detailed information of these objects and phenomena can be collected. For more results that are efficient, remote sensing data must be analyzed together with further data gained from the ancillary ground to obtain more accurate information about the objective or phenomenon under study likely to be integrated into Geographical Information System (GIS).

3.2.1 Remote sensing methodologies

To give a clear perception of the decrease in vegetation cover in the study area, Remote sensing techniques represented by supervised classification and Normalized Differences Vegetation Index (NDVI) adopted to display the effects of desertification in the study area for the period from 1992 to 2016 according to available remote sensing data. ERDAS Imagine v.13 software used for analyzing the vegetation cover changes where the obtained results represented by accurate maps. These methodologies illustrated briefly in the following sections.

3.2.1.1 Normalized difference vegetation index (NDVI)

Vegetation cover decreasing and desertification are important issues to many meteorological, hydrological, ecological and social etc. researches. Many vegetation indices derived from satellite data in the optical and infrared wavelengths. Each of these datasets has been derived to overcome some limitation in existing indices. The most

widely used remotely sensed vegetation index in detecting and investigating drought effects is the NDVI. For desertification studies NDVI providing a measure of canopy greenness, which is related to the quantity of standing biomass. A main challenge associated with NDVI is that although biomass and productivity closely related in some systems, the results gained from NDVI can differ widely the changes of vegetation cover across land uses and ecosystem types (Liu and Huete 1995).

Based on the electromagnetic spectrum of the vegetation that fluctuating between red and near infrared, numerous vegetation indices formulated for detecting and evaluating the vegetation cover (Johnson and Kasischke 1998; Dymond and Johnson 2002). According to Lunetta, 2006, the most used vegetation indices for vegetation analysis listed in (Table 3.2). In this study, the Normalized Difference Vegetation Index (NDVI) used in this study to find the changes in the vegetation cover in the study area.

Table 3.2 : Different vegetation indices techniques.

| Vegetation Indices | Formulas |
|---|---|
| Difference Vegetation Index (DVI) | $DVI = \text{Band 4} - a \times \text{Band 2}$ |
| Normalized Difference Vegetation Index (NDVI) | $NDVI = (NIR - RED) / (NIR + RED)$ |
| Perpendicular Vegetation Index (PVI) | $PVI = \text{Band 4} - a \times \text{Band 2} - b / \sqrt{1 + a^2}$ |
| Ratio Vegetation Index (RVI) | $RVI = \text{Band 4} / \text{Band 2}$ |
| Soil Adjusted Ratio Vegetation Index (SARVI) | $SARVI = \text{Band 4} / (\text{Band 2} + (b/a))$ |
| Soil Adjusted Vegetation Index (SAVI) | $SAVI = (1 + L) \times (\text{Band 4} - \text{Band 2}) / (\text{Band 4} + \text{Band 2} + L)$ |

The Normalized Difference Vegetation Index (NDVI) is a quantified vegetation remote sensing index, which measures the differences between red and near-infrared spectrum that reflected or observed from the vegetation cover. It is mostly used to discriminate the vegetated areas from un-vegetated areas; also, it can be used to evaluate the vegetation healthy status (Ahmad et al, 2018). Rouse et al. used the index for the first time in 1973. It is represented mathematically using equation 3.1 as follows.

$$NDVI = (NIR - RED) / (NIR + RED) \quad (3.1)$$

Where,

NIR - reflection in the near-infrared spectrum

RED - reflection in the red range of the spectrum

The result of this formula generates a value between -1 and +1 where the values from -1 to zero represent non-vegetated areas such as abandoned land or urban land and values greater than zero to +1 represent existing vegetation in the area under study. In other words, a high NDVI value yield when low reflectance in the red channel and high reflectance in the NIR channel observed, and vice versa.

In particular, using NDVI is important in three sectors, firstly in evaluate, differentiate and demonstrate the global vegetation cover represented by the green biomass of farming, forests and rangeland vegetation cover. Secondly, NDVI can used as an indicator of drought providing an early warning procedure. Thirdly, NDVI can used as an indicator of earth surface moisture. NOAA platforms, LANDSAT satellite and Earth Resources Technology Satellite (ERTS) imagery dataset, which became early sensors that can supply red and near infrared, and thermal infrared measurements of the reflectance of the planet. Where their spectral resolution enables them to detect the vegetation targets and separate them on different other plant targets easily.

3.2.1.2 Image enhancement

Before digital image processing and in order to improve obtaining wealthy information from the available images. Image enhancement techniques algorithms are the best procedure are commonly applied. The results of image enhancement techniques displayed as special images that can adopted in further analysis. The most common practices of image enhancement techniques are False Colors Compositions FCC and density slicing.

A multispectral image consists of several bands that displayed in a grayscale level that cover the entire spectrum. When a combination made based on three bands (red, green, blue). A False Color Composite image was obtained that usually named FCC image which allows to sight the wavelength range that the human eye cannot see as in (Figure 3.2) that illustrated the vegetation looks in red colour, because the high reflects of near-infrared wavelength and not appear like the usual green (Rees and Pellika 2010). As illustrated in (Table 3.3) there are many band combinations that each of these combinations gives analytic visualization for any task of image processing purpose.

Taking into account the possibility of finding new combinations using the method of trial and error, which may appear new information or objectives cannot shown in the usual combinations.

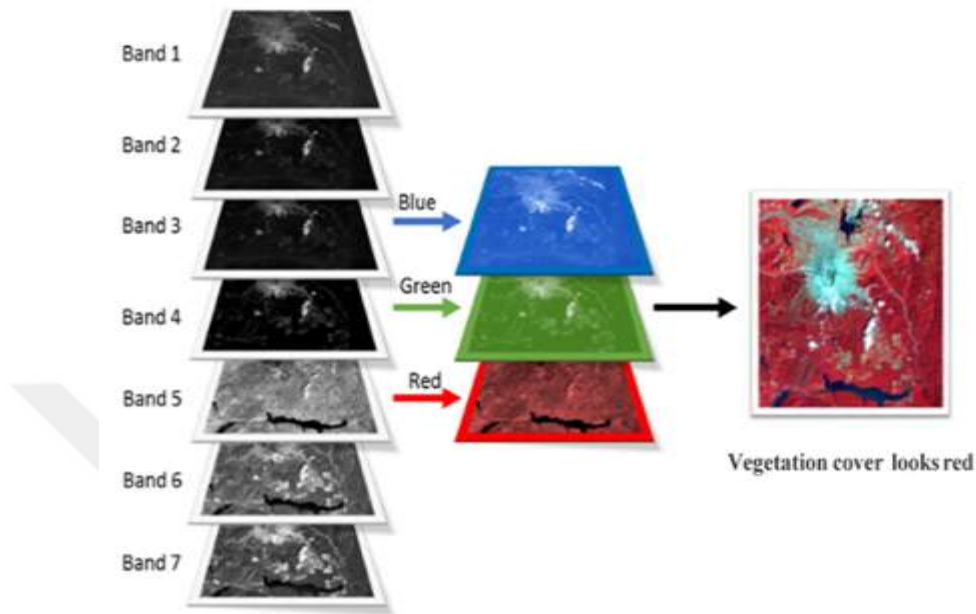


Figure 3.2 : FCC combination (modified after Rees and Pellika 2010).

Table 3.3 : Different band combinations False Colors Compositions images.

| Composite Order | Used Bands |
|----------------------------------|------------|
| Natural Color | 4 3 2 |
| False Color (urban) | 7 6 4 |
| Agriculture | 6 5 2 |
| Healthy Vegetation | 5 6 2 |
| Land/Water | 5 6 4 |
| Natural With Atmospheric Removal | 7 5 3 |
| Color Infrared (vegetation) | 5 4 3 |
| Shortwave Infrared | 7 5 4 |
| Vegetation Analysis | 6 5 4 |

Density slicing converts the continuous grey tone of an image into a series of density intervals or each corresponding to a specified digital range. Slices may displayed as areas bounded by contour lines. This technique emphasizes subtle grayscale differences that may be imperceptible to the viewer. Grayscale values (0-255) converted into a series of intervals or slices, and different colours assigned to each slice. Density slicing used to highlight variations in vegetation.

3.2.1.3 Supervised classification

Classification of remote sensing imagery is the process that land covers objects can be classified to several of individual classes based on the spectral properties of these objects. There are many specialist techniques for classifying images. Supervised classification among them that consider as essential extinction in many remote sensing software like ERDAS Imagine that can use it for detecting the land use/cover changes.

In supervised classification, spectral signatures of known target areas on an image are specified to be a confidence reference data (training signature data), that used for classified the image pixels and gathered them in groups (classes) according to their spectral signatures. The training signature data has special characteristics that should be included to get confidence classification, where relatively homogeneous, numerous, classes representability and large data as possible are the most characteristics of training signature data. There are many parametric rules (classifier algorithms) like Maximum Likelihood, Mahalanobis Distance, Minimum Distance, Parallelepiped etc. Maximum Likelihood (ML) classifier adopted in this study where the assumption of this classifier is each class in each band are normally distributed and calculates the probability that a given pixel belongs to a specific class. Unless a probability threshold selected, all pixels are classified. Each pixel assigned to the class that has the highest probability.

In this study, the supervised classification extension in ERDAS Imagine used for comparing the changes in vegetation cover through the two-time period. Several basic steps must follow them carefully when trying to operate the supervised classification extension in ERDAS Imagine to get accurate classification results. According to the complexity of digital classification due to the differences in classified classes, classification accuracy has taken seriously. Therefore, it is essential to the researchers how studied the land use/cover practices have full knowledge in two factors, firstly the nature of the studied area in terms of variety of classes and secondly the good consideration to the accuracy assessment techniques (Foody 2002).

A confusion matrix (or error matrix) usually used as the quantitative method of characterizing image classification accuracy. Confusion matrix is a table that shows correspondence between the classification result and a reference field data. A classification error matrix typically contains tabulation results of an accuracy

evaluation of a thematic classification, such as that of a land use and land cover map. There are many different ways to look at the thematic accuracy of a classification. The error matrix allows calculating the overall Accuracy, user's accuracy and producer's accuracy to evaluate the classification results (Hammond and Verbyla 1996; Costa, 2018).

The overall accuracy is essentially tells out of all of the reference sites what proportion were mapped correctly. The overall accuracy usually expressed as a percent, with 100% accuracy being a perfect classification where all reference site classified correctly. Overall accuracy is the easiest to calculate and understand but ultimately only provides the map user and producer with basic accuracy information. Producer's Accuracy is the map accuracy from the point of view of the mapmaker (the producer). This is how often are real features on the ground correctly shown on the classified map or the probability that a certain land cover of an area on the ground classified as such. It is also the number of reference sites classified accurately divided by the total number of reference sites for that class. The User's Accuracy is the accuracy from the point of view of a map user, not the mapmaker. The User's accuracy essentially tells how often the class on the map will actually be present on the ground. The User's Accuracy is calculating by taking the total number of correct classifications for a particular class and dividing it by the row total.

3.3 Geographic Information System (GIS)

There are broad definitions of Geographic Information System (GIS), these definitions provided by many researcher and agencies, the most acceptable definition of GIS is the hardware and software system that has many facilitates for solving complex issues in different life applications like land use planning, transportation, environmental analysis, urban planning, ecosystems modelling and many other applications (Konecny, 2002). GIS as a tool consists of many extinctions that can handle much analysis needs like hydrology analysis, mapping locations, quantities or densities. GIS deal with many data type where remote sensing images, GPS, variables databases and digitized data are the most data kind that can feed in GIS system (Bernhardsen, 2002). Geographical Information System (GIS) is a representation of a long-term decision support system for varied applications that deals with environmental issues trough detect risk areas and assess environmental phenomenon impacts. The characteristics

of GIS that can, retrieving, manipulating and storing a huge amount of data enabling it to be an effective tool for analysis and management environmental issues. This system has many output forms as suitability maps, reports, diagrams and query system that help decision-makers to make the critical decisions and devise plans according to the environmental problem under study.

3.3.1 GIS methodologies

To find the changes and anomalies in drought levels over the actual and predicted periods, the used spatial analysis method gives a very clear output in maps form showing these changes clearly. In addition, this method used to find the dust and sand materials origin sources that carried out from the main source area by winds and deposits in the study area. GIS system provides procedures for tracking environmental phenomena like hurricanes or dust storms events where the paths of these events can be vitalized using real-world dataset (Badarinath et al, 2010). In the following two sections, the used GIS methods briefly discussed.

3.3.1.1 Spatial analysis

Spatial analysis is a geographic analysis and data management procedure that performs operations like statistics, spatial statistics, modelling or cartographic analysis etc. on an input dataset to obtain a new output dataset. The spatial analysis considered as the crux of GIS because it has the ability to add values to the used geographic data through many analysis procedures like transformations or manipulations to detect all changes and anomalies that were not clear at the beginning of the analysis. This method can provide answers to simple or complex spatial questions related to many studies under consideration. The Spatial Analyst Toolbox provided by Arc View v.10.3 software has eighteen extensions deals with different kind of spatial analysis fields like surface analysis, hydrology and groundwater as examples. The most important extensions are distance, density and hydrology that they provide a realistic spatial analysis to a geographical dataset. Generally, using spatial analysis methods installed in GIS system in studying environmental phenomena has very important advantages in the analysis that can be gained, where a new data can be estimated and a complex dataset can be visualized in time and space also the boundaries between values can be created.

3.3.1.2 Tracking dust and sand storms events

For displaying, analyzing and investigating phenomena such as environmental phenomena (hurricanes or sand storms etc.), GIS can provide particle tracking models. These models can be run in real-time during a disaster or can be used as a part of a scientific study or field research project (Vance et al, 2009). Particle tracking models can display the paths of these phenomena. Arc GIS Engine supported by Environmental System Research Institute (ESRI) used in this study for tracking dust and sand event in the study area. The last dust and sand storms event accrued in March-24- 2017 that classified under Haboobs storm type was tracked using GIS by adopting tracking analysis procedures to identify the theoretical storm paths by specifying the direction and wind speed of which controls the storm where the average wind speed in Nineveh is about 2.8 m/s. The storm is drawn and divided into small parts where the centres of all parts are identifying to specify the decrease or increase in storm size as a result of its movement, the storm affecting the province within one 18 hours.

The covering area of this storm classified into three phases as seen in (Figure 3.3). According to the formation form at hour 0 the first and second stages began to form the shape of these phases that changed into cumulative and continues marching until the hour 4 where it enters the study area. At hour 12, this storm becomes more active and covering all the study area where the third phase begins in this period. Six hours later, this storm is gradually disappearing and leaving the study area to the adjacent provinces to become less powerful and ends after a while.

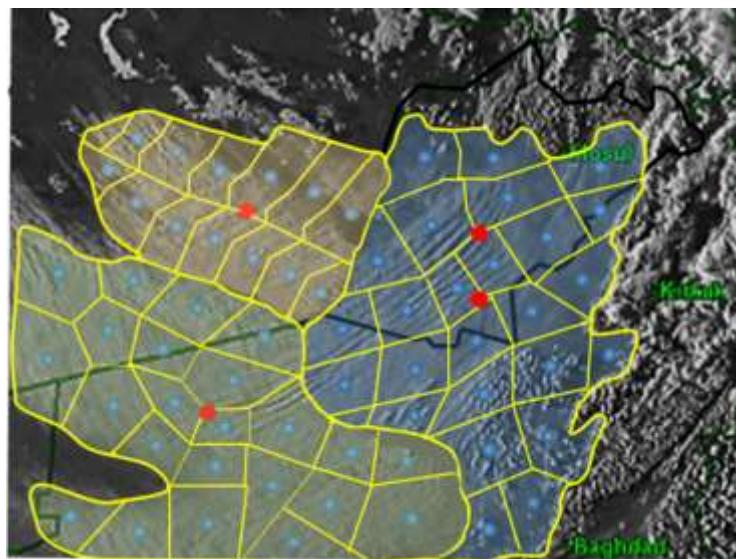


Figure 3.3 : Dividing the storm into small parts.

The shapefiles of the three phases have been divided into nested regions where the centre of these parts was identified to prepare tracking analysis to find the theoretical paths of this storm which lasted 18 hours. The movement of this storm has tracked through Playback Manager. This method gives the sequence of the actual wind movement during the 18 hours within the specified hours. On this analysis, the most affected centre points of the storm emphasized where two theoretical paths tracked.

3.4 Computational Methods

To study desertification closely, there are many mathematical methods derived to find some relationships or factors that prove the presence of this phenomenon or one of its factors in the area under study. Drought indices and runoff estimation methods are the most famous computational methods used for studying desertification. In the following two sections the Standardized Precipitation Index (SPI) and the Soil Conservation Service (SCS-CN) are briefly discussed.

3.4.1 Standardized precipitation index (SPI)

Over the years, many drought indices developed and used by meteorologists and climatologists around the world (Bayissa et al, 2018). Those indices ranged from simple such as Percentage of Normal Precipitation Index and Precipitation Percentiles Index more complicated indices such as the Palmer Drought Severity Index. However, scientists realized that these indices should be simple, easy to calculate and statistically relevant and meaningful where the deficit of precipitation has different impacts on groundwater, reservoir storage, soil moisture, snowpack and streamflow.

Meteorologists and climatologists around the world used to use a different kind of drought indices that ranged from simple to complicated indices. However, in 1993 three scientists from Colorado State University named as McKee, Doesken, and Kleist, they succeeded to develop a meaningful and statistically relevant index called it Standardized Precipitation Index (SPI) for drought estimation. The required input parameter for this index formula is only precipitation values making it easy to simulate the drought levels in any area. This index provides early warning and useful assessing procedure for drought severity calculation. Standardized Precipitation Index (SPI) acts as an indicator for drought monitoring in terms of early warning, which helps to assess the extent and severity of the drought. The basic statistical analysis of SPI depends on

how time-series data converted into normal distributions using the Gamma Distribution Probability Function in which the arithmetic mean is equal to zero (Türke and Tatlı 2009). SPI is a dimensionless probability index where it is conducted after sequence the mathematical procedures. Firstly, the precipitation values are fitted to gamma distribution which can represent the precipitation time series well as found by (Thom 1958) as illustrated by equation 3.2.

$$g(x) = \frac{1}{\beta^\alpha \Gamma(\alpha)} x^{\alpha-1} e^{-x/\beta} \quad \text{for } x > 0 \quad (3.2)$$

Where $\alpha > 0$ is a shape parameter, $\beta > 0$ is a scale parameter, Γ is the gamma function, and $x > 0$ is the precipitation amount.

$$\alpha = \frac{1}{4A} \left(1 + \sqrt{1 + \frac{4A}{3}} \right) \quad (3.3)$$

Where,

$$A = \ln(x) - \sum \frac{\ln(x)}{n} \quad (3.4)$$

n = number of precipitation observations

$$\beta = \frac{x}{\alpha} \quad (3.5)$$

Secondly, Integrating the probability density function with respect to x and inserting the estimates of a and b yields an expression for the cumulative probability $G(x)$ of an observed amount of precipitation occurring for a time as illustrated in equation 3.6.

$$G(x) = \int_0^x g(x) dx = \frac{1}{\beta^\alpha \Gamma(\alpha)} \int_0^x x^{\alpha-1} e^{-x/\beta} \quad (3.6)$$

Since the gamma distribution is undefined for $x = 0$ and a precipitation distribution may contain zeros, the cumulative probability becomes as shown in equation 3.7.

$$H(x) = q + (1-q) G(x) \quad (3.7)$$

Where, q is the probability of a zero. If there are zeros in a precipitation time series Thom, 1966 suggested that q could be estimated by m/n where m represents the number of zeros.

Thirdly, the cumulative probability distribution is then transformed into the standard normal distribution to yield the SPI. The equations from equation 3.2 to equation 3.7 are formatted in Microsoft Excel to create templates that are ready to calculate the values of SPI as seen in (APPENDIX B). The SPI is computed by dividing the difference between the normalized seasonal precipitation and actual precipitation on the standard deviation as equation 3.8.

$$SPI = \frac{X_n - X_a}{\sigma} \quad (3.8)$$

Where,

X_n is normalized seasonal precipitation

X_a actual precipitation

σ is its standard deviation.

Positive values of the SPI index indicate that there is an increase in precipitation from the annual average, which is defined as a wet period. The difference between the positive values and the annual average of precipitation represents a surplus in precipitation while negative values mean that there is a deficit from the annual average of precipitation, defined as a drought period. The deficiency represents the difference between the negative values and the annual average of precipitation in the investigated year (Keyantash and Dracup 2002). McKee et al. 1993 established rules for classifying the dryness levels where values of -1 or less indicate conditions of drought and values of 1 or more indicate conditions of wetness as shown in (Table 3.4).

Table 3.4 : Classification of the Standardized Precipitation Index (SPI) values.

| SPI Classes | SPI Value |
|----------------|---------------|
| Extremely wet | 2.0 + |
| Very wet | 1.5 to 1.99 |
| Moderately wet | 1.0 to 1.49 |
| Near normal | -0.99 to 0.99 |
| Moderately dry | -1.0 to -1.49 |
| Severely dry | -1.5 to -1.99 |
| Extremely dry | -2.0 and less |

It can be observed from (Figure 3.4) that the positive values of the SPI index represent the wet years while the negative values represent the dry years. Therefore, the difference between the precipitation value and the annual precipitation rate represents the annual deficit precipitation. Drought duration (DI) can be defined as the successive drought period within the time series precipitation records. While the drought magnitude (Dm) can be defined as the amount of deficit precipitation during the time period and the average drought (Da) can be defined as the quotient of the drought magnitude (Dm) on the drought duration (DI) (Livada and Assimakopoulos 2007) as illustrated in equation 3.9. Moreover, conditions of wetness as shown in (Table 3.4).

$$D_m = \sum X' - X_i \quad (3.9)$$

Where,

D_m = the amount of total drought

X' = the average of precipitation record

X_i = the precipitation value at time i

m = the numbers of times of the deficit precipitation within the drought period

$$D_a = D_m / D_I \quad (3.10)$$

(D_I) = Drought duration

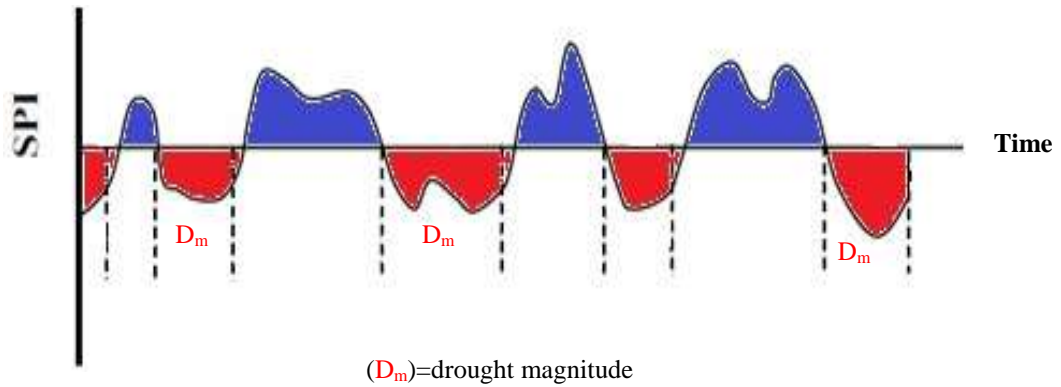


Figure 3.4 : SPI analysis for precipitation record.

The SPI value varies based on the timescale where the small timescales like 1-month make the SPI move frequently above and below zero while longer timescales like 12-month make the SPI change slowly due to changes in precipitation. The soil moisture can be considered as evidence of precipitation anomaly in a relatively short time while

groundwater with all its properties of reservoir and flow is evidence of long-term precipitation anomalies. In other words, from SPI-1 to SPI-6 are a good indicator for agricultural drought estimation and assessment while SPI-12 to SPI-24 is a good indicator for hydrological drought analyses and applications (Huang et al, 2016).

In this study two SPI timescale (SPI-3 and SPI-12) adopted to assess the drought, the forty-six monthly average of approved meteorological data obtained from Mosul station for the period from 1970 to 2017 used to assess the drought situation. Drought duration (DD), Average drought intensity (ADI), and Drought magnitude (DM) estimated to identify drought in the study area.

3.4.2 The SCS-CN Curve number method

Watershed runoff can be determined through many approaches where the Soil Conservation Service Curve Number (SCS-CN) one of them. SCS-CN is the most famous formula used to estimate the runoff in rural areas developed by the U.S. Department of Agriculture also known as the Hydrologic Soil Cover Complex Method (USDA, 1972). This procedure depended essentially on the rainfall records of an area as input data taking into account the watershed wetness (Mishra and Singh 2013). The mathematical form of the SCS-CN method described as given in equation 3.11 below.

$$Q = \frac{(P - I_a)^2}{(P - I_a) + S} \quad (3.11)$$

Where,

Q = Runoff

P = Rainfall

I_a = Initial abstraction

S = Potential maximum retention after runoff begins

Watershed wetness used as indicator to find a dimensionless parameter called curve number (CN) which has a value ranged from 1 (minimum runoff) to 100 (maximum runoff), this parameter depends on several criteria like hydrologic soil group (HSG), land use, land cover, hydrologic conditions and antecedent moisture condition (AMC) (Ponce and Richard 1996; Michel et al. 2005). The U.S. Department of Agriculture developed a guide to adjusting CN according to watershed wetness. Based on the total

rainfall in the 5-day period preceding a rainstorm as known as Antecedent Moisture Condition AMC that can defined as an index of watershed moisture and availability of Storage the soil moisture before the storm occurs, and can have a significant effect on runoff volume. There are three levels of AMC for dry, normal, and wet conditions as illustrated in (Table 3.5) for the normal case, the CN values documented to adjust the CNs for other cases (dry and wet) by applying equation 3.12 and equation 3.13 (Silveira et al. 2000).

Table 3.5 : Seasonal rainfall limits for three antecedent moisture conditions.

| AMC | Total 5-days Antecedent Rainfall (mm) | |
|--------|---------------------------------------|----------------|
| | Dormant season | Growing season |
| Dry | 12.7< | 35.6< |
| Normal | 12.7-27.9 | 35.6-53.3 |
| Wet | 27.9> | 53.3> |

$$CN_{(I)} = \frac{4.2 * CN_{(II)}}{10 - (0.058 * CN_{(II)})} \quad (3.12)$$

$$CN_{(III)} = \frac{23 * CN_{(II)}}{10 + (0.13 * CN_{(II)})} \quad (3.13)$$

Where,

$CN_{(I)}$ Is the curve number for dry condition, $CN_{(II)}$ is the curve number for normal condition, $CN_{(III)}$ and $CN_{(II)}$ is the curve number for wet condition.

equation 3.14 represents the rainfall-runoff equation used by the SCS for estimating depth of direct runoff from storm rainfall as below.

$$Q = \frac{(P - 0.2S)^2}{(P + 0.8S)} \quad (3.14)$$

Where,

S is the watershed storage, Q is the actual direct runoff and P is the total rainfall. The equation has one variable P and one parameter S where, equation 3.15 as relates S to curve number (CN).

$$S = \frac{25400}{CN} - 254 \quad (3.15)$$

The Hydrologic Soil Group (HSG) is a soil classifier depends on the minimum infiltration rate of soils after a long period of moisturizing. This classifier divided the soil into four types (A, B, C, and D) from the lowest to the highest runoff potential (Stewart et al, 2011) as illustrated in (Table 3.6).

Table 3.6 : Different soil group classifications.

| Soil characteristics | Soil group |
|--|------------|
| Deep sand, deep loess, and aggregated silt | Group A |
| Shallow loess and sandy loam | Group B |
| Clay loams, shallow sandy loam, soils low in organic content, and soils usually high in clay | Group C |
| Soils that swell significantly when wet, heavy plastic clay, and certain saline soils | Group D |

3.5 Artificial Intelligent (AI)

Artificial Intelligent (AI) can defined as a space of computer science applications that simulates a human ability to learn and make logical decisions. Artificial Intelligent provides solve complicated problems that face humanity with the best reliability and cost-effectiveness. Many tasks can Artificial Intelligent provides where decision-making, speech recognition, images recognition, predict variables etc. Artificial Intelligent consists of six branches as Machine learning, Evolutionary computation, Fuzzy systems, Computational creativity, Probabilistic methods and Chaos theory.

An Artificial Neural network (ANN) classified under machine learning as a branch of Artificial Intelligent where many applications can studied using (ANNs) like pattern recognition, control nonlinear system, prediction, function approximation and data classification etc. Fuzzy logic classified under Fuzzy theory that can described as a powerful theoretical framework that identifies the relationship between linguistic input data and human expertise in one scenario. For obtaining good results and high correlation between input and output dataset, Artificial Neural networks and fuzzy logic can connect them together in one Artificial Intelligent model named the adaptive Neuro-Fuzzy Inference System (ANFIS). To use the Artificial Intelligent procedure in this study, the basic concepts of Artificial Neural Network and Fuzzy Logic theory

discussed. The pioneering spirit of this chapter is to design and development models consist of Artificial Intelligent functions and Neuro-Fuzzy model, which can use them as tools for combating desertification in the study area as follows.

1. Designing weather forecasting model for Nineveh governorate based on three Artificial Neural Networks (ANNs) approaches (RBF, FCM, and NARX Neural Networks). The model performance accuracy was tested using weather data that belong to Nineveh governorate meteorological stations.
2. Develop Artificial Neural Network consist of RBF and NARX for predicting runoff in ungauged basin within Nineveh governorate boundary.
3. Develop Artificial Intelligent model consist of ANFIS and NARX for predicting SPI based on the correlation between five chosen weather variables and actual SPI.

3.5.1 Artificial neural network- basic concepts

The revolution of neural networks began to appear for the first time in (1943) when it pointed out by both (McCulloch and Pitts, 1943) through their research that considered as the first spark to start the history of the evolution of neural networks. From that time until today, many scientists have developed various neural networks based on several theories that aim to address many problems that require an effective and accurate processing mechanism. There are many definitions of the term neural networks but the most prominent ones as defined by.

Nigrin, (1993), *“An artificial neural network (ANN) is an interconnected group of artificial neurons which have a natural property for storing experiential knowledge and making it available for use”*

Hung et al, (2009), *“A neural network is a circuit composed of a very large number of simple processing elements that are neurally based. Each element operates only on local information. Furthermore, each element operates asynchronously; thus there is no overall system clock.”*

Walczak, (2019), *“An artificial neural network (ANN) is essentially a learning algorithm deals with specified oriented problems of both time-series and classification pattern by creating different kinds of interconnected neurons. These are then organized in one or multiple layers”*

According to the above definitions, the Artificial Neural Networks (ANNs) can be defined as a highly efficient processor that analyzing a huge dataset in various forms, extracting useful information in most scientific fields. It is a part of Artificial Intelligence that designed in mathematical models that simulates the nervous system in the human mind to recognize a specified pattern behaviour for a different time series to resolving real-world problems that need complex calculations. Prediction, classification, data association, data conceptualization and data filtering are the main five applications of neural networks. Seven key components need to be provided to structure any given artificial neural network. Each of them is responsible for achieving a specific task where their results are integrated to achieve the ultimate goal of the artificial neural network. These components are weighting factors, summation function, transfer function, scaling and limiting, output function, error function and learning function (Anderson and McNeill, 1992).

There are three essential categories assigned to the types of neural networks, firstly the learning process that is divided into supervised and unsupervised learning algorithms. Secondly is how the dataset flows through the parts of the neural network. The third category is the quantity and quality of the available data (Lippmann, 1987). There are two paths to flowing data in a network. The first one is when the data travels in one direction from the first layer of the network until it reaches the last layer of the network, this path is called feedforward. The second path is called feedback that means the data flows through two or multi-direction inside the artificial neural network layers.

3.5.2 Artificial neural networks - biological design

The structure of neural networks derived from the biological design of the human brain, which runs by numerous nerve units or neurons. In particular, these neural networks mimic the nature of the human brain, but with a few sets of biological neural systems. All artificial neural networks have a specific main architecture that contains layers connected by neurons as seen in (Figure 3.5). These neurons can be defined as important linking tools where they work as communication lines between other ordering neural network parts.

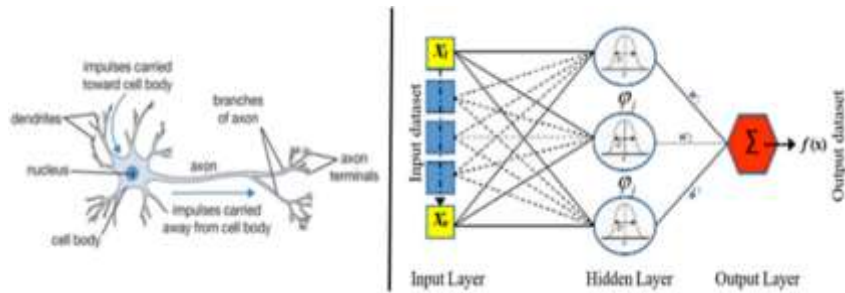


Figure 3.5 : Biological neurons versus artificial neural network.

The first layer is the input layer where the data received from different data sources and mostly organized in the form of matrices. The inputs data transferred to the second layer named by hidden layers (there may be one or several hidden layers) by neurons where the data mathematically processed through functions designed for a specific purpose. The results obtained from the processed layer are transferred to the third layer (output layer) providing a feed-forward path by another group of neurons. There is an additional type of connection called feedback connection. This is where the output of one layer needed to route back to a previous layer for more calculations (Lapedes and Farber, 1987). According to the main architectures, the neural networks can classified. Different structural of artificial neural networks designed as seen in (Figure 3.6) to cover different applications.

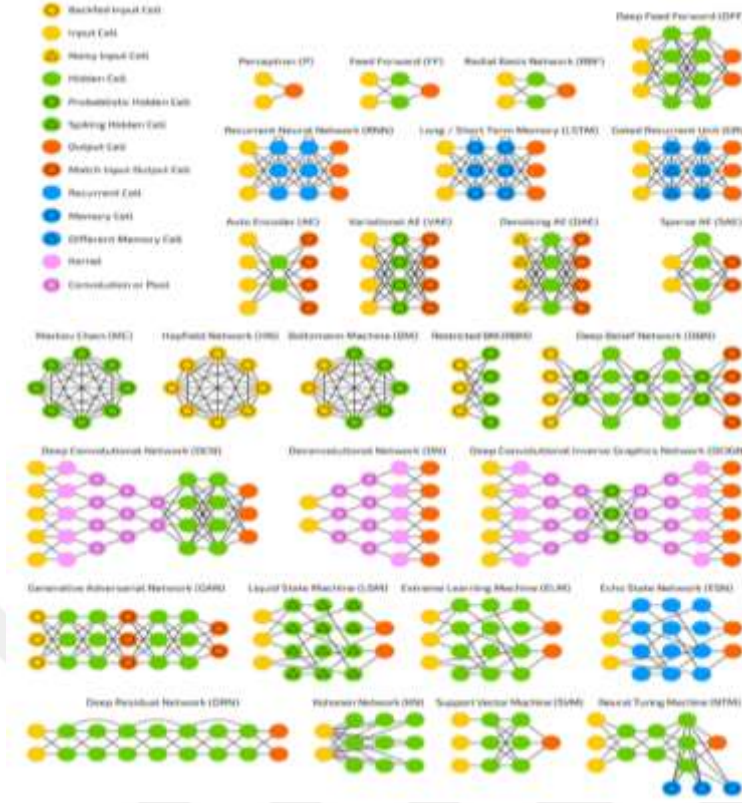


Figure 3.6 : Different artificial neural networks types (Url-3).

The Artificial Neural Networks work smoothly and simply when necessary components are available. These components are summed up by the neurons number and primary weights. Simple mathematical procedures are carried out with each input data individually. Then the obtained information is passed into the hidden layers through the neurons for processing using the activation functions that have been chosen for these networks. The results are passed gain by the neurons to the output layers to obtain the final desired results.

Mathematically the neural networks can be described as below as equation 3.16.

$$y(t) = F \left(\sum_{i=0}^m w_i(t) \cdot x_i(t) + b \right) \quad (3.16)$$

Where,

$w_i(t)$ is weight value in discrete time t where i goes from 0 to m

$x_i(t)$ is input value in discrete time t where i goes from 0 to m

b is bias,

F is a transfer function,

$y(t)$ is output value in discrete time t .

3.5.3 Artificial neural networks activation functions

For accomplished learning process and for determined the output results of artificial neural networks a kind of computationally efficient mathematical functions named activation functions or some time called it threshold functions are employed. Many kinds of activation functions designed for solving many real-world problems as for an example, nonlinear activation function that contained many types, Sigmoid Functions and Hyperbolic Tangent Function, Radial Bases Function

3.5.4 Artificial neural networks training algorithms

A kind of mathematical algorithm used for training artificial neural networks. These algorithms based on representation foundations and evaluation by training process. These algorithms try to learn how to visualize the pattern of the input data (testing data), as well as define the relationship between testing data and which data points are more frequent compared with the other points. These algorithms evaluate the performance of the first phase (representation) by estimating the training accuracy performance using some errors criteria like Root Mean Square Error (RMSE) and then it will be ready to expose to unknown data. Supervised learning and unsupervised learning are the most common training algorithms where each of them has the responsibility to find the best artificial neural network that gives the best results as far as possible.

3.5.5 Artificial neural networks design procedure

There are several essential requirements to develop any artificial neural network, these requirements can classified as dependent elements into three groups, learning algorithms, network designed architecture and activation functions. Therefore, a procedure can follow listed in steps for designing ANNs as illustrated below.

1. Provide an appropriate amount of input data. For high-performance neural networks, plentiful raw data must provided. The size of the input dataset divided into three groups as training, validating and testing dataset.
2. Splitting data. They are many data splitting methods that depending on statistical principles were simple random sampling, trial-and-error methods and convenience

sampling are the most famous data splitting methods. According to the hyperparameter of the developed artificial neural networks, the percentage training, validating and testing dataset area changing taking into account that the high percentage always go to training dataset estimated at 60% to 80% of the initial raw data size. The rest of the well divided into validating and testing dataset.

3. Define networks architecture. According to the purpose of developing the artificial neural networks the number of the hidden layers, a number of neurons and suitable activation function must carefully chosen.

4. Select a learning algorithm. It is important to adopt a learning algorithm for ANNs when developing models. According to given criteria, all the requirements like weights optimized (adjusted). These learning procedures capabilities are the strengths key of high-performance ANNs.

5. Training process. It is a repeatable process stopped when reached acceptable error value.

6. Validation process. It is a fitting process that evaluates the performance of the Training process.

7. Testing process. It is the process used to evaluate the model after training and validation processes are complete.

To ascertain a good performance accuracy of the designed ANN models, several error criteria chosen to test the testing process (Tiwari et al, 2018; Ghorbani et al, 2019) where these criteria are the Coefficient of Determination (R^2), Root Mean Square Error (RMSE), Nash-Sutcliffe coefficient (CE) and Mean Absolute Percentage Error (MAPE). The computations formula of these criteria as follows.

$$RMSE = \sqrt{\frac{\sum_{i=1}^n (X_{actual,i} - X_{predict,i})^2}{n}} \quad (3.17)$$

$$CE = 1 - \frac{\sum_{i=1}^n (X_{actual,i} - X_{predict,i})^2}{\sum_{i=1}^n (X_{actual,i} - \overline{X_{actual}})^2} \quad (3.18)$$

$$MAPE = \frac{1}{n} \sqrt{\sum_{i=1}^n (\text{actual}(i) - \text{predicted}(i)) / \text{actual}(i)} \quad (3.19)$$

The model accuracy can be calculated as.

$$\text{Model Accuracy} = 100 - \text{MAPE} = ? \%$$

Where, X_{actual} is actual values and X_{predict} is predicted values at time/place i .

3.6 Designing ANNs Models

3.6.1 Model description

Identification of suitable models for future weather forecasting in long-term prediction is a significant precondition for effective climate change management. These models have received enormous consideration of researchers in the last few decades and many models for weather forecasting have been designed to improve the climate changes in different study areas (Yahya and Seker 2019). Weather forecasting can be defined as the application that inserts many scientific technologies to predict the atmosphere status for the future time for specific locations (Sheridan 2002) where forecasted weather variables are very important in addressing future environmental and industrial planning. For forecasting local-scale weather variables, the empirical approaches used as weather forecasting methods if data are plentiful.

To forecast weather variables in a very effective way, Artificial Intelligent procedure represented by artificial neural networks (ANNs) can be used, which have the ability to simulate nonlinear input data and generate artificial mechanism to study the pattern of observed data and train it to predict future weather data. The artificial neural network designed in the form of a mathematical model that simulates the nervous system in the human mind to resolve real-world problems that need complex calculations. All artificial neural networks have a specific structure contains layers connected by neurons. These neurons can be defined as important aspects of neural networks where they work as communication lines between the network parts (Kosko 1992). The technology that is used for predicting weather variables model for the study consists of mathematical equations that are related to ANNs that are named RBF, NARX, FCM clarified as follows, and as illustrated in (Figure 3.7) that represent the designed flowchart structure of the developed model steps.

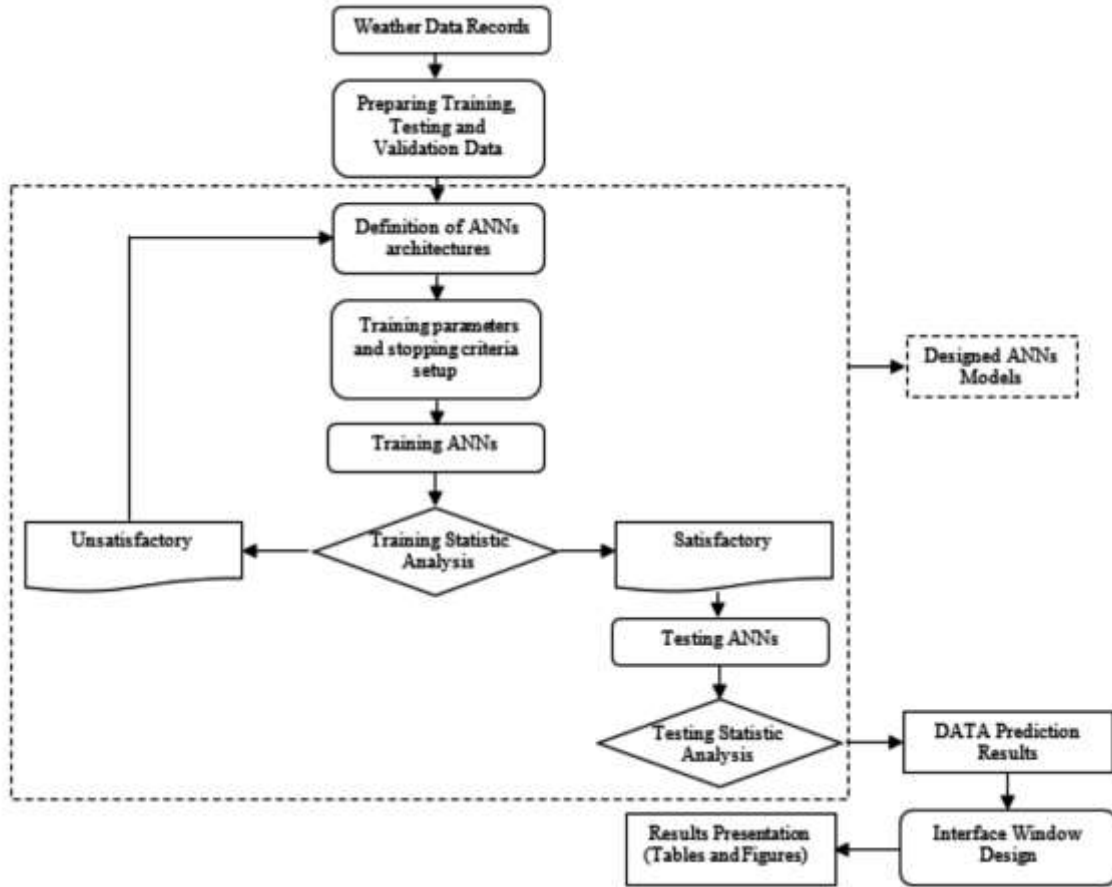


Figure 3.7 : Designed flowchart structure of the developed model.

First, Radial Basis Function RBF can be defined as feed-forward neural network that used as a strong tool offering many advantages in modelling the nonlinear system. The RBF function consists of three layers where the first layer can be described as a not weighted linear layer that transmit input data through the hidden nodes into the next layer. The second layer called hidden layer, maybe there are one or more of this layer in the designed neural network, and it is also a not weighted linear where input data in this layer were processed. To reduce the complexity and capability of the designed neural network the hidden layer must be chosen carefully. Producing the output results depend on the third layer that recognizes as a weighted nonlinear layer. Radial basis functions (RBFs) used as activation function where they are several types of these activation function like Gaussian, Multi-quadric or Inverse Quadratic etc. (Walczak, 2019), in this study Gaussian function was used where it can be mathematically defined as equation 3.20 and equation 3.21 (Wei 2012).

$$\varphi_j = \exp\left(-\frac{\sum_{i=1}^n (x_i - w_{ij})^2}{2\sigma^2}\right)$$

(3.20)

Where,

$x = (x_1, x_2 \dots x_n)$ is the input vector, w_{ij} represent the center vector and σ^2 represent the width parameter.

The production of the output as a weighted sum can represented as shown by equation 3.21.

$$y(t) = \sum_{j=1}^n w_{ij} \cdot \phi_j + w_o \quad (3.21)$$

Where,

Φ_j represent the basis functions set,

w_{ij} the associate weights for every Radial Basis Function (RBF)

w_o is the bias weight of output.

Second, the Nonlinear Autoregressive Network with Exogenous Inputs Neural Network NARX is suitable estimation algorithm that used for modelling and predicting time series in moderately nonlinear dynamic systems (Lin et al. 1996). In this function the input data can be feedback using the output results therefor it can classified as a feed-forward neural network. To deduce the dynamic model of the realized neural network system, the NARX model represented by equation 3.22 as follows.

$$y(k+1) = f_{ANN}(y(k), y(k-1), \dots y(k-n+1), u(k), u(k-1), \dots u(k-m+1)) + k(k) \quad (3.22)$$

Where,

$y(k+1)$ is model predicted output, f_{ANN} is a non-linear function describing the system behavior, $y(k)$, $u(k)$, $k(k)$ are output, input and approximation error vectors at the time instances k , n and m the order of $y(k)$ and $u(k)$ respectively.

Third, Fuzzy C-Means Clustering (FCM) is defined as the unsupervised clustering algorithm based on the fuzzy theory that was submitted for the first time by Bezdek in 1973 (Suganya and Shanthi 2012). FCM can classified under classical fuzzy clustering algorithms that are based on an idea of dividing a single dataset or a time series into several groups that have specific attributes for each group (Fan, 2003). FCM is

employed fuzzy partitioning to find cluster centers by minimizing a dissimilarity function such that a data point can belong to all groups with different membership grades between 0 and 1. To accommodate the FCM design procedure, the following mathematical steps proposed by Bezdek, 1981 (Shahi et al, 2009) can be illustrated below.

Step 1. Randomly initialize the membership matrix (u) that has constraints in equation 3.23.

$$\sum_{i=1}^c u_{ij} = 1, \forall j = 1, \dots, n \quad (3.23)$$

Where,

u_{ij} is a membership matrix that initialized randomly.

Step 2. Define the dissimilarity function which is used in FCM is given equation 3.24 to Compute dissimilarity.

$$J(U, c_1, c_2, \dots, c_c) = \sum_{i=1}^c J_i = \sum_{i=1}^c \sum_{j=1}^n u_{ij}^m d_{ij}^2 \quad (3.24)$$

Where,

u_{ij} is between 0 and 1

c_i is the centroid of cluster i

d_{ij} is the Euclidian distance between ith centroid(c_i) and jth data point

$m \in [1, \infty]$ is a weighting exponent.

Step 3. Calculate centroids (c_i) by using equation 6 that represent a minimum of dissimilarity function.

$$c_i = \frac{\sum_{j=1}^n u_{ij}^m x_j}{\sum_{j=1}^n u_{ij}^m} \quad (3.25)$$

Step 4. Use equation 5 to compute dissimilarity between centroids and data points

Step 5. Compute or update the new partition matrix U using equation 3.26.

$$u_{ij} = \frac{1}{\sum_{k=1}^c \left(\frac{d_{ij}}{d_{kj}} \right)^{2/(m-1)}} \quad (3.26)$$

Ideally, the analysis using ANNs need continues time-series dataset (Zhang and Hu 1998). Furthermore, it is logical to insert the weather data records of all meteorological stations within a selected region when designing a weather forecasting model to ensure obtaining realistic results. The study area contains six meteorological stations (Mosul, Tal Afar, Sinjar, Hadher, Rabiaa and Bashigah stations) as seen in (Figure 3.1).

As a result of the difficult circumstances that faced Iraq in general and Nineveh province in particular as a result of wars when it fell under the control of terrorist organizations during the previous five years which caused some stations to stop working, it was difficult to obtain accurate weather variables records of all stations. To complete this study, five weather variables records (rainfall, temperature, humidity, wind speed and sun shine) belong to Mosul station for the period 1972 to 2017 used as 540 samples for each variable to train and test the designed neural networks models. Those variables arranged in MATLAB workspace. Due to the lack of available data, and to ensure the best results in training, validation and testing process, the volume of data has tripled to become 1620 by simply appending it with itself three times. Out of the 1620 samples, 70 % of samples called the training data that randomly selected by (nntool) for training ANNs. To measure the popularization of the network 15 % of samples called validation data feeds the ANNs as data has not been dealing with or seen before. To get an independent measurement of the ANNs performance in terms of Root Mean Squared Error (RMSE) the rest 15 % dataset (testing set) used to accomplish this stage. In this study, one variable (rainfall) has examined for all designed ANNs approaches where the necessary parameters prepared during experimentation. The same technique followed in designing the rest of the ANNs to suit other variables.

Three different neural network approaches, RBF, NARX and FCM, used to develop different neural network sub-models collected together in one model used for local weather forecasting in the study area. The Neural Network Fitting Tool Box (GUI) available in MATLAB platform used to develop the designed ANNs (Qi and Zhang 2001). Define samples (inputs and outputs), create a network, Define ANN topology, select transfer function and configure network are the first steps that must be done to create the initial model structure as shown in MATLAB script codes as illustrated in (Table 3.7) and as seen in (Figure 3.8). Many trials and error attempts have carried out to set up the fit number of hidden layers and the best number of artificial neurons

to reach optimal performance. RMSE, MAPE and R^2 used as performance criteria. Furthermore, these three used ANN approaches shortly described.

Table 3.7 : MATLAB script codes, for design ANN structure.

```

% create network
net = network( ...
1,      ...      % numInputs, number of inputs,
2,      ...      % numLayers, number of layers
[1; 0], ...      % biasConnect, numLayers-by-1 Boolean vector,
[1; 0], ...      % inputConnect, numLayers-by-numInputs Boolean
                matrix,
[0 0; 1 0], ...  % layerConnect, numLayers-by-numLayers Boolean
                matrix
[0 1]      ...    % outputConnect, 1-by-numLayers Boolean vector);
% view network structure
view(net);
% number of hidden layer neurons
net.layers{1}.size = 5 ;
% hidden layer transfer function
net.layers{1}.transferFcn = 'logsig'
';
view(net) ;
% configure network
net = configure(net,inputs,outputs);
view(net);

```

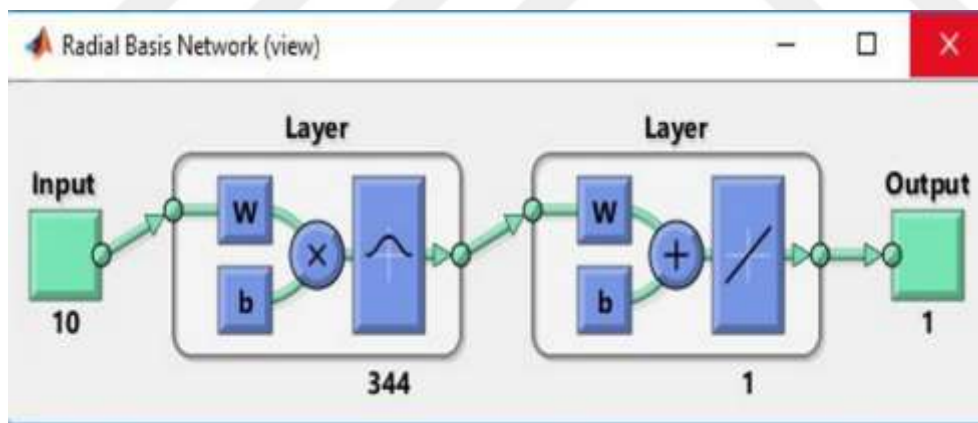


Figure 3.8 : RBFNN design structure.

A Radial Basis Function Neural Network (RBFNN) is a special type of feeding forward neural network that uses RBF as its activation function to control the behaviour of this neural network. RBFNN structure consists of three layers; the first layer is not weighted linear layer that has a role to transmit input data by the neurons into the next layer. The second layer is not weighted nonlinear layer called hidden layer (may be one or more) where in this layer, the hidden neurons process the input

data. The number of neurons in the hidden layer must be chosen carefully because they affect the complexity and capability of the network (Basheer and Hajmeer 2000). The third layer is the output layer, which can be defined as a weighted nonlinear layer that has a role in producing the output results.

The Nonlinear Autoregressive Network with Exogenous Inputs Neural Network (NARXNN) is a powerful procedure for modelling and predicting time series taking into account the complexity and nonlinearity of time series patterns (Diaconescu, 2008). This ANN is classified as a feed-forward neural network where the input can be feedback using the output results. Fuzzy C-Means Clustering (FCM) algorithm defined as the unsupervised technique based on the fuzzy theory that was submitted for the first time by Li, et al, 2008). FCM can be classified under classical fuzzy clustering algorithms that are based on an idea of dividing a single dataset or a time series into several groups that have specific attributes for each group (Fan, et al. 2003).

To gain the best performance model, the model structure designed in four stages. All sub-models work separately in the first stage called training stage then their results were gathered and fed back to working in the second stage also named testing stage where in this stage, the performance accuracy of the all designed sub-models were evaluated. The third stage is the prediction stage, where the data records are processed to estimate the predicted data of five weather variables (rainfall, temperature, humidity, wind speed and sun shine).

The final stage called the presentation stage where an interface window designed to be an easy facility to work on this model without any difficulty or complexity. A designed window shows several options to make it easier for the user to work on this model, where the type of weather variables, method of prediction, data record length and prediction period in years can be chosen. In addition, this window has the ability to show the tested and forecasted results in tables and figures formats as seen in (Figure 3.9).

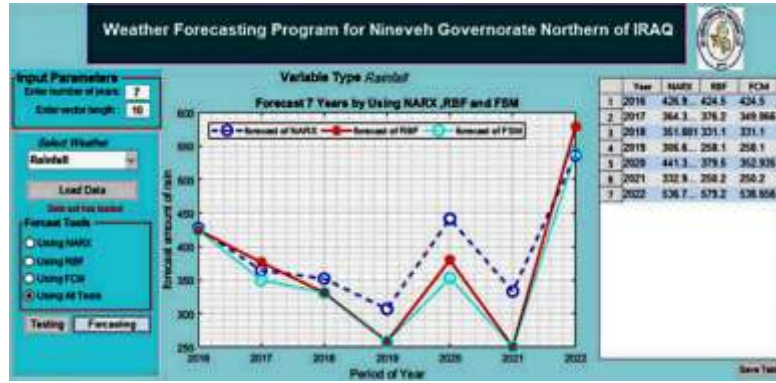


Figure 3.9 : The designed interface window for the develop model.

The designed structure of the developed model illustrated in (Figure 3.7) where this chart represents the steps that carried out to develop the model. Fifteen ANN sub-models designed as three sub-models for each variable where the number of hidden layers and the number of neurons in each sub-model found by experimentation. The designed sub-models of rainfall variable (RBF-R, NARX-R and FCM-R) discussed in details as an example of all designed sub-models for the rest of the variables. To clarify the names of the sub-models, the arrangement of RBF-1 structure is 10-344-1 as example indicates the number of neurons in the input layer as the first number, the second one represents the neurons in one hidden layer and the last number represents the neurons in the output layer. The same format used to define NARX sub-models. Since FCM, sub-models do not contain hidden layers and neurons in their structures, so they will described as shown in (Table 3.8). The designed sub-models described in detail as follows.

Table 3.8 : Architectures design of develop ANNs sub- models.

| Variables | RBF Models | RBF structures | NARX Models | NARX structures | FCM Models |
|-------------|------------|----------------|-------------|-----------------|------------|
| Rainfall | RBF-R | 10-344-1 | NARX-R | 10-32-4-1 | FCM -R |
| Temperature | RBF-T | 10-300-1 | NARX-T | 10-42-4-1 | FCM -T |
| Humidity | RBF-H | 10-266-1 | NARX-H | 10-34-4-1 | FCM -H |
| Wind speed | RBF-W | 10-310-1 | NARX-W | 10-40-6-1 | FCM -W |
| Sun shine | RBF-S | 10-286-1 | NARX-S | 10-38-4-1 | FCM -S |

1- Develop RBF Sub-Model

Five RBFNNs architectures designed for forecasting five weather variables (rainfall, temperature, humidity, wind speed and sun shine). RBF-R discussed in detail as an example of the five sub- models illustrated by the following stages below.

Stage one. The function (newrb) used to create an RBF structure where the hidden nodes were adding until meeting the specified root mean squared error RMSE goal to approximate the function in the training procedure. Three arguments must taken into account to ensure that this function works correctly. Firstly, set up the training process limitation by setting up the minimum RMSE error where in this study, the RMSE set up equal to 0.0000001 and the training process will terminated when reaching this number. Secondly, RBF spread default set up equal to 1.0. Thirdly, to guarantee that the network works satisfactorily without any complexity the fit number of hidden nodes was carefully selected by trial and error strategy where it was found that the most appropriate number of hidden nodes equals to 100 which gave acceptable best performance results as seen in (Figure 3.10). The factors that affect the performance of RBF tested where these factors are the epoch, learning rate and the duration of the iteration time. The faster iteration has achieved in 12 sec and reached the epoch 160.

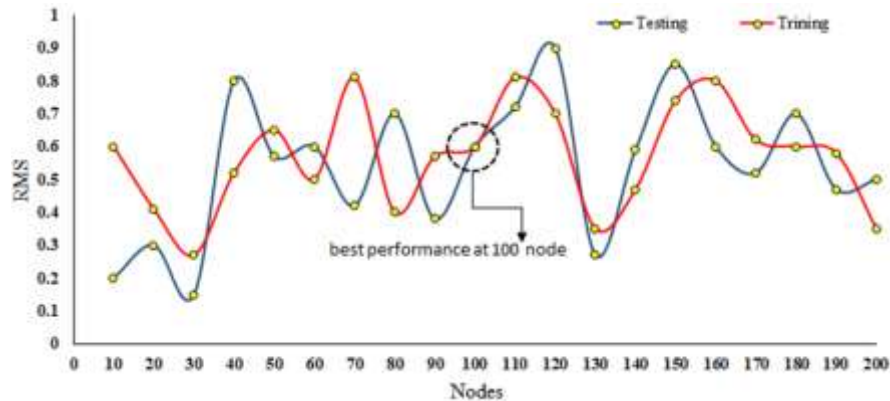


Figure 3.10 : The perfect selected number of hidden nodes.

Stage two. RMSE and R^2 estimated to find prediction accuracy of designed RBF where the best performance training obtained RMSE equal 0.0099 and best R^2 result was 0.998. The relationship between the observed and output dataset obtained as seen in (Figure 3.11).

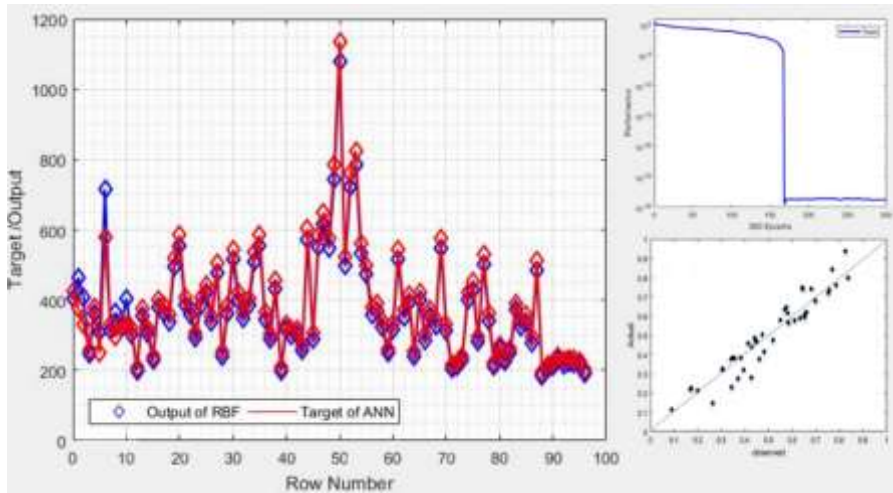


Figure 3.11 : RBF-R sub-model training results.

2- Develop NARX Sub-Model

For designed NARX-R sub-model, ten variables entered as input data with one exogenous input and two feedback delays. The model structured as two hidden layers with 32 and 8 hidden nodes for the first and second layer, respectively. The 1620 dataset was divided into 3 sets using the divide block function where 70% of it that equal 1134 used as training dataset and 30% of the total data used in both validation and testing procedures as 486 dataset. The activation functions *narxnet* and *closeloop* were used to activate sigmoid functions. Levenberg–Marquardt used for training of the network using the *trainlm* function. The performance accuracy of a trained procedure evaluated using RMSE and R^2 . The average R^2 for training, validation and testing datasets was $R^2 = 0.987$ simulated mathematically by function formed as (output = $0.99 \cdot T + 0.31$), and the root mean squared error was RMSE = 0.0032 as given in (Figure 3.12).

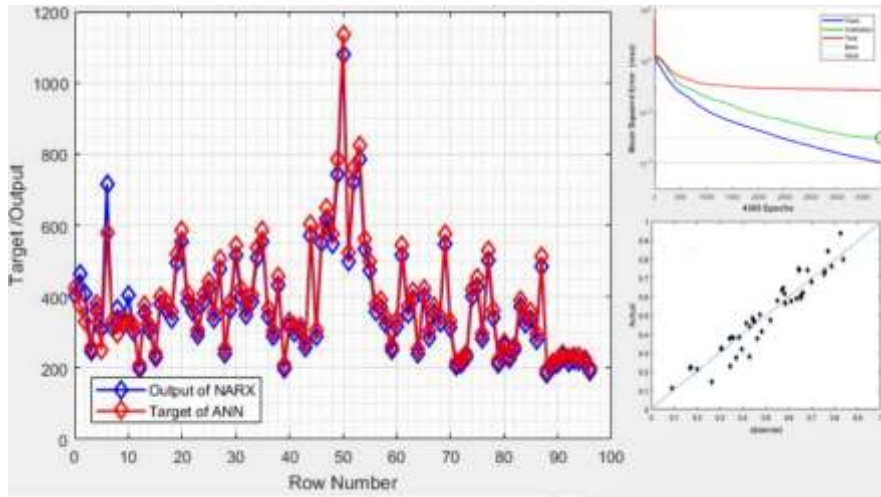


Figure 3.12 : NARX-R sub-model training results.

3- Develop FCM Sub-Model

For designed FCM-R, in the first stage, the real data will read and pre-processed to apply to the prepared fuzzy inference system with input parameters. To design fuzzy inference system structure in MATLAB workspace, *genfis3* function was used (Astakhova, et al. 2015). The input parameters that must interred to generate this function are the input dataset matrix (one-dimensional dataset in this study) and the radii as a vector that specifies a cluster centers range of influence in the input dataset where the radii parameters are tuned equal to 0.06 for subtractive clustering. This automatically generates the number of clusters where three clusters generated. The number of clusters is input to the FCM algorithm as a starting point only. The membership functions will created where the sum of all membership functions must be 1.0. The generated number of membership function rules was 23. The sub-model is trained using hybrid learning algorithm to identify the membership function parameters of single output where the sugeno-type fuzzy inference systems for fuzzyfication process adopted to complete training phase. FCM clustering is an iterative process. The process stops when the maximum number of iterations reached or when the objective function improvement between two consecutive iterations is less than the minimum amount of improvement specified. For this sub-model, the total number of iteration tuned as default equal to 500. The model stopped when it reach 148 iteration with RMSE= 0.019 and $R^2=0.895$ as given in (Figure 3.13).

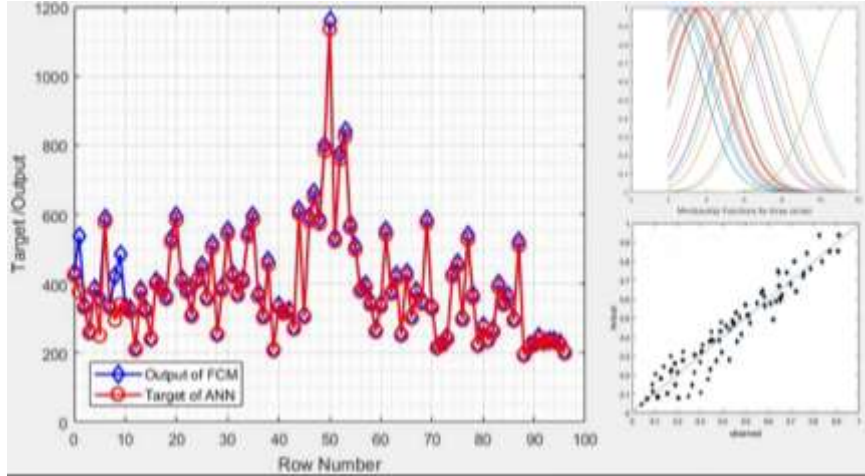


Figure 3.13 : FCM-R sub-model training results.

Training, tasting and prediction errors estimated to ensure the performance accuracy of the developed sub-models as follows.

a. Error analysis in the training stage

During the training process of the RBF, NARX and FCM networks, the obtained average RMSE shows significant values close to 0 and R^2 close to 1.0 as seen in Table 3.9. Comparatively, the training accuracy of RMSE and R^2 for NARX sub-models are best than RMSE and R^2 gained from RBF and FCM that is mean the NARX sub-models gives strong training performance than the RBF and FCM.

Table 3.9 : Training process analysis of designed sub-models.

| Designed sub-models | R^2 | Ave. R^2 | RMSE | Ave. RMSE | Iteration and Epoch |
|---------------------|-------|------------|--------|-----------|-----------------------------------|
| RBF-R | 0.998 | 0.914 | 0.0064 | 0.0041 | 12 seconds, reached the epoch 160 |
| RBF-T | 0.894 | | 0.0028 | | 26 seconds, reached the epoch 240 |
| RBF-H | 0.891 | | 0.0049 | | 16 seconds, reached the epoch 120 |
| RBF-W | 0.876 | | 0.0026 | | 32 seconds, reached the epoch 180 |
| RBF-W | 0.812 | | 0.019 | | 40 seconds, reached the epoch 210 |
| NARX-R | 0.927 | 0.928 | 0.0013 | 0.0019 | 13 seconds, reached the epoch 185 |
| NARX-T | 0.931 | | 0.0016 | | 14 seconds, reached the epoch 195 |
| NARX-H | 0.942 | | 0.0021 | | 16 seconds, reached the epoch 210 |
| NARX-W | 0.914 | | 0.0025 | | 15 seconds, reached the epoch 185 |
| NARX-S | 0.901 | | 0.003 | | 22 seconds, reached the epoch 230 |
| FCM -R | 0.894 | 0.864 | 0.0078 | 0.0077 | 50 seconds, reached the epoch 250 |
| FCM -T | 0.891 | | 0.0082 | | 55 seconds, reached the epoch 270 |
| FCM -H | 0.852 | | 0.0080 | | 58 seconds, reached the epoch 300 |
| FCM -W | 0.821 | | 0.0068 | | 59 seconds, reached the epoch 310 |
| FCM -S | 0.782 | | 0.0091 | | 61 seconds, reached the epoch 420 |

b. Error analysis in the tasting stage

Based on Table 3.10, the designed ANN sub-models show performance accuracy range fluctuated as 67.9% to 84.2% represented by performance Criteria. Comparatively, the average accuracy of NARX sub-models are higher than the average accuracy of the other designed sub-models.

Table 3.10 : Testing process analysis of designed sub-models.

| Designed sub-models | Performance Criteria | | | | | |
|---------------------|----------------------|-------|-----------|-------|----------|---------------|
| | R ² | RMSE | CE | MAPE | Accuracy | Ave. Accuracy |
| RBF-R | 0.861 | 0.812 | 0.74 fair | 18.6% | 81.4% | 79.35% |
| RBF-T | 0.854 | 0.751 | 0.72 fair | 19.7% | 80.3% | |
| RBF-H | 0.825 | 0.624 | 0.78 good | 22.8% | 77.2% | |
| RBF-W | 0.795 | 0.698 | 0.76 good | 21.5% | 78.5% | |
| RBF-S | 0.791 | 0.618 | 0.75 good | 21.1% | 77.2% | |
| NARX-R | 0.905 | 0.721 | 0.83 good | 15.2% | 84.8% | 83.75% |
| NARX-T | 0.941 | 0.742 | 0.82 good | 15.8% | 84.2% | |
| NARX-H | 0.923 | 0.715 | 0.80 good | 16.1% | 83.9% | |
| NARX-w | 0.939 | 0.736 | 0.79 good | 17.9% | 82.1% | |
| NARX-S | 0.934 | 0.718 | 0.76 good | 18.1 | 79.1% | |
| FCM -R | 0.911 | 0.785 | 0.82 good | 19.8% | 80.2% | 78.10% |
| FCM -T | 0.925 | 0.810 | 0.81 good | 16.2% | 83.8% | |
| FCM -H | 0.934 | 0.734 | 0.83 good | 19.5% | 80.5% | |
| FCM -w | 0.742 | 0.654 | 0.72 fair | 32.1% | 67.9% | |
| FCM -S | 0.722 | 0.634 | 0.7 fair | 31.5% | 63.4% | |

c. Prediction error analysis

After analysis the training and testing error criteria of the designed sub-models and after making sure that it works in an acceptable manner these sub-models are gathered in one model where has been run to predict weather variables after feeding the model with the available weather variables time series. It observed that the sub-models start to collapse and their results are irrational in different predicted years as seen in (Table 3.11). In order to unify the highest predicted time for all the sub-models, the year 2050 chosen as the highest year that the model could predict logical results.

Table 3.11 : Predicted period with irrational results after collapsing stage.

| Designed Sub-models | Predicted Period | Predicting logical data at 2040 | Collapsing after the year | Predicting irrational data after collapsing |
|---------------------|------------------|---------------------------------|---------------------------|---|
| RBF-R | 2017-2050 | 424.5 | After 2051 | 2156.5 |
| RBF-T | 2017-2050 | 27.6 | After 2052 | 11.2 |
| RBF-H | 2017-2050 | 52.65 | After 2051 | 8.5 |
| RBF-w | 2017-2050 | 1.7 | After 2052 | 0.1 |
| RBF-S | 2017-2050 | 8.9 | After 2050 | 115 |
| NARX-R | 2017-2050 | 426.9 | After 2050 | 841.99 |
| NARX-T | 2017-2050 | 28.18 | After 2050 | 45.2 |
| NARX-H | 2017-2050 | 51.36 | After 2050 | 1000.1 |
| NARX-w | 2017-2050 | 1.6 | After 2050 | 5.6 |
| NARX-S | 2017-2050 | 8.2 | After 2050 | 115 |
| FCM -R | 2017-2050 | 424.5 | After 2050 | 1008 |
| FCM -T | 2017-2050 | 27.74 | After 2050 | 33.7 |
| FCM -H | 2017-2050 | 53.47 | After 2050 | 400.7 |
| FCM -w | 2017-2050 | 1.7 | After 2050 | 0.2 |
| FCM -S | 2017-2050 | 5.8 | After 2050 | 220 |

3.7 Fuzzy Logic

The Fuzzy Logic is designed to simulate the human nature thinking about an issue, which the answer is not necessarily to be yes or no (classical logic), the answer may be going to another stage like vague, uncertain, and indecisive (Kosko, 1992). To get a perfect understanding of the Fuzzy Logic as a tool used to modelling different aspect of humankind activities, two characteristics might mentioned. First, in any activity, the degrees of relationship can be modelling. Second, it is easy for the planner person to find close links to cope with reality when using Fuzzy Logic model. The principles of Fuzzy Logic depends generally on the “trial and error” task according to many studies in this field. Where the chosen fuzzy set and linguistic values are the keys for the best model that give results with a high degree of credibility close to reality (Zadeh, 1973; Wang, and Vachtsevanos, 1992; Hong, and Lee, 1996).

Many kinds of research and practices indicate that Fuzzy Logic is an effective procedure in solving problems have unique tasks to which traditional methods are powerless. In the field of engineering, Fuzzy Logic has a special fingerprint in many engineering application where it can process many engineering problems like (control, modelling, estimation, identification, classification and prediction). The paragraphs below describe the application of Fuzzy Logic in hydrologic or environmental

engineering throughout building a Fuzzy Logic system for drought prediction in the study area. The Fuzzy Logic theory and concepts must defined positively and Fuzzy Logic control system categories must stated in details.

3.7.1 Fuzzy logic theory basics and concepts

Fuzzy Logic based on fuzzy set theory in which a particular variable or element has a degree of membership in a given set which may be anywhere in the range of truth. This is different from a conventional set theory based on Classic Logic in which a particular object or variable is either true or false but never is in between or both. An expert system involves the human experience about many processes like data analysis, prediction, and classification using the suitable data sets together with an inference engine for evaluating the rules base for a given problem (Siler and Buckley 2005). In simpler words, the Fuzzy Logic system deals with a large number of inputs belong to the scientific issue that will simulated. The inputs will processed according to human knowledge and experience using simple rules (covering all the scenario of reality) in simple language words. Then these rules converted to single output decision represents a close value to the reality of the problem to simulate as seen in (Figure 3.14).

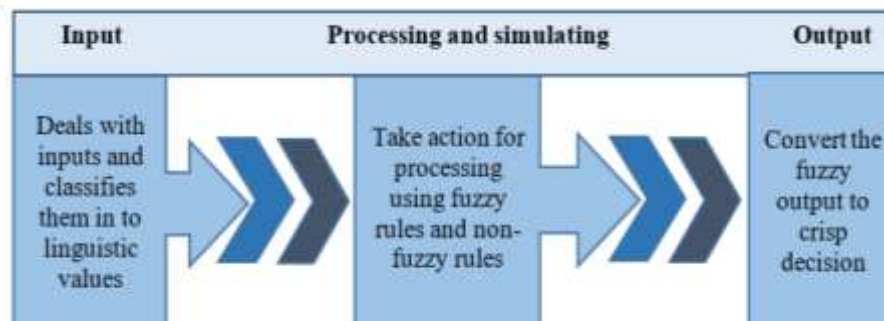


Figure 3.14 : The fuzzy logic theory.

Many tasks can accomplished by using fuzzy controller system monitoring, classification controlling, diagnosing, prediction, querying, and optimizing. The basic components of a Fuzzy Logic Control system FLC can divided into four categories as seen in (Figure 3.15).

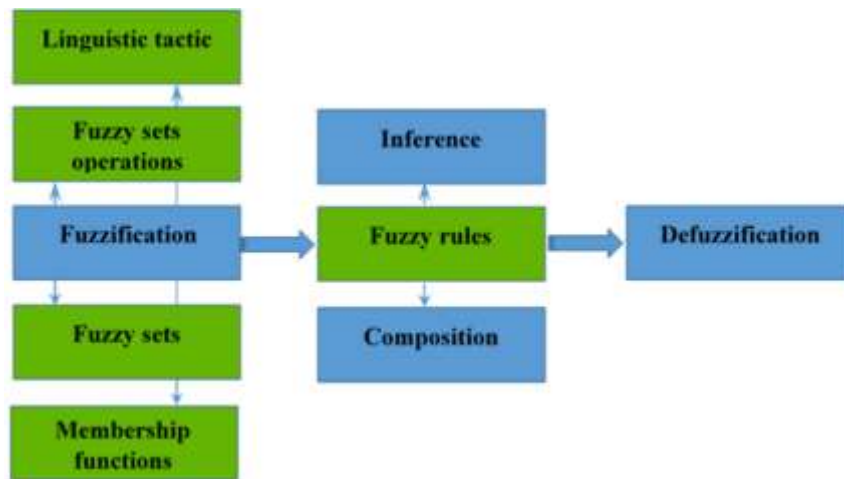


Figure 3.15 : Fuzzy Logic Control system FLC categories.

Fuzzification is the first step in the fuzzy inferencing process. In this step crisp inputs that measured by a traditional method (such as temperature, pressure, rain, etc.) are transformed into fuzzy inputs. The fuzzy inputs in this step classified into linguistic values according to an expert decision. In this step, Membership Functions set out and fuzzy operations are used. Then the results of this step passed into the second step to finish the modelling using Fuzzy Logic approach. To ensure success of fuzzification process the following requirements must met.

It is known that the human mind can analyze, infer, and classify dependence on completely or partially information. In this sense, Zadeh, 1965 tried to find a somewhat similar way of human thinking by finding logical forms to simplify the input date in the fuzzy controller system process. In engineering problems, variables used to define or describe the problems as input data sets to estimate or produced the output data sets are a result of that problem. In Fuzzy Logic, the input data sets decomposed into one or more fuzzy sets, with each set describing variable's values in a wide-ranging character. As an example, the concept of precipitation records can modelled around a variable rainfall. The value of this variable can be Convictional rainfall, Cyclonic rainfall or Orographic rainfall. This range of values may decomposed into a number of sections –very low rain, low rain, moderately rain or heavy rain – each of them representing a fuzzy set associated with the variable rainfall.

Fuzzy sets are mapped in the form of wide range expansion of (membership values) using theoretical functions. The example above shows that a fuzzy set is a set without sharp values (crisp), that is mean there is a kind of membership connection between

the fuzzy set elements. Fuzzy set is different from the classical crisp set because members of a crisp set must have full membership in that set. Mathematically, the difference between the classic sets (crisp sets) and the fuzzy sets can explained by.

In classic sets theory concepts we can assuming universal set X such that A is a crisp subset of X (sharp edge value). Then the function can be define as below.

$v : X \rightarrow \{0,1\}$ Such that $v(x)$ is 1 if $x \in A$ and $v(x)$ is 0 when $x \notin A$ this function describe the classical set or crisp set that every variable has only one predefined confirmed value.

Where in fuzzy sets theory concepts the function that established to describe the fuzzy theory contains all ranges of possible values in the unit interval. This known as the membership function.

For a given crisp set A , this function assigns a value μ_F to every $x \in A$ such that

$$\mu_F(x) = \begin{cases} 1, & \text{if and only if } x \in A \\ 0, & \text{if and only if } x \notin A \end{cases} \quad (3.27)$$

Thus, the function maps elements of the universal set to the set containing 0 and 1. This can indicated by.

$$\mu_F = X \text{ where } X \in F$$

Where the membership function denoted by μ_F for the fuzzy set theory. The range between 0 and 1 is referred to the membership grade or degree of membership (Klir, and Yuan 1995).

A fuzzy set P defined below as.

$$P = \{(x, \mu_F(x)) \mid x \in P, \mu_F(x) \in [0,1]\} \quad (3.28)$$

Where $\mu_F(x)$ is a Membership Function MF or degree of truth belonging to the interval $[0, 1]$ as illustrated in (Figure 3.16). Membership Function MF can defined as a curve that each point in the input space is represented to a membership value (or degree of membership) between 0 and 1.

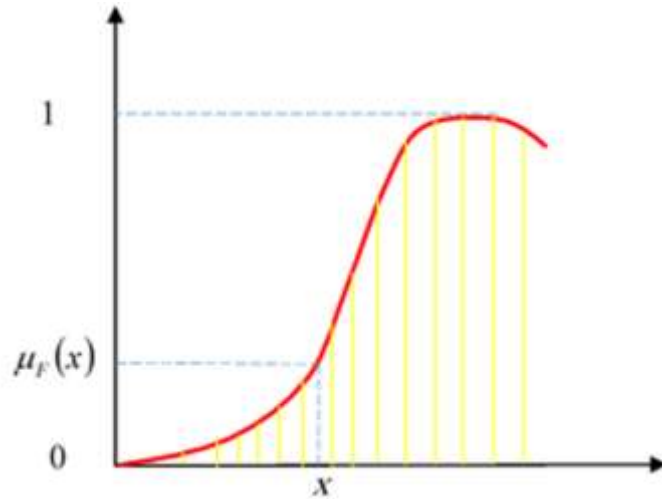


Figure 3.16 : A membership function definition.

The Membership Functions mathematically represented by functions with special characteristics and shapes. Membership Functions can be symmetrical or asymmetrical with one-dimensional or multidimensional universes. The favourite functions that widely used in the modelling of the logic system are triangular, trapezoidal, s-shaped, and Gauss function. The shape of each function has classified into three parts as seen in (Figure 3.17).

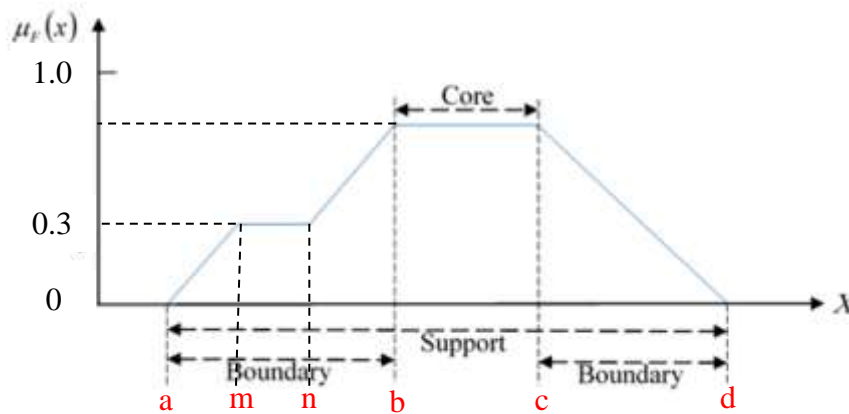


Figure 3.17 : A membership function parts (modified after Ross, 2005).

The first part called (core) and it represents the part of the selected function that elements have full membership for a given set. The second part called (support) and it represents the part of the selected function region that elements have nonzero membership for a given set. The third part called (boundary) and it represents the part of the selected function region that containing elements have nonzero membership and

not complete membership for a given set. The fuzzy set can be presented graphically using the MFs where the x-axis represents the universe of discourse, whereas the y-axis represents the degrees of membership in the [0, 1]. The best way to define an MF is to express it mathematically and specify its parameters clearly. As shown in an example submitted by (Ross 1993), the MFs consisting of a mixture of triangular and trapezoidal function and these functions can be defined mathematically by four parameters {a, b, c and d} as illustrated by equation 3.29 interval as seen in (Figure 3.17).

$$MF(x; a, b, c, d) = \begin{cases} 0 & x \leq a \\ \frac{x-a}{m-a} & a < x \leq m \\ 0.3 & m \leq x \leq n \\ \frac{x-n}{b-n} & n \leq x \leq b \\ 0.8 & b \leq x \leq c \\ \frac{d-x}{d-c} & c \leq x \leq d \end{cases} \quad (3.29)$$

Moreover, by using min and max rules, the alternative expression for equation 3.27 can be state as seen in equation 3.30 and used in the Fuzzy Logic approach as.

$$MF(x; a, b, c) = \max\left(\min\left(\frac{x-a}{b-a}, \frac{c-x}{c-b}, 0.3, \frac{x-n}{b-n}, 0.8, \frac{d-x}{d-c}\right), 0\right) \quad (3.30)$$

The Linguistic tactic is original idea invented by Zadeh it includes two interrelated approaches, the linguistic variables and the linguistic values that can defined as a measurable data set, stated in objectively or subjectively manner, like rainfall, temperature, or wind speed etc. In other words, linguistic variables are variables that give a true and logical description of a set of elements representing a given situation. The linguistic values represent the domain of the related linguistic variables as example the domain of rainfall can classified in many linguistic values (low rain, moderate rain and high rain as example) as seen in (Figure 3.18).

The most theoretic operations that used in Fuzzy logic unions, intersection and complement. Considering we have two fuzzy sets A and B then these operations represented as following in (Figure 3.19).

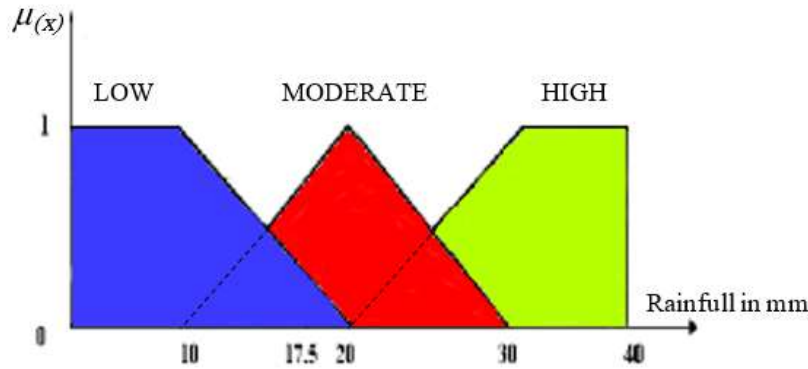


Figure 3.18 : Membership functions for linguistic variable (rainfall).

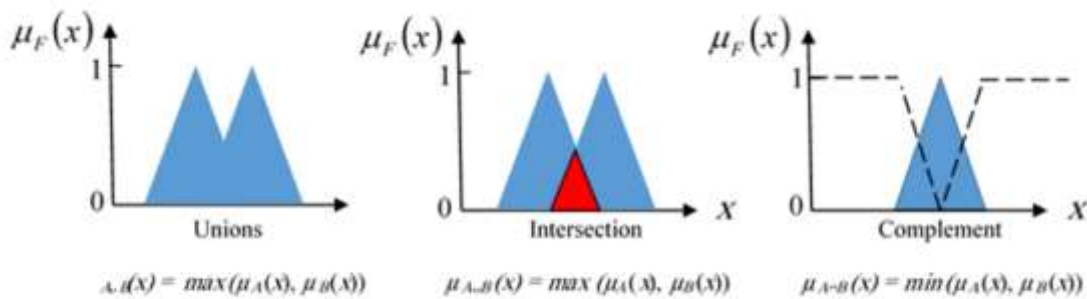


Figure 3.19 : Fuzzy sets operations

Depending on the linguistic values, fuzzy rules designed to cover all possible scenarios for the problem under study. The if-then rules implemented to achieve the goal where the true value of each computed fuzzy rule. Fuzzy rule or (decision matrix) as seen in (Table 3.12). Mimic human beings thoughts when the decisions made. It classified as one type of Artificial Intelligent. Fuzzy rule operated by using most common statement a series of IF “predicate” - THEN “conclusion” and it contains properties of fuzzy sets operations. When the fuzzy rules are set up according to the expert experience these rules will become the core or the knowledge base that used to solve the problem under the study. In some times not all the expert knowledge that translated to rules are useful sometimes, some of the rules can be redundant.

Table 3.12 : A decision matrix representation.

| | | Output (y) | | |
|-----------|----------|------------|----------|----------|
| | | Low | Moderate | High |
| Input (x) | Low | Low | Low | Moderate |
| | Moderate | Low | Moderate | High |
| | High | Moderate | Moderate | High |

In this study, Fuzzy rules expressed mathematically in the way proposed by (Li et al, 2002). Rules usually written in the form.

IF x_1 is L , x_2 is T , ..., x_n is S , Then output of y is A

Where,

x is linguistic variables (input data or control variable).

L , S and T are fuzzy sets.

y is linguistic variables (output solution).

The relationships between input and output variables in a fuzzy system can expressed in following equation.

$$y = \sum_{p=1}^P \mu_p(x_1, x_2, \dots, x_n) \bullet A_p(x_1, x_2, \dots, x_n) \quad (3.31)$$

Where, the fuzzy rules are always written in the following form [*if* (input 1 is membership function 1) *and/or* (input 2 is membership function 2) *and/or...then* (the output is output membership function). For example on the fuzzy rules that used in this study where the characters of six variable give one output variable (extremely dry) based on (IF-THEN) rule and (AND) operator as.

IF (high wind speed) and (high temp.) and (very low rainfall) and (high evaporation)
THEN (drought is extremely dry).

Composition refers to the organization and combination of fuzzy set output. Max, Min, OR (probabilistic) and Sum (simply the sum of each rule's output set) operators are

used in this process. All these aggregation operations have been placed together to show how the output of each rule is combined (Klir and Folger 1988; Wang 1997). Mathematically these operators can be stated as.

$$\mu_{A \wedge B}(x) = \min(\mu_A(x), \mu_B(x)) \quad (3.32)$$

$$\mu_{A \vee B}(x) = \max(\mu_A(x), \mu_B(x)) \quad (3.33)$$

A fuzzy subsystem $\mu(y)$ with x as inputs and one output y can be decomposed into n fuzzy subsystems. Membership functions of y are the results of multiplying those of fuzzy subsystems as in equation 3.34.

$$\mu(y) = \sup [\mu_A(x) * \mu_B(x,y)] \quad (3.34)$$

This process achieves the following objectives.

1. Select the suitable membership function to evaluate degree of membership of inputs and estimating the min value for each rule.
2. Inference, which rules, are effective for inputs.
3. Gather the rules in groups according to what the output they calculate.
4. Determine mathematically the max value of each groups in step 3, using the min values that calculated in step 1.
5. Consider the output answer that having maximum value.

Defuzzification process represents the final step of the fuzzy inference system. In this process, the fuzzy output set that is obtained from the composition process will be converted to a scalar value. A defuzzification process is needed to translate the output fuzzy set into real numbers that are used to define the problem in reality. Seven methods are used to get the scalar value of the fuzzy output. These methods are Max-membership principle, Centroid method, Weighted average method, Mean-max membership, Center of Gravity method, Center of the largest area and First of maxima or last of maxima (Murshid et al, 2011). The famous one that is used in the study is the Center of Gravity method. To find the centre of gravity of (Figure 3.20) that represents a logical union of the three fuzzy sets where equation 3.35 was used to solve this problem as below.

Assume, x is the x -coordinate of center of gravity

$\int \mu_c(x) dx$ denotes the area of the region bounded by the curve μ_c .

If μ_c defined with a discrete membership function, then COG can stated as equation 3.35.

$$X^o = \frac{\sum_{i=1}^n x_i \cdot \mu_c(x_i)}{\sum_{i=1}^n \mu_c(x_i)} \quad (3.35)$$

Where, x_i is a sample element and n represents the number of samples in fuzzy set c .

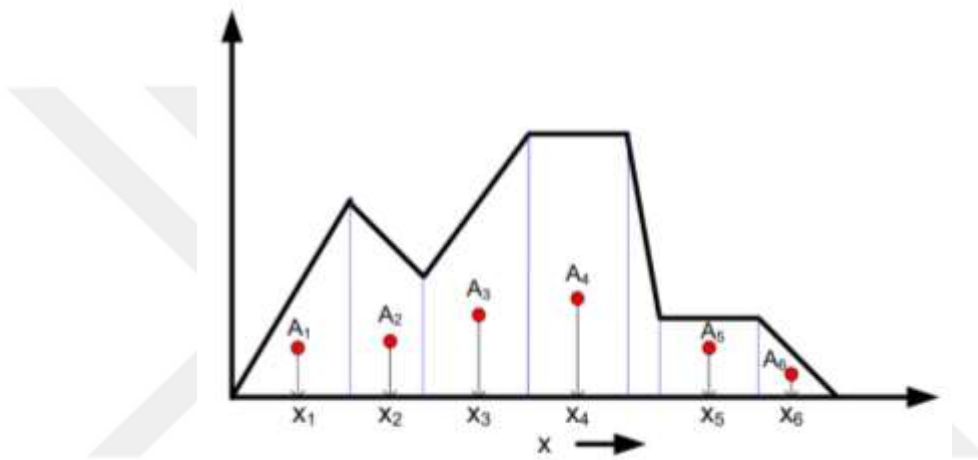


Figure 3.20 : Center gravity method (modified after Ross, 2005).

The steps for solving COG can illustrated, as the entire region must divide into a number of small regular regions (e.g. triangles, trapizoid etc.).

As seen in (Figure 3.20) Let $A_i = 1 \dots n$ denotes the area (regular regions) and x_i denotes the center of these area then the center of gravity X^o of the i -th regular regions can be found by applying equation 3.35.

The fuzzy inference system can defined as the method that used to found the fuzzy output. There is a two kind of fuzzy inference methods (direct and indirect) the most popular methods is the direct method like Mamdani, Takagia and Surgeon's methods Mamdani, et al, 1975. The Mamdani method adopted in this study for building the fuzzy controller system as seen in Figure 3.21. It is an intuitive theory based on fuzzy set theory that has wide acceptance in the Fuzzy Logic scientific field proved to suitable for building control system and decision processes for solving most applications problems. Based on Zadeh's 1973 research in the field of Fuzzy Logic for

complex controller systems, Mamdani 1975 formulated this method, which known by his name as an attempt to control a steam engine and boiler combination that was a pioneering step for using fuzzy logic in engineering applications.

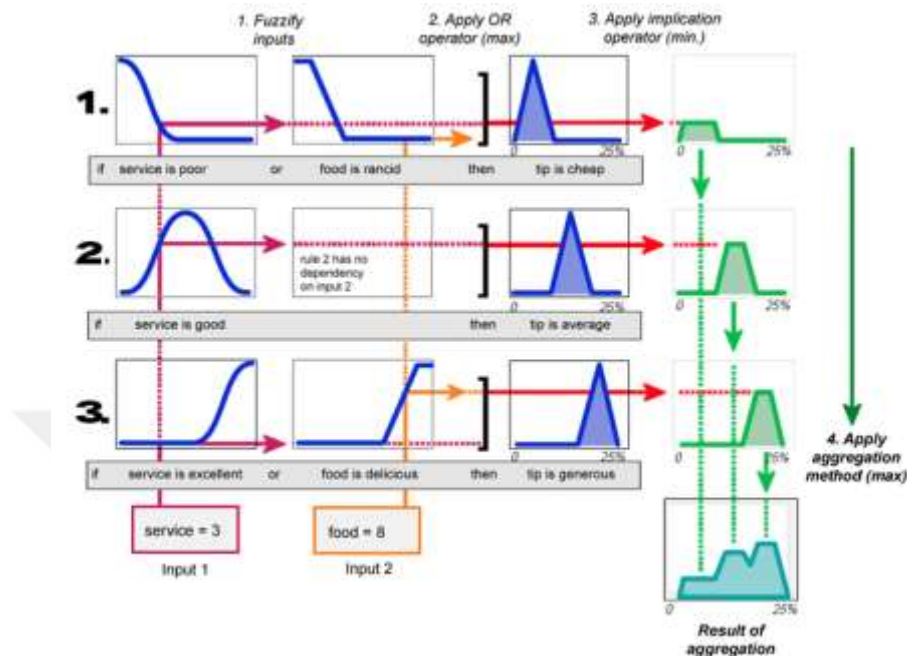


Figure 3.21 : Mamdani method inference example (Url-4).

This method can be defined as a simple structure based on min-max operations to convert the fuzzy set for each output variable to a concept number representing reality. Mamdani method used in this work as one of fuzzy control system methodology that translates the fuzzy set theory based on human experiences. To ensure that this method works correctly six steps have to follow as.

1. Determining a set of fuzzy rules.
2. Fuzzifying the inputs using the input membership functions.
3. Combining the fuzzified inputs according to the fuzzy rules to establish a rule strength.
4. Finding the consequence of the rule by combining the rule strength and the output membership function.
5. Combining the consequences to get an output distribution.
6. Defuzzifying the output distribution.

3.7.2 Adaptive neuro fuzzy inference system (ANFIS)

The Adaptive Neuro-Fuzzy Inference System (ANFIS) is a combination of Fuzzy Logic and Artificial Neural Networks developed to facilitate learning and adaptation (Jang, 1993). ANFIS is a graphical network representation of Sugeno-type fuzzy systems connected with the neural learning capabilities. For achieving the desired performance, ANFIS can modify its membership functions and tuning them through it is flexible design structure (Xue and Xiao 2019). Multi-layer perceptron (MLP) network as known, as a supervised network is the most common network that can connected with fuzzy systems. This network is comprised of nodes with specific functions collected in layers. ANFIS can construct a network realization of IF / THEN rules that has expressed by (Jang, 1993) that represented mathematically in equation 3.36 and equation 3.37 and as seen in (Figure 3.22).

$$\text{If } x \text{ is } A_1 \text{ and } y \text{ is } B_1, \text{ then } f_1 = p_1x + q_1y + r_1 \quad (3.36)$$

$$\text{If } x \text{ is } A_2 \text{ and } y \text{ is } B_2, \text{ then } f_2 = p_2x + q_2y + r_2 \quad (3.37)$$

Where,

A_1 ; A_2 and B_1 ; B_2 are the member functions (MFs) for inputs x and y , respectively, and p_1 ; q_1 ; r_1 and p_2 ; q_2 ; r_2 are the parameters of the output function.

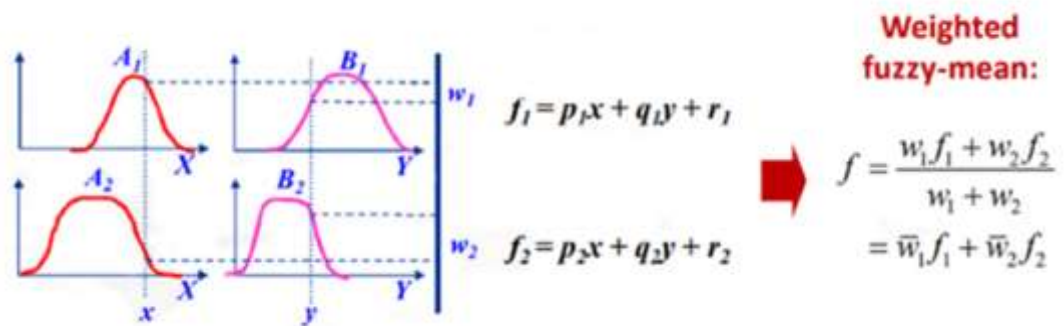


Figure 3.22 : The basic mathematics of ANFIS model (modified after Jang, 1993).

The corresponding equivalent ANSIS structure can be presented in a diagram form that contains five main layers as shown in (Figure 3.23) that works together as one system as illustrated below.

Layer 1. It is a fuzzy layer where this layer has (n) nodes which (n) is the number of inputs datasets to the system. Every node i in this layer is an adaptive node.

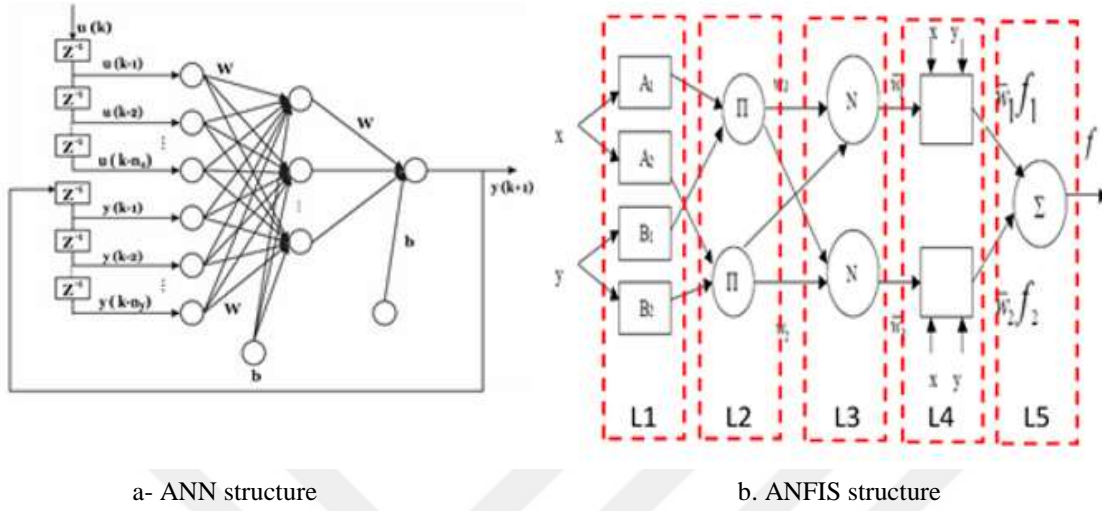


Figure 3.23 : A typical architectures of ANFS model (modified after Jang 1993).

These inputs data will processed according to human knowledge and experience using simple rules covering all the scenarios of reality as shown in mathematical equations, equation 3.38 and equation 3.39.

$$F_i^n = \mu_{A_i}(x) \quad \text{for } i=1, 2, \dots, n \quad (3.38)$$

$$F_i^n = \mu_{B_i}(y) \quad \text{for } i=1, 2, \dots, n \quad (3.39)$$

Where, x (or y) is the input to the node; A_i (or B_i) is a fuzzy set (a linguistic terms, such as low or high) associated with this node, characterized by the shape of the MFs in this node.

Layer 2. In this layer, the weights have checked in each membership function. This layer deals with the incoming signals (x) from the first layer and evaluate the rules results by multiplies incoming signals and sending the product output. The output in this layer can represented using equation 3.40.

$$F_i^n = \mu_{A_i}(x), \mu_{B_i}(x) \quad \text{for } i=1, 2, \dots, n \quad (3.40)$$

Layer 3. The nodes calculate the ratios of the rule's firing strength to the sum of all the rules firing strength. The result is a normalized firing strength. The output of this layer can expressed as equation 3.41.

$$F_i^n = w_i = \frac{w_i}{\sum w_i} \quad \text{for } i=1, 2, \dots, n \quad (3.41)$$

Layer 4. This layer is the feed-forward artificial neural layer, in this layer, the weights will determine by the backpropagation algorithm during the data training process. The results of this layer have minimized the error between the real and the expected values.

Layer 5. In layer five, the single node is a fixed node indicating the overall output as the summation of all incoming signals.

ANFIS can be trained using the hybrid learning algorithm that developed by (Jang et al, 1997) where this algorithm has two faces the first one is “forward pass face” that depend on the least squares method to optimize the consequent parameters, while, the second face is “backward pass face” used to adjust the premise parameters based on backpropagation (BP) algorithm. MATLAB platforms provide training routine for training ANFIS based on hybrid learning algorithm method. In forward pass face, the output values from the ANFIS model estimated while the output error can be estimated used backward pass face. This procedure repeated until reached the predefined error.

3.8 Development Neuro-Fuzzy Inference System (ANFIS)

3.8.1 Model description

Neuro-Fuzzy Inference System model represented by Fuzzy Logic model and Artificial Neural Network consisting of Nonlinear Autoregressive Network with Exogenous inputs (NARX) was developed to predict SPI depending on predicting weather variable records for six meteorological stations as seen in (Figure 3.24) that illustrate the flow chart of developed ANFIS.

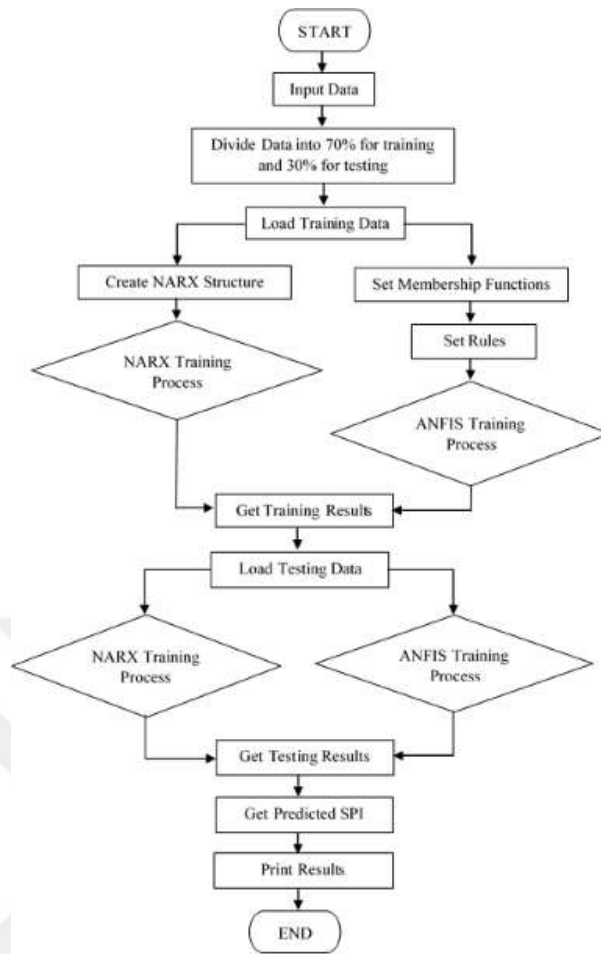


Figure 3.24 : Designed flowchart structure of the developed ANFIS.

The adopted meteorological records contained six weather variables (wind speed, temperature, rainfall, sunshine, humidity and evaporation) were used to developed ANFIS model. For adopting these variables as linguistic variables, it was essential to analyze them to find their relationships with the actual SPI by finding the correlation coefficient R^2 among these variables and actual SPI. This analysis showed two of these variables (sunshine and humidity) had a weak correlation coefficient compared to other variables, so they were excluded from the list of linguistic variables as input dataset and adopting the other four variables (wind speed, temperature, rainfall, and evaporation) as input dataset that they show good relationship with actual SPI as seen in (Figure 3.25).

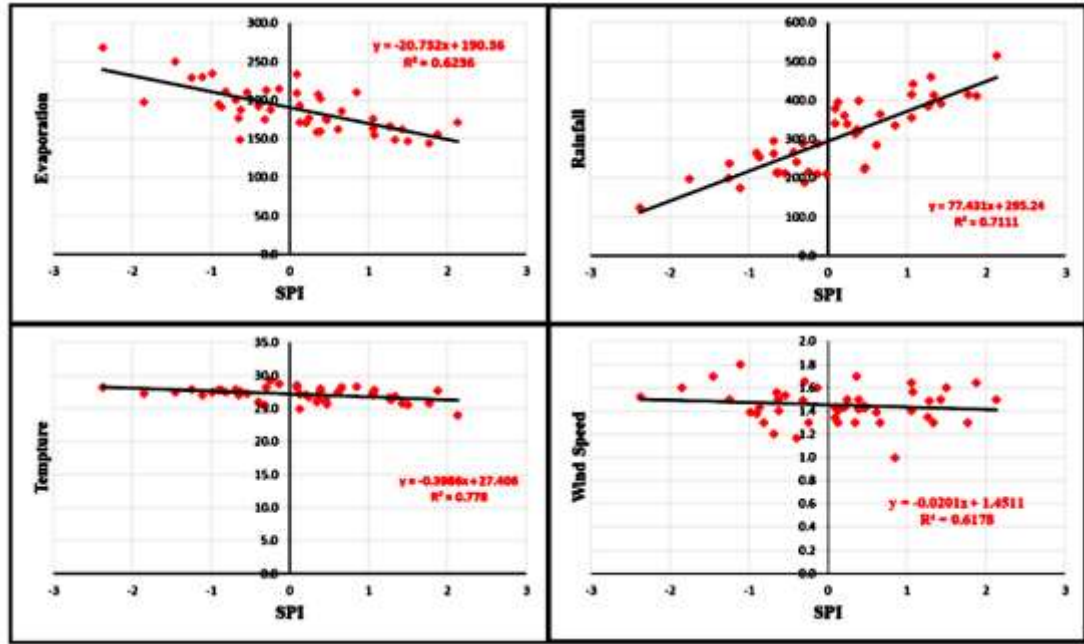


Figure 3.25 : Correlation relationship between the input variables and actual SPI.

The first step in developing a fuzzy model is defining the linguistic variables with a membership function (fuzzification phase). The advantages of the linguistic variables are to describe the fuzzy sets qualitatively and quantitatively to make them useful and give understandable meanings to experts and for computer processors to get accurate output values. The inputs dataset according to fuzzy sets for wind speed, temperature and evaporation variables classified as low, moderate and high while rainfall categorized as very low, low, semi-moderate, moderate, high and very high. Membership Functions (MFs) defined for each input and output variable. These functions must designed to verify the main condition where the designed MFs must overlap with the closest MF. As suggested by various experts, the overlap of fuzzy regions should average somewhere between 25% and 50% of the fuzzy set base (Yen and Langari 1998). For the input dataset (wind speed, temperature, rainfall, and evaporation), normal trapezoidal membership function and special trapezoidal (R-functions and L-functions) membership functions chosen to map these inputs as shown in (Figure 3.26).

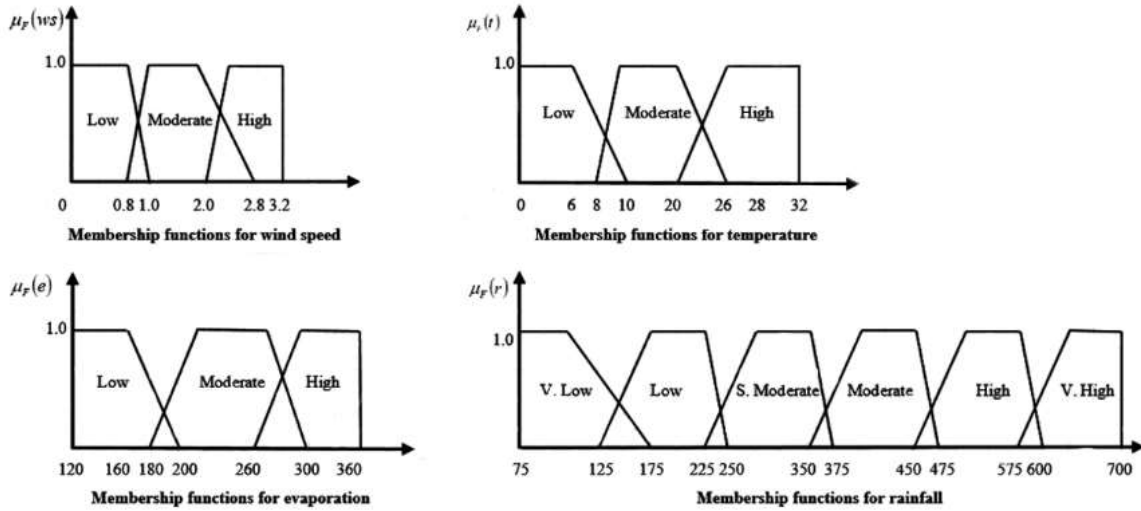


Figure 3.26 : Designed membership functions for inputs dataset.

Drought MFs are the output of the developed fuzzy model. The drought divided into seven fuzzy sets similar to the SPI categories described by McKee et al. 1993 as extremely wet, very wet, moderately wet, near normal, moderately dry, severely dry, and extremely dry. Three types of MFs selected. First, R and L shape type trapezoidal functions used for extremely dry and extremely wet categories. Second, the normal trapezoidal function used for near normal, severely dry, moderately dry, moderately wet and very wet as shown in (Figure 3.27).

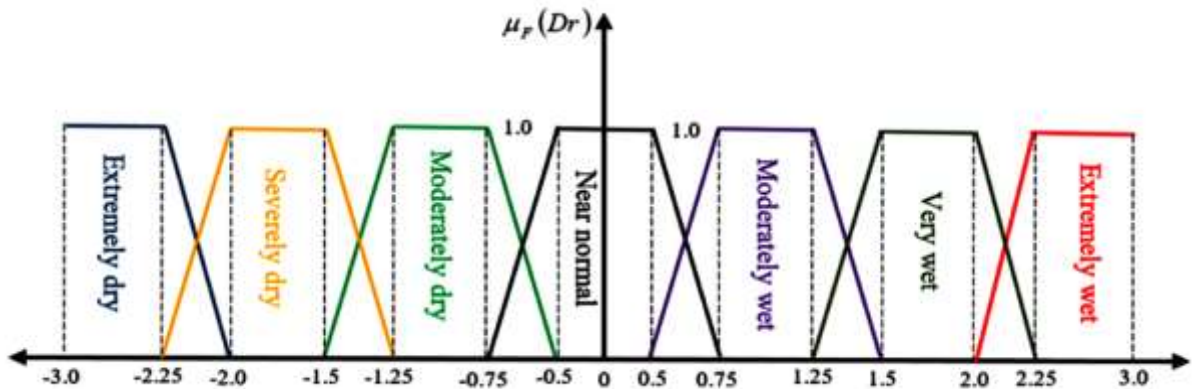


Figure 3.27 : Designed membership functions for drought.

To calculate the degree of matching between inputs and fuzzy rules derived from experience, fuzzy logic operators were used to accomplishing this phase. The main operator (AND) was used to build the fuzzy rules of the system. AND operator is a conjunction tool used to combine rules that have multiple conditions therefore (*min*)

the fuzzy operator takes all the minimum degrees of the membership taking into account all the conditions.

For example, if input data represented an input fuzzy set classified as minimum inputs. wind speed=0.6, temperature=8, evaporation=165 and rain=125 are fuzzy *min* operator that applied to those inputs, the result will be 1, 0.65, 0.8, and 0.5, respectively where the smaller value (0.5) is taken as the solution to representing the fuzzy (*min*) operator as shown in equation 3.42.

$$\mu_{wstner}(x) = \min (\mu_{ws}(x), \mu_t(x), \mu_e(x), \mu_r(x)) \quad (3.42)$$

Fifty fuzzy rules described and applied to cover all scenarios of the drought event as shown in (Table 3.13). Where the rules from 1 to 5 describing extremely dry events when there is no rainfall or it is very low and other variables waver between moderate and high, the rules from 6 to 13 inventory all the extremely wet events when rainfall is very high and other variables are low. Rules from 14 to 21 describe all cases of nearly normal drought when all variables waver between very low and moderate. The rules from 22 to 29 describe a severe drought event when rainfall wavers between very low and low and other variables between moderate and high and the rules from 30 to 37 describe a moderate drought event when rainfall wavers between very low and semi-moderate and all variables waver between moderate and high. A rule from 38 to 45 describes all cases of very wet conditions when rainfall wavers between semi-moderate and very high and all variables waver between low and moderate. Rules from 46 to 50 describe all cases of moderately wet when rainfall wavers between semi-moderate and high and all variables waver between low and moderate. A sample of the overall fuzzy inference system given in (Figure 3.28).

Table 3.13 : Some of the fuzzy rules covering extremely dry drought scenario.

| Rules | IF (Antecedent) | | | | THEN (Consequent) |
|-------|-----------------|----------|-------------|----------|----------------------|
| | Wind speed | Temp. | Evaporation | Rainfall | Drought |
| R1 | Moderate | High | High | Very low | Extremely dry |
| R2 | High | Moderate | High | Low | Extremely dry |
| R3 | High | High | Moderate | Low | Extremely dry |

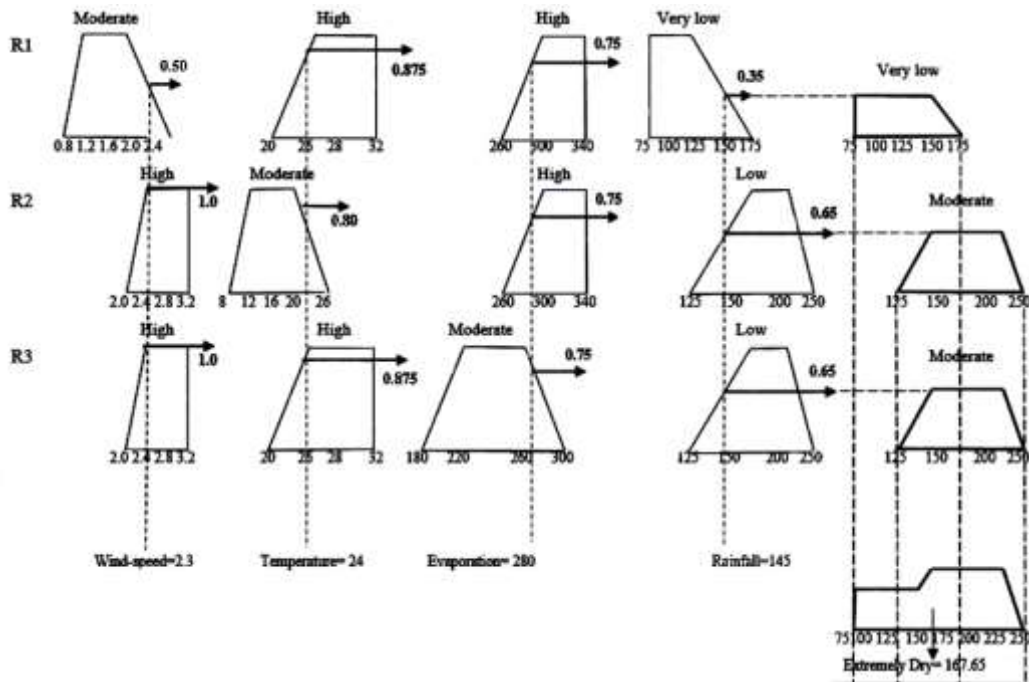


Figure 3.28 : Mamdani fuzzy inference system.

The schematic of a four input and one output the ANFIS structure depicted as seen in (Figure 3.29). For obtaining better results in ANFIS, several parameters should adjusted where number and type of input and output MF, training error goal and training epoch number should be selected carefully. For the developed ANFIS model in this study, the inputs set are rainfall, temperature, evaporation and wind speed while the output is SPI values.

For testing the generalization, capability of the ANFIS at each epoch the command *genfis1* function used. A validation process done to over fit the data that used for training ANFIS model, for each training epochs. After 52 epochs of batch learning, the developed ANFIS model showed good stability and validity. To ensure the efficiency performance of ANFIS model. The Coefficient of Determination $R^2=0.905$, Root Mean Square Error RMSE=0.935, Nash-Sutcliffe coefficient CE=0.83 (between 0.75–0.85 the model performance level acceptable or satisfactory is good according to Altunkaynak and Nigussie, 2016), and Mean Absolute Percentage MAPE=17.39% where the performance accuracy was 82.61%, which makes the system reliable and efficient for SPI prediction for the study area.

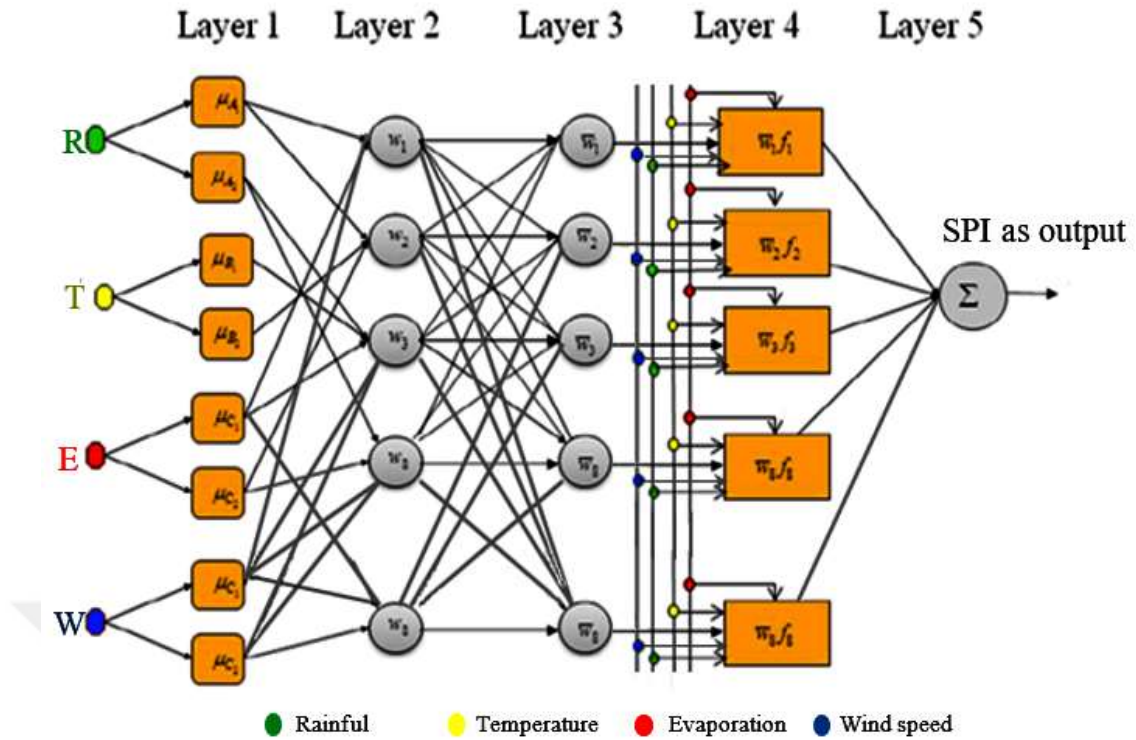


Figure 3.29 : Developed ANFIS model.

For developing an artificial network based on NARX, rainfall time series belong to six stations for the period 1972 to 2017 were used as 540 samples for each one to train and test six designed neural network models. These time series arranged in Excel file sheets that are imported into the MATLAB workspace (MATLAB R2017a 2017). Due to the lack of available data. To ensure the best results in the training and testing of the neural network, the volume of data has tripled to become 1620 for each record by simply appending it with itself three times. Out of the 1620 samples, 70 % of those samples that called the training data are randomly selected by (nntool) for training ANN. To measure the popularization of the network 15 % of samples called validation data feeds the ANNs as data has not been dealing with or seen before. To get an independent measurement of the ANN performance in terms of Root Mean Squared Error (RMSE) the rest 15 % dataset (testing set) used to accomplish this stage.

Ten variables are entered as input variables with 1 exogenous input delays and 2 feedback delays. NARX has two hidden layers with 32 and 4 neurons for the first and second layer respectively. NAEX Neural network learning was limited to a maximum of 1000 epochs. The activation functions in developed NARX models are sigmoid functions, and for more efficient training algorithm narxnet, closeloop functions used

to obtain best result. Levenberg-Marquardt as better performance than all other training algorithms is used for training of the network using the trainlm function that can be defined as network training function that updates weight and bias values according to Levenberg-Marquardt optimization. The performance of a trained model evaluated using RMSE and R^2 .

The average R^2 for training, validation, and testing datasets was $R^2=0.987$ simulated mathematically by function formed as (output= $0.99 \cdot T + 0.31$), and the root mean squared error was $RMSE=0.000326$. In order to determine the best prediction performance accuracy the statistical errors criteria $R^2=0.9699$, $RMSE=0.8467$ and $MAPE=0.8538$ were calculated to prove the prediction accuracy. The developed NARX give predicted rainfall data for nine years that means the input rainfall time series was predicted from (1970-2017) to (2017- 2026) for all rainfall records for the six stations. The new rainfall time series used to calculate the SPI. After testing the system CIM (NARX and ANFIS) and running it, a significant convergence shown between the predicted SPI values by CIM and predicted SPI values by ANFIS. The average prediction error found to be 27.78% as illustrated in (Figure 3.30).

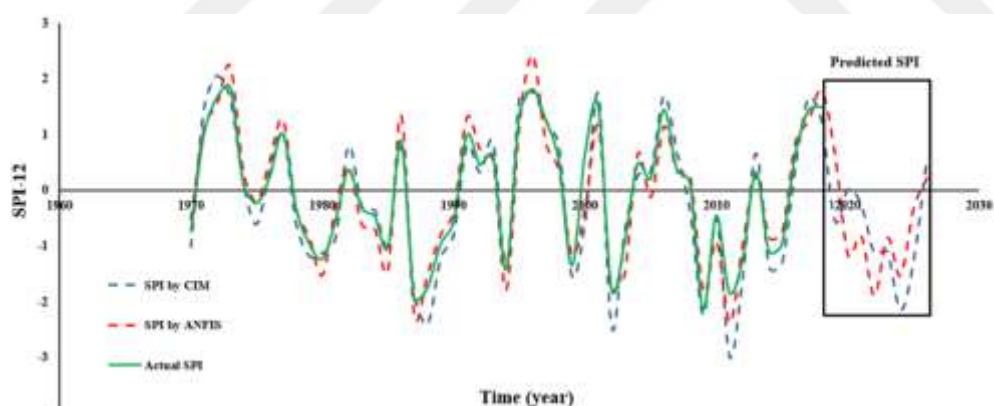


Figure 3.30 : Comparing actual and predicted SPI values.

4. RESULTS AND DISCUSSIONS

Desertification can be defined scientifically when the factors causing this phenomenon which have been specified under human activity, climate change and other indirect causes like poverty are defined. It is not possible to predict a specific place or accurate time for the occurrence of this phenomenon, but its effects are obvious in many regions, especially in arid and semi-arid regions. Because of the wars and the international hurdles with the terrorist organizations that occupied Nineveh for three years and until they liberated from these gangs, the process of combating desertification has eliminated in this period. Therefore, this reason taken into consideration as one of the factors that contributed to the danger of this phenomenon in the study area. Accurate and reliable data integrated with suitable functions and algorithms are the key that can be used to combating this phenomenon. To combat this threat, the use of modern technologies such as Artificial Intelligent, remote sensing and geographic information systems in monitoring, Analysis, update databases and develop mathematical models and tracking system in combating or at least minimizing the impact of this phenomenon.

In this study, remote sensing, geographic information system, Artificial Intelligent, computational methods (Standardized Precipitation Drought Index and Soil Conservation Service (SCS-CN)), and statistical analysis (Temporal variations analysis and Spearman's rank correlation techniques) were applied to find solutions for combating for desertification in the study area. The obtained results, conclusions and recommendations given in the following sections. To achieve the objective of this study and to match the aims and the research questions as referred to in the first chapter, the results obtained from the different used methods in this study presented as follows.

4.1 Remote Sensing Techniques

Remote sensing techniques can be considered as very useful tools for monitoring the land cover change detection in any area under investigation providing updated, consistent, sequentially, low-cost effective data. Many remote sensing techniques used to estimate the change detection such as supervised classification, remote sensing indices, image differencing and ratios or correlation. Remote sensing indices considered as robust, simple and easy used techniques for estimating the quantitative information of the vegetation cover for all the pixels of an image. In this study, remote sensing images for a part of the study area covering 1000 km² (Dataset path 170 row 35 on 25/4/1992 and 16/5/2016 taken by Enhanced Thematic Mapper (ETM+) sensor board on landsat7) specified for monitoring and estimating the percentage of land cover changes. To prove the effects of this phenomenon on the study area in general. Image enhancement, supervised classification and Normalized Differences Vegetation Index (NDVI) techniques were prepared to complete the requirements of this part of the study.

Image enhancement by adopting false-colour composite techniques that are usually composed of three bands to get new images, where the features reflection in these images appear to be different as a reality to make easily distinguished by the human eye. These images named False Colour Composite (FCC) images where it is necessary to know the reflection characteristics of the basic cover types of the earth surface depending on the purpose of the study. Several FCC combinations were analyzed to produce a visual interpretation scene where the best combination was 4, 3, 2 (RGB) for ETM+ bands as seen in (Figure 4.1) where the vegetation appear in red.

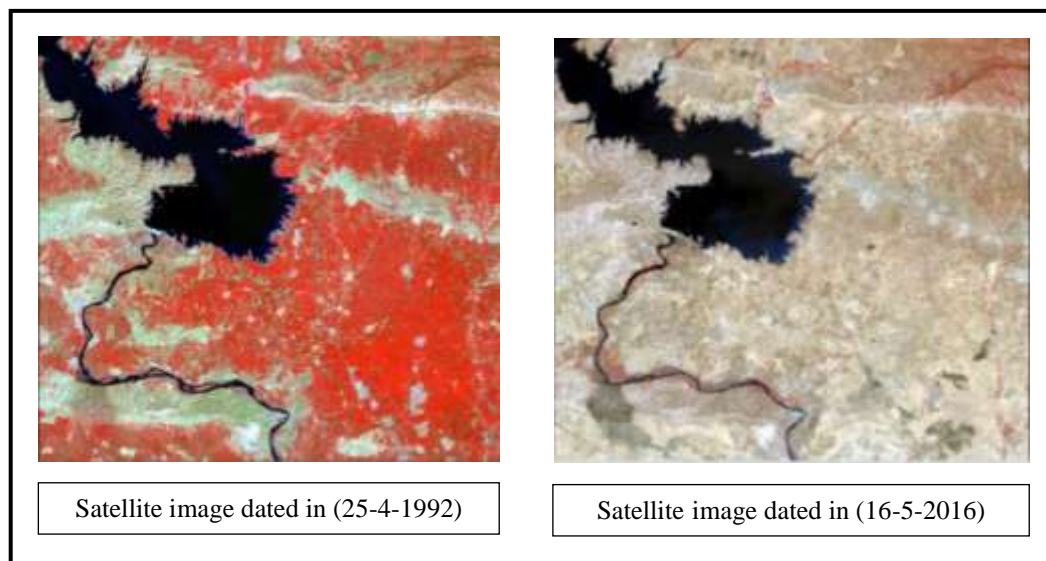


Figure 4.1 : Landsat TM FCC 4,3,2 of the study area with different date.

The results obtained from this technique give a clear perception of decline in the vegetation cover in two comparison periods, indicating that the desertification phenomenon increasing in the study area strikingly. To strengthen the results of the visual interpretation, the NDVI levels were estimated, where it found that vegetation levels were ranged from -0.1 to 0.642 and from -0.548 to 0.28 for images (25-4-1992) and (16-5-2016), respectively as seen in (Figure 4.2).

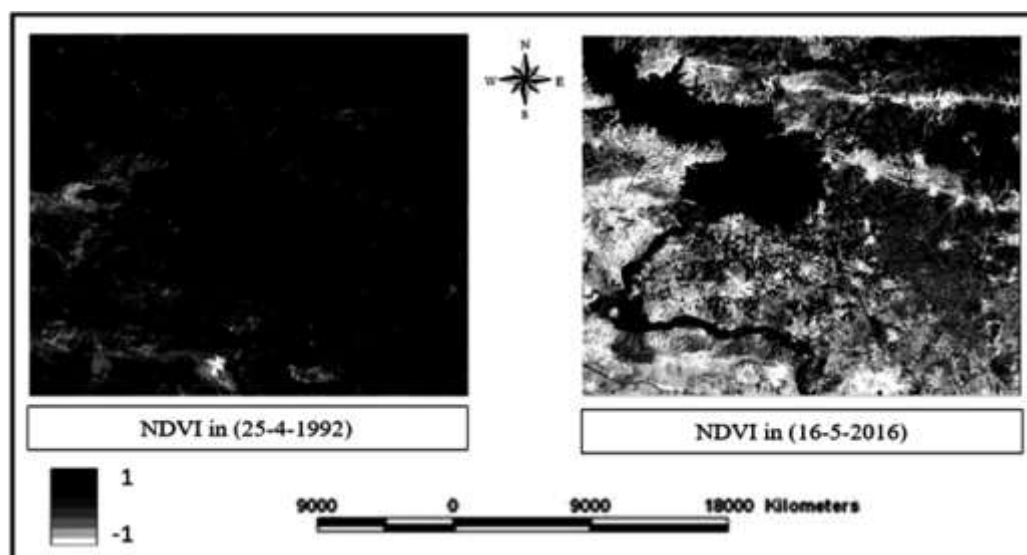


Figure 4.2 : NDVI analysis for a part of the study area.

The images obtained by this technique appeared at gray levels, making it impossible for the human eye to distinguish these levels. To separate them easily and to make the NDVI result more clear and to estimate the impact of vegetation changes, the density

slicing method was used to classify the NDVI ranged level, which was divided into three classes according to available vegetation in the study area. These levels are a non-vegetation area when NDVI is below zero, low vegetation area when NDVI ranged between (0.0-0.2), and high vegetation area when NDVI is greater than 0.2. The classification results show that the low-density vegetation cover class decreased by 20% and the high-density vegetation cover class reduced by 80%, thus the percentage of land classified under the class non-vegetation increased as seen in (Figure 4.3).

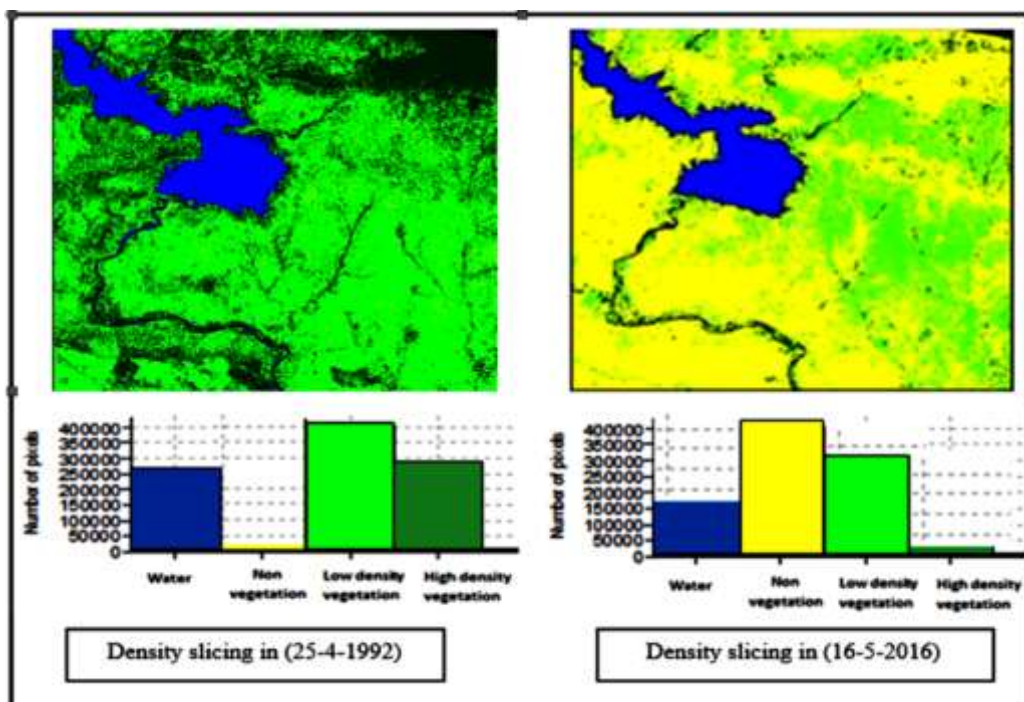


Figure 4.3 : NDVI density slicing maps.

The digital analysis resulting from the supervised classification in the period from 1992 to 2016 showed four classes (water, non-vegetation cover, low-density vegetation cover and high-density vegetation cover) where the area of the vegetation cover class decreased by 17.7 % from 592.3 km² in 1992 to 487.46 km² in 2016. The percentage of area transferred to non-vegetation cover (drought area) class that increased from 251.1 km² in 1992 to 355.94 km² in 2016 as shown in (Figure 4.3).

The supervised classification results, showed four classes (water, vegetation cover, barren land and settlement). The comparison of the two images shows 17.7 % decreasing in the area of vegetation cover class from 592.3 km² in 1992 to 487.46 km²

in 2016 and the percentage of area transferred to barren land (drought area) class increased from 251.1 km² in 1992 to 355.94 km² in 2016 as shown in (Figure 4.4).

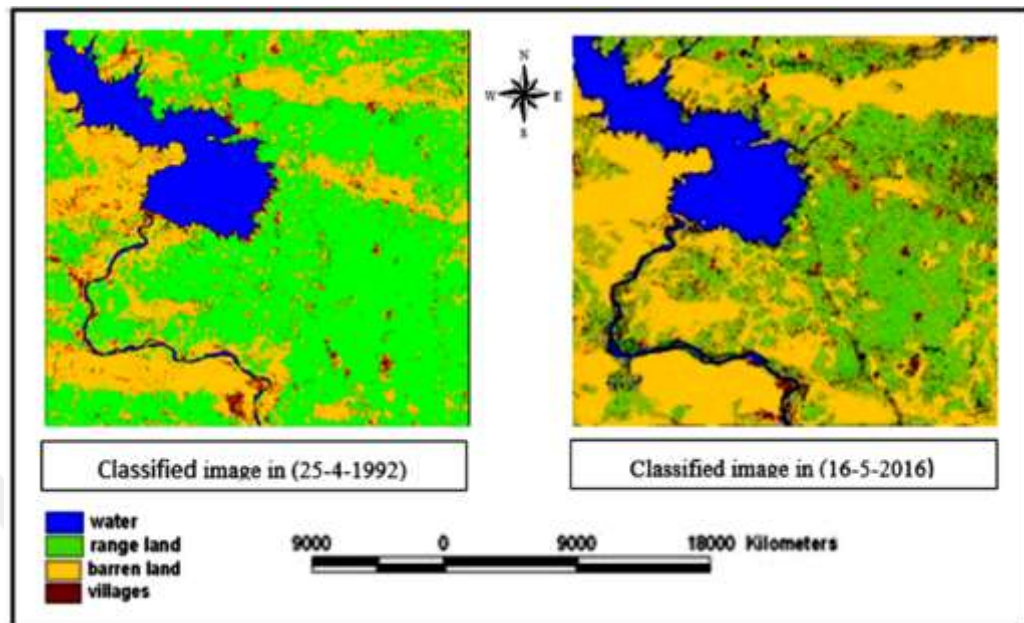


Figure 4.4 : Supervised classification analysis.

The accuracy of supervised classification result calculated based on additional actual ground information (ground training data) as illustrated in (Table 4.1 and Table 4.2). The classification accuracy of supervising classified maps was 87.56% for the image dated 1992 and 85.63% for the image dated 2016.

Table 4.1 : Error matrix of ground training samples for image dated 1992.

| Classes | Reference Data | | | | | Total |
|---------------------|----------------|---------------------|-------------|----------|-------|-------|
| | Water | Vegetation Cover | Barren Land | Villages | Other | |
| Water | 64 | 0 | 2 | 0 | 1 | 67 |
| Vegetation Cover | 8 | 256 | 12 | 3 | 2 | 281 |
| Barren Land | 0 | 2 | 127 | 0 | 3 | 132 |
| Villages | 0 | 0 | 0 | 42 | 0 | 42 |
| Other | 0 | 0 | 0 | 0 | 13 | 13 |
| Total | 72 | 258 | 141 | 45 | 19 | 535 |
| User's Acc. | 87.56% | | | | | |
| Prod. Acc. | 79.34% | | | | | |

Table 4.2 : Error matrix of ground training samples for image dated 2016.

| Classes | Reference Data | | | | | Total |
|------------------|----------------|------------------|-------------|----------|-------|-------|
| | Water | Vegetation Cover | Barren Land | Villages | Other | |
| Water | 56 | 0 | 1 | 0 | 5 | 62 |
| Vegetation Cover | 8 | 188 | 24 | 3 | 15 | 238 |
| Barren Land | 0 | 2 | 283 | 2 | 9 | 296 |
| Villages | 0 | 0 | 0 | 42 | 0 | 42 |
| Other | 0 | 0 | 0 | 0 | 23 | 23 |
| Total | 64 | 190 | 308 | 47 | 52 | 661 |
| User's Acc. | 85.63% | | | | | |
| Prod.Acc. | 77.58% | | | | | |

The results of supervised classification and NDVI showed deterioration in the vegetation cover. The rate of this deterioration reached 17.7% in less than 24 years, and it is expected to accelerate because of the desertification phenomenon in the region in addition to other reasons including uncontrolled overgrazing methods used by livestock breeders and large numbers of inhabitants who turned away from agriculture and migrated to the cities. Furthermore, to give a clear perception of the decrease of vegetation cover in the study area. Vegetation health index VHI maps produced by the NOAA STAR center, were derived for the study area for the years 2010, 2014, and 2016 in a specific day (eight of April) that represent the beginning of the spring season in the study area (Figure 4.5).

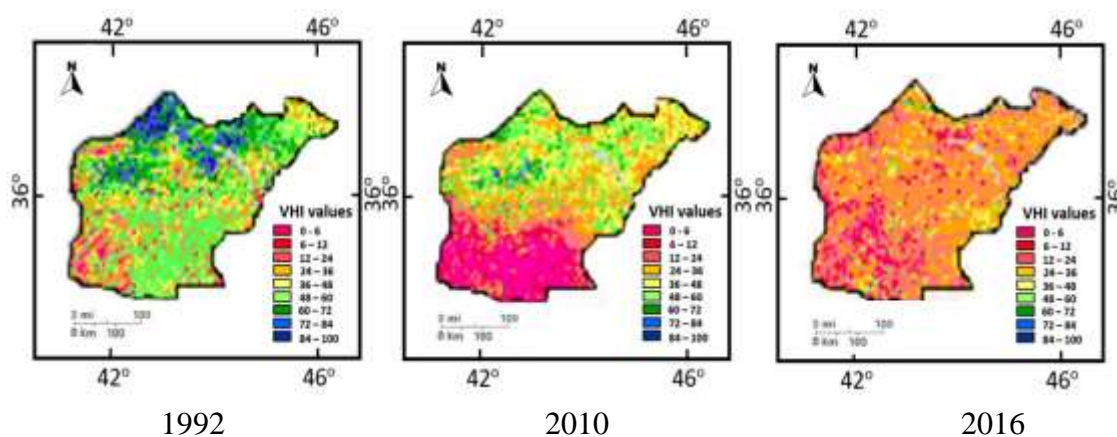


Figure 4.5 : Vegetation health index VHI maps.

When comparing the digital analysis resulting in obtaining from these maps, a significant collapse in vegetation health have been observed reaching 50% in the year 2016 when a comparison is made with the year 1992. For the drought, expansion analysis driven from drought change maps produced by the NOAA STAR center as seen in (Figure 4.6), the digital analysis resulting showed three classes (drought, desert, and land).



Figure 4.6 : Drought expansion maps.

In these maps, the class of drought area and the class of desert area were expensive because of the land area class. Where the area of the land class decreased continuously by 0.7% in the year 2014 and 2.2% in the year 2016 when a comparison is made with the year 1992 meaning that 2.2 % of the study area transformed to drought and desert areas. After identifying the extent of the desertification problem in the study area a seasonal valley named Wadi AL-Mleh basin chosen to apply theoretical analysis using virtual GIS to design rainwater storage lakes as one of rainwater harvesting techniques. There are many kinds of rainwater harvesting-technologies. One of them adopt constructing small dams on the main valleys where this technology classified under macro techniques. There are many kinds of these dams (earth-fill dams, rock-fill dams, valley dams, and regulating dams etc.) based on their use, construction material, size and shape (Salih et al, 2012).

Many requirements should taken into account when designing these dams, economic and environmental issues are examples of these requirements. Many data used for designing and constructing procedure like (hydrologic, geologic, hydraulic and cultural data etc.) The most suitable site should achieve many criteria where geologic studies must done and soil conditions must be suitable (Weerasinghe et al, 2011).

These dams guarantee the formation of seasonal artificial lakes that can be utilized in many activities such as irrigation and nomad's resettlement.

Appropriate sites investigated for constructing small dams on the main waterways of the Wadii AL-Mleh basin in order to create theoretical rainwater storage lakes. The first step was to identify the surface drainage network, which is an important step in hydrological, geological and geomorphologic studies. The surface drainage network of Wadii AL-Mleh basin derived using the hydrological analysis function in ARCGIS 10. The results showed that the stream flow order of Wadii AL-Mleh basin is six according to classification (Strahler, 1964). This level indicates that the basin receives large amounts of seasonal water in the form of surface runoff as shown in (Figure 4.7).

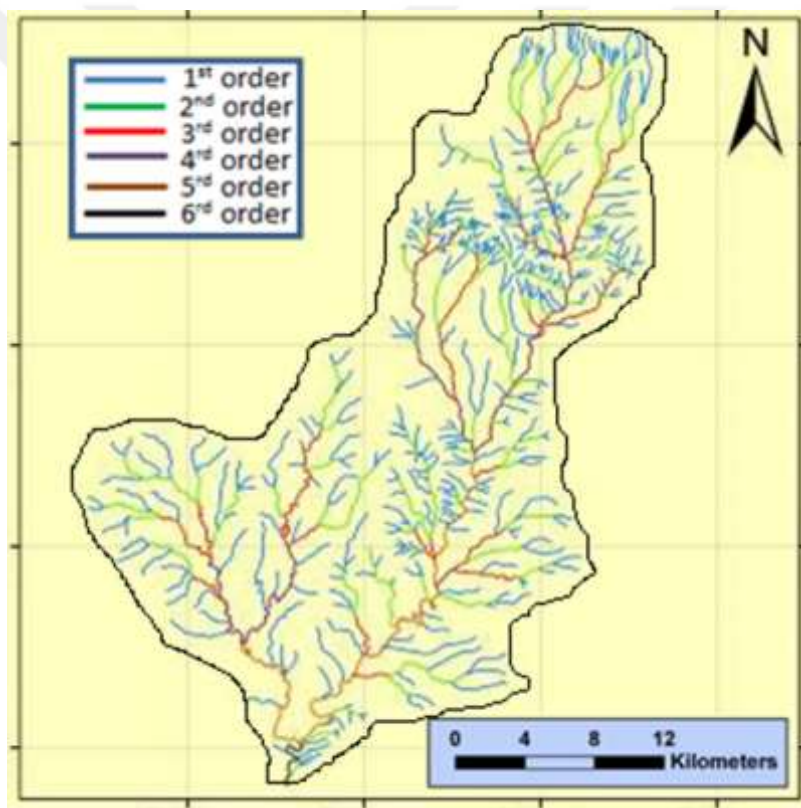


Figure 4.7 : Surface drainage network map.

These quantities are lost due to several factors, including evaporation and uncontrolled rapid flow into the Tigris River causing several problems, like soil erosion. To give a sufficient description of the geometry of the drainage basin and its river system, the results of the morphometric analysis of the drainage network elements are required. Four morphometric properties chosen to illustrate the characteristics of the basin from the hydrological point of view as follows.

a. Stream order. The study of the Stream order very important to know the amount of discharge and this property reflect the erosion and deposition ability of the basins stream order (strahler, 1964). The stream order of the Wadii AL-Mleh basin are six that means the biggest amount of discharge flow as annual runoff.

b. Area consistency ratio. This ratio signs to the basin convergence or diverge range from the circular shape and its value ranges between (0-1). The values closer to one usually mean the basin in a circular. The result for Wadii AL-Mleh basin was (0.62) this value explain the basin have irregular discharge.

c. Basin elongation. This character controls the amount of annual runoff that flow in the main stream (Pike, 1999) and its value ranges between (0-1). The value of this character for all basins was the same and equal to (0.67) and this value was an account from (1) that mean the main canal receive a massive amount of annual runoff.

d. Bifurcation ratio. This ratio controls the average of discharge and its value ranges between (5-3) for normal basins. (Pike, 1999) Prove the relationship between the period of discharge and the Bifurcation ratio whenever this ratio approach to (3) that mean the amount of discharge increase in Wadi AL-Mleh basin.

For designing artificial lakes in the study area, a procedure of three steps carried out as shown below.

a. Derive the Contour Map. A digital elevation model (30) meter was used to classify the study area slope, a contour map with an interval of (25) m was derived using (Global mapper v.13) as seen in (Figure 4.8).

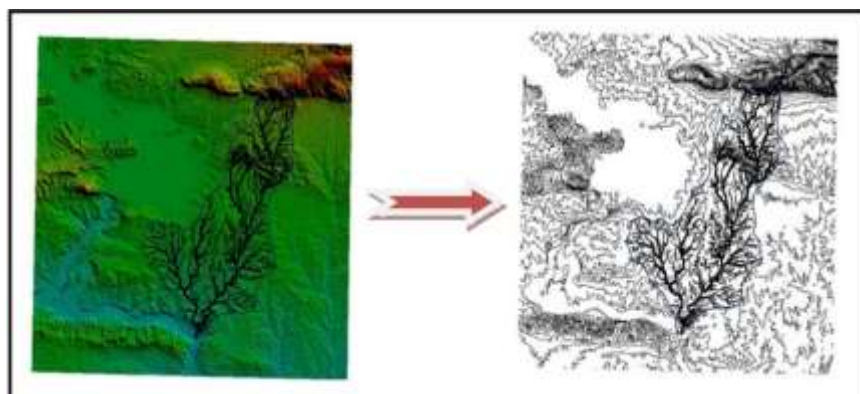


Figure 4.8 : Deriving the contour map using (Global map v.13).

The land gradient is very important in selecting rainwater-harvesting methods (Gutiérrez et al, 2004). This feature gives a clear picture of the topography of the basin, which helps to determine the most suitable locations where the greatest amount of rainwater can be harvested as illustrated in (Figure 4.8) and (Table 4.3). The most suitable sites chosen for dams' construction as shown in (Figure 4.9). The results of this analysis can be used in the future as a database to identify the surface area of the established lakes and determine the area of land that is subsequently flooded when the lakes are formed.

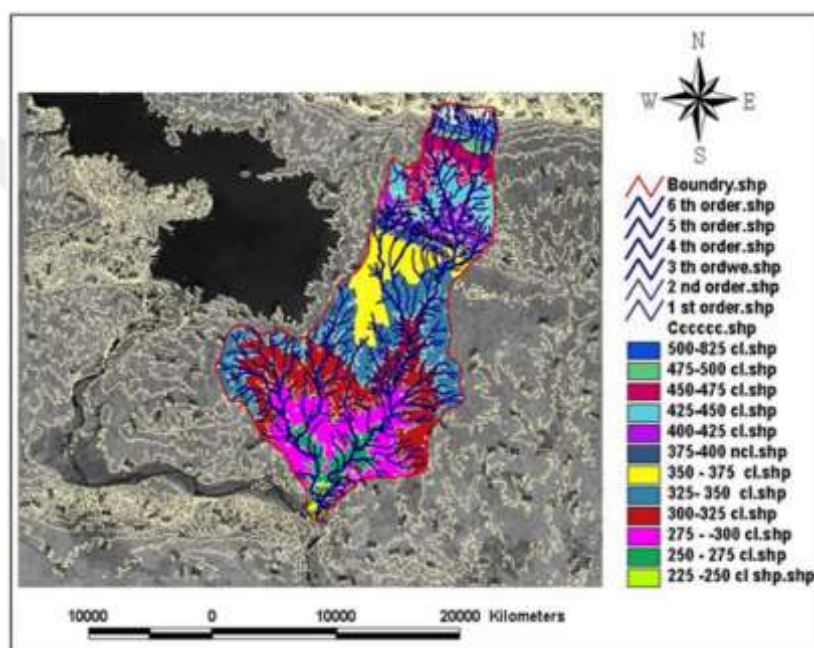


Figure 4.9 : Gradients and contours intervals classification.

Table 4.3 : Gradient analysis and the area between the contours intervals.

| Contour level (m) | Land gradient (%) | Area between contours intervals (km ²) |
|----------------------|----------------------|---|
| 225-250 | 0.13 | 3.46 |
| 250-275 | 0.13-0.15 | 16.36 |
| 275-300 | 0.15-0.2 | 57.75 |
| 300-325 | 0.4-0.6 | 41.56 |
| 325-350 | 0.6-0.7 | 115.85 |
| 350-375 | 0.7-1.0 | 22.85 |
| 375-400 | 1.0- 1.25 | 10.56 |
| 400-425 | 1.25-1.75 | 15.33 |
| 425-450 | 1.75-2.5 | 17.75 |
| 475-500 | 4.0-4.5 | 4.47 |
| 500-825 | 4.5-5.0 | 9.81 |

b. Finding the cross-section of the best location. By tracking the mainstream drainage network, the suitable positions for the six small dams found based on the digital elevation model (DEM). The lowest depth found for these sections is 10 meters. Therefore, the actual height of the dams to be constructed has assumed 4 meters. This assumption was only to show how the simulation procedure work to establish the seasonal lakes and how much water supposed to be stored on these lakes that's mean the height of the dams could be any number depending on the height of the cross-section of the valley at a chosen point as shown in (Figure 4.10).

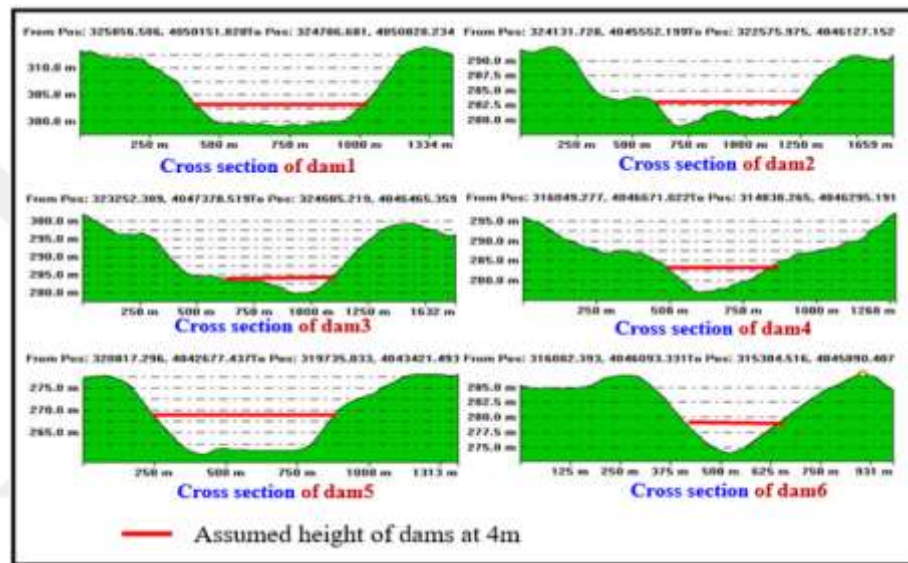


Figure 4.10 : Cross section sites for selected dams.

c-According to the digital elevation model and the remotely image for the study area, ERDAS v.13 software used to create a realistic simulation that shows the location of the selected dams' sites and the default artificial lakes that formed behind these dams using virtual GIS. The first step for creating the water layer is to display the DEM that manipulated with considered specific assumed elevation to be 4 meters at the selected dams' sites. The second step is to overlay the raster image and activate the water function then we can fill the proposed artificial lake slowly using water elevation function as shown in (Figure 4.11).

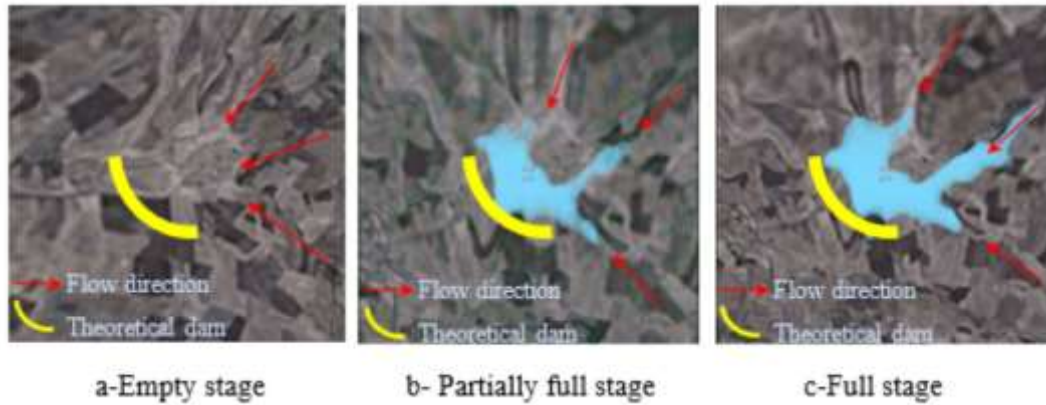


Figure 4.11 : Simulation procedure for creating rainwater storage lake (L3).

After filling the lakes with water at the specified height (4) m, the amount of water that can be harvested was calculated automatically also the surface area of each lake is calculated as illustrated in (Table 4.4).

Table 4.4 : Expected rainwater harvested volume.

| Lakes no. | Surface area (km ²) | Expected harvesting (m ³) |
|-----------|------------------------------------|--|
| L1 | 1.02 | 283,824.7 |
| L2 | 1.134 | 182,475.5 |
| L3 | 2.02 | 284,910.8 |
| L4 | 1.187 | 298,586.8 |
| L5 | 1.321 | 217,625.2 |
| L6 | 1.125 | 196,827.4 |
| Total | 6.887 | 1,464,250.4 |

The total volume of the theoretical amount of harvested water in the study area was (1,464,250.4) cubic meters with the assumption that the height design of the dams was (4) m and a total surface area of the six default artificial lakes is (7.807) km². The final 3D simulation scene for the study area shows the theoretically designed rainwater storage lakes as shown in (Figure 4.12) and (Figure 4.13).

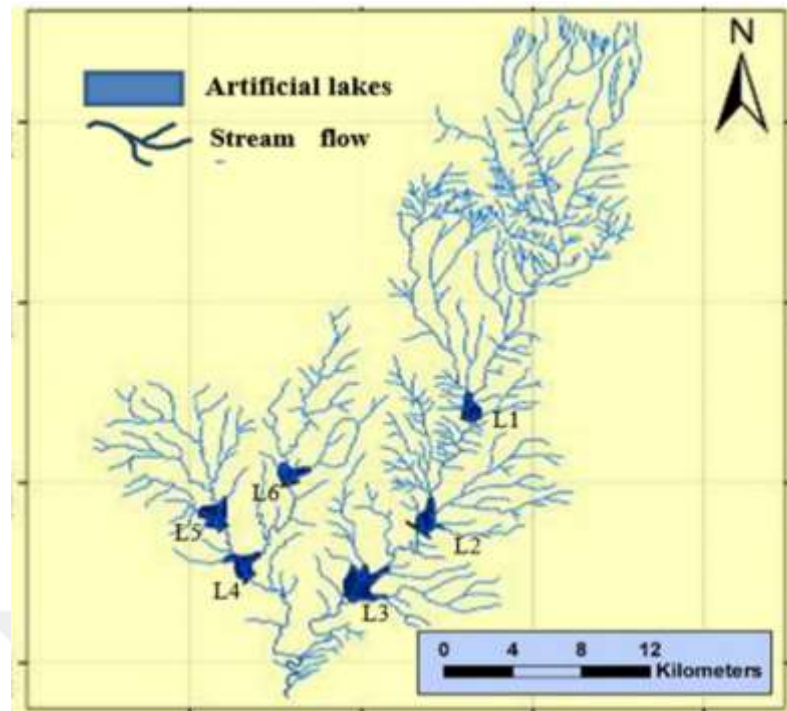


Figure 4.12 : The default artificial lakes that formed behind the dams.



Figure 4.13 : Final 3D vision for the study area.

Storing water in temporary seasonal lakes behind the established dams in a specified area and based on the topography of the area behind the dams has important implications for the future of the region. The desertification phenomenon is threatening the daily life and health of inhabitants. These proposed lakes can provide part of the

drinking water for most villages and residential complexes in the area. The water collected in these lakes can also be used for supplementary irrigation and will revive partly agriculture in the region. These seasonal lakes will undoubtedly restore life to the area and will turn the area into tourist attractions if planned correctly.

The surface area and the amount of water that can be harvested annually in the region were calculated, this amount of harvested water represents the full capacity of all reservoirs taking into account the assumed height of dams of 4 m. The accurate amount of water of these reservoirs might be calculated yearly and that depends on the amount of annual precipitation that falls on the study area. The main aim of this study is to find a natural reservoir to harvest rainwater safely every year and that may help to develop the agricultural activities, combating desertification resulting from the drought, and reduce soil erosion resulting from seasonal floods in the valleys of the study area.

4.2 Geographic Information System (GIS)

Various activities conducted using GIS in this study where the results related to GIS can be illustrated as follows.

a. Dust and sandstorms effective feeding-regions map was prepared using GIS technique based on forty MODIS satellite images as seen in (Figure 4.14) where these images show a sequence of dust and sandstorms events that hit the study area between the periods from 2005 to 2018. By geometry option, in GIS platform, the centroid of each storm was found and the boundaries drawn as a shapefile-contained information about each storm. The Geostatistical analysis technique adopted using the Inverse Distance Weighted (IDW) technique as a spatial interpolation procedure to create this map (Baddock et al, 2009). By this, map four feeding-sources areas detected two of them from outside the Iraqi border and the other two sources within the Iraqi border.

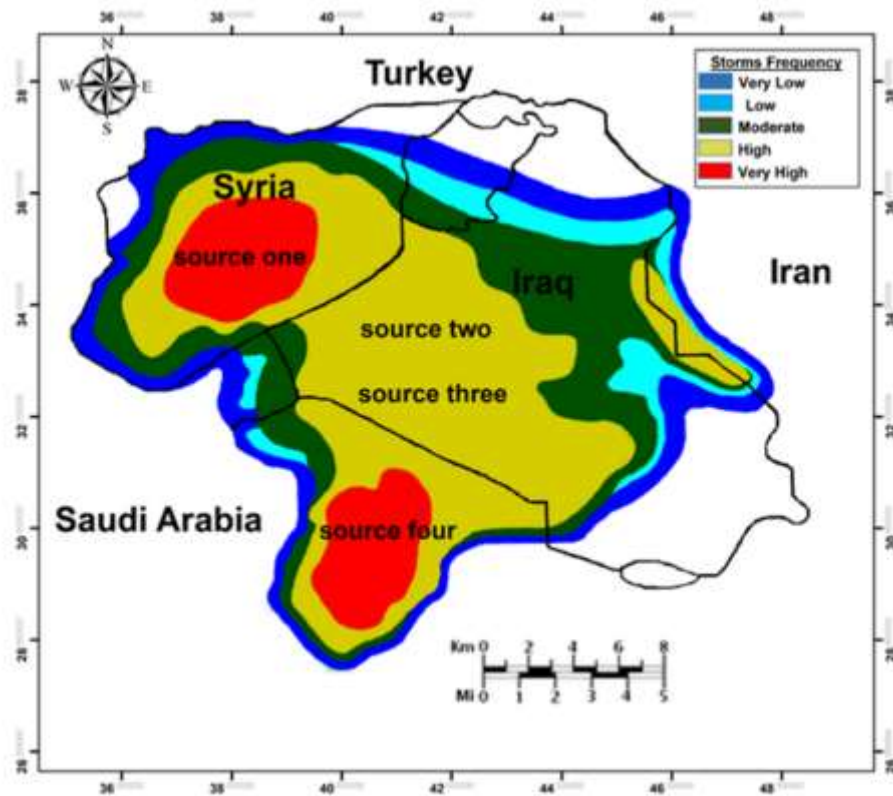


Figure 4.14 : Dust and sand sources effective regions.

The sources areas identified as below where the dust and sand storms fluctuated between very low to very high and storms affecting the study area fluctuated between moderate to high as follows.

1. Source one is foreign source represented by the area located outside the Iraqi border region to the west of the study area about 300 km within the Syrian borders. This source directly affects the formation of the storms destined to the study area.
2. Source two is local source represented by the area located inside Iraqi border to western parts of the Samera and Tikrit provinces in Iraq and the south-west of Anbar desert in about 485 km far from the study area. This source directly affects the formation of the storms destined to the study area.
3. Source three is local source represented by the area located inside Iraqi border in Muthanna desert that located in Muthanna province southeast of Iraq about 650 km far from the study area. This source indirectly affects the formation of the sandstorms destined to the study area.
4. Source four is foreign source represented by the area located outside Iraqi border to the south of the study area within the Saudi Arabia border more precisely the northeast

of Saudi Arabia desert about 1100 km far from the study area. This source indirectly affects the formation of the storms destined to the study area.

Using the middle East dust loads map, the storms materials loads were classified as fluctuated between very low to moderate. The sequencing frequency of all dust and sandstorms classified into three groups according to their potential sources areas as local, foreign or mixed dust and sand grain feeding areas. Furthermore, by this classification, the frequent months of these storms occurrence found and the percentage of each type of storms calculated according to available storm-frequency data. The result of this classification shows that the most local storms happened in July is (33.87%), most foreign storms were in March is (44.35%) while most mixed storms occurred in October is (21.77%) as illustrated in (Figure 4.15.)

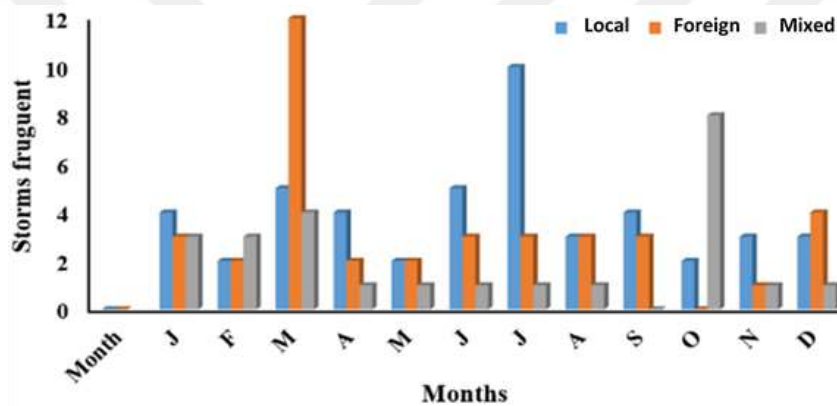


Figure 4.15 : Storms events classification according to their detected origin sources.

The wind rose diagram drawn to recognize the possible pathways of all wind events that blowing into the study area where the analysis of this diagram shows that most wind events blow from southwest to northeast. This diagram proves that these winds are carrying the dust and sand grains from the detected feeding sources areas. That mean if the winds are blowing from this direction (effective dust and sand regions) then the areas to the north and northwest of the study area will affected in the seasons of dust and sandstorms occurrence as seen in (Figure 4.16).

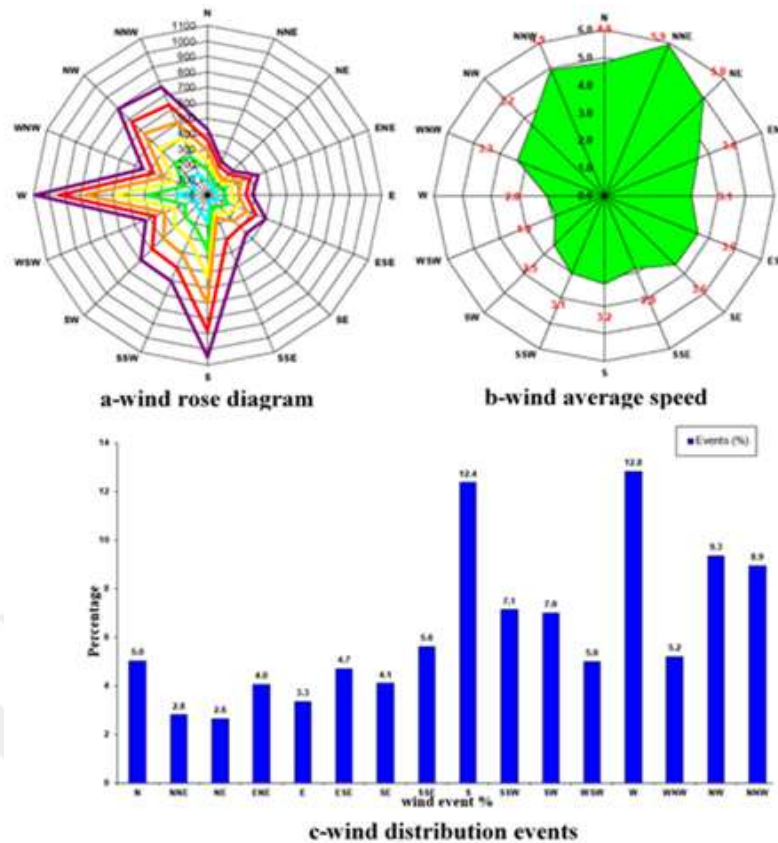


Figure 4.16 : Wind regime analysis.

By particle-tracking algorithm procedures using Playback Manager Tool, a realistic example was analyzed to prove the results above by tracking a dust and sandstorm event that occurred on 24 March 2017 with a 36-hour duration, which is classified under ‘foreign storm’. The covering area of this storm classified into three phases as seen in Figure 3.3. According to the form of formation were at hour 0, the first and second stages began to form and the shape of these phases’ changes into cumulative and continues marching until the hour 4 where it enters the study area. At hour 12, this storm becomes more active and covering all the study area where the third phase begins in this period. Six hours later, this storm is gradually disappearing and leaving the study area to the adjacent provinces to become less powerful and ends after a period. The storm tracking results show that this storm has two theoretical paths as seen in (Figure 4.17) where the wind direction and storm control wind specified. The theoretical paths of this storm proved that the dust and sand grain materials carried out from the source number one that proven by dust and sandstorms effective feeding-regions map. In addition, the average-wind-speed diagram drawn where the results of this diagram show that the prevailing wind speed fluctuates between 1–5 m/s with an average speed of 2.8 m/s, prevailing west wind of 12.8% and a prevailing south wind

of 12.4%. These prevailing wind speeds percentages are very important in studies that applied to estimate the speed of dust and sand storms materials transportation.

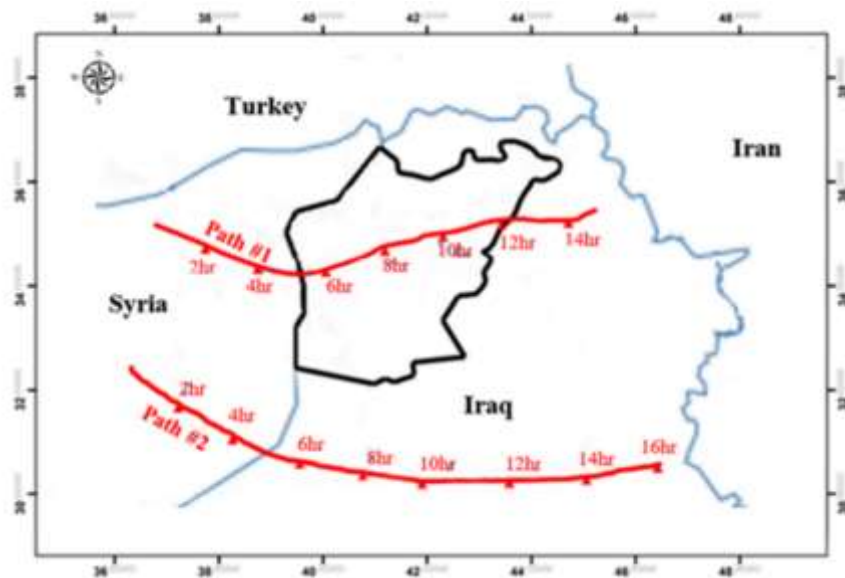


Figure 4.17 : The movement paths of the last dust and sand storm.

b- For assessing the drought conditions and distribution in the study area a GIS project was built up for preparing a long-term spatial distribution map as seen in Figure 4.18 based on actual and predicted SPI-12. This map discussed according to drought levels where moderate drought, severe drought, and extreme drought probably accrued in the study area in the predicted period from 2017 to 2026.

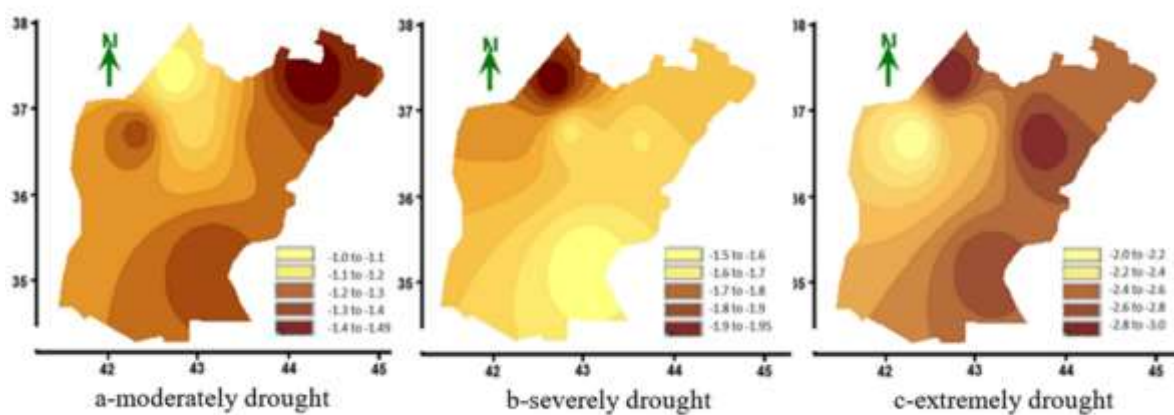


Figure 4.18 : Spatial distribution of long term SPI-12 in the study area.

c- For managing and future planning of water quantities in Al Murr basin (ungagged basin within the study area). A GIS project created according to the availability of data using Arc Map v.10.2. The GIS database established through the primary available

data for the study area, which includes Landsat satellite image dated 16/5/2015 that took by Enhanced Thematic Mapper (ETM+) sensor on board of Landsat 7 with 30 m Digital Elevation Model (DEM) resolution and actual and predicted rainfall time series. The basin boundary and surface water network were extracted using hydrology extension. The basin divided into 20 sub-basins (from B1 to B20) where the area of these sub-basins calculated as seen in (Figure 4.19).

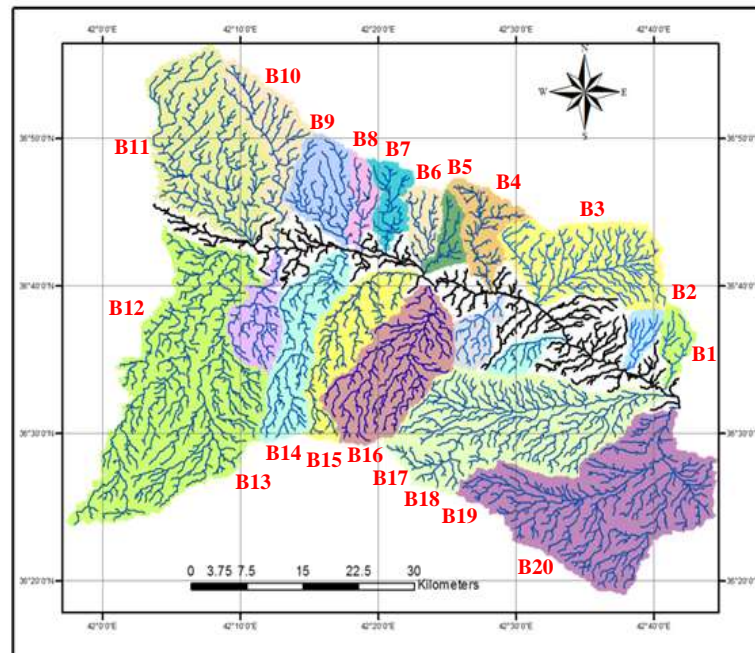


Figure 4.19 : Al Murr basin analyze by Arc Map v.10.2.

The amount of runoff for the actual and predicted period was calculated and entered as the table's forms in the developed GIS database. With the change of global climate, forecasting models are more relevant for forecasting weather variables into 20 years forward at least (Lohani et al., 1998). On the other hand, runoff changes may be observed when long-term weather variables prediction as compared to the corresponding short-term prediction (Sivakumar et al., 2001). Trend line analysis as linear least squares regression was carried out to explain the difference between short-term versus long-term runoff forecasting as shown in (Figure 4.20 and Figure 4.21).

For short time predicted analysis for the period 1956 to 2017, ten years' time-series data predicted until 2027 where the estimated average runoff shows slightly increased by the value of the trend line slope over time. This short time predicted indicator is not sufficiently clear or cannot adopted due to climate change effects as illustrated in

(Figure 4.20). Moreover, the longtime predicted analysis for the period 1956 to 2017 thirty-three years' time-series data were predicted till 2050 where the average runoff shows decreasing trend giving a realistic impression of what might happen as a result of climate change in the study area as illustrated in (Figure 4.21).

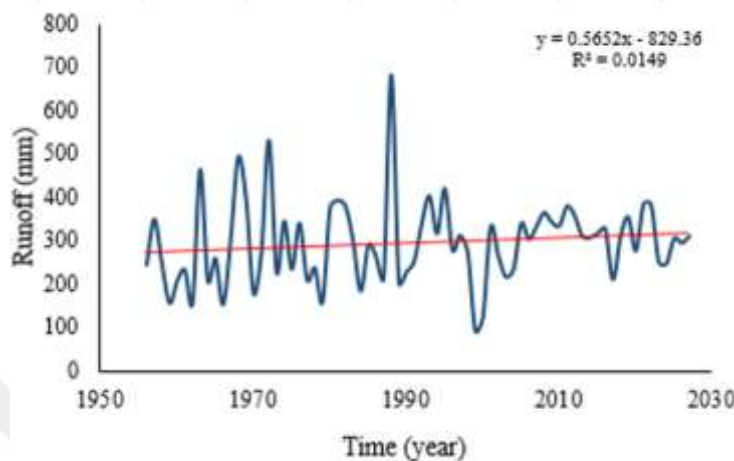


Figure 4.20 : Short term predicted analysis.

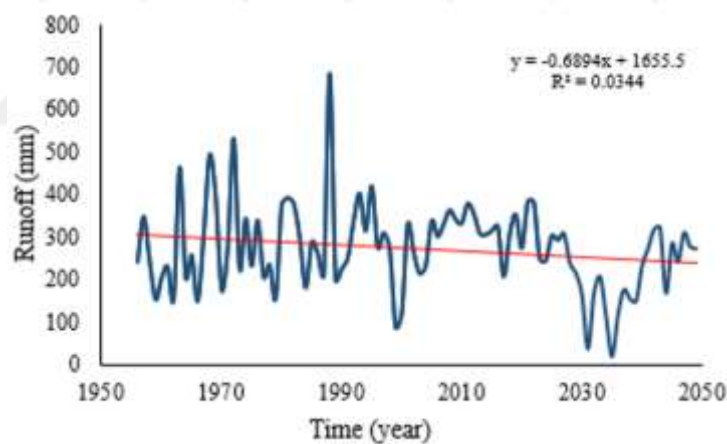


Figure 4.21 : Long term predicted analysis.

For managing and future planning of water quantities in Al Murr basin for the actual and predicted runoff time series (1956-2050) that equal to 93 years the basin was divided into three periods as (1956-1987), (1987-2018) and (2018-2050) where the calculation results of average runoff based on SCS-CN for each sub-basin were estimated. It has been noted an increase in the average runoff for the two periods (1956-1987) and (1987-2018) by 22.45 mm, with a decrease in the average runoff for the predicted period (2018-2050) as 65.35 mm as seen in (Figure 4.22).

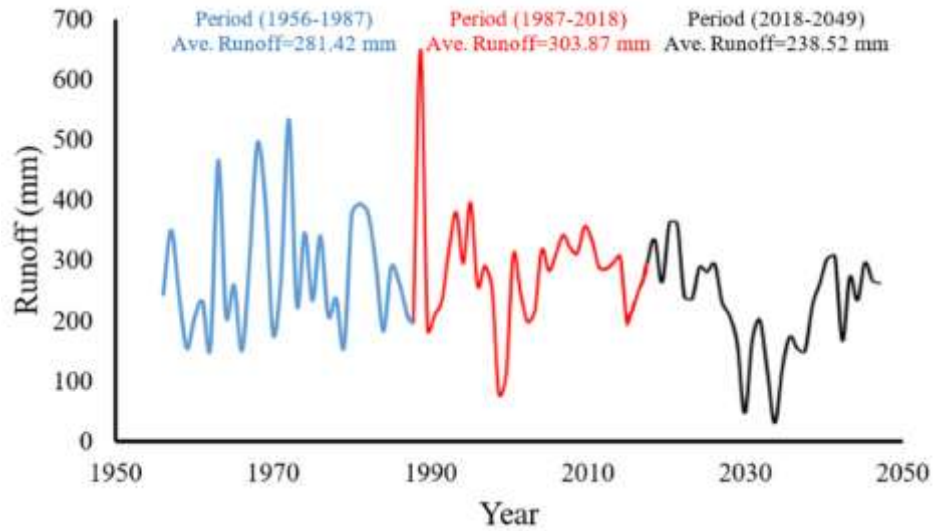


Figure 4.22 : Runoff distribution for actual and predicted time (1956-2050).

The actual and predicted runoff analyzed as a spatial distribution when GIS project developed as illustrated in (Figure 4.23). The spatial analysis shows changes in the runoff distribution with time for the actual and predicted periods, where many reasons caused this changing in runoff distribution like climate changes effects and increasing sandstorms frequency in the study area as mentioned in many previous studies (Kobler 2013; Yahya and Seker 2018). A kind of induction and inquire system was established in this project that can be developed by adding many layers using remote sensing data like land use/cover map, morphological map, hydrological map etc.

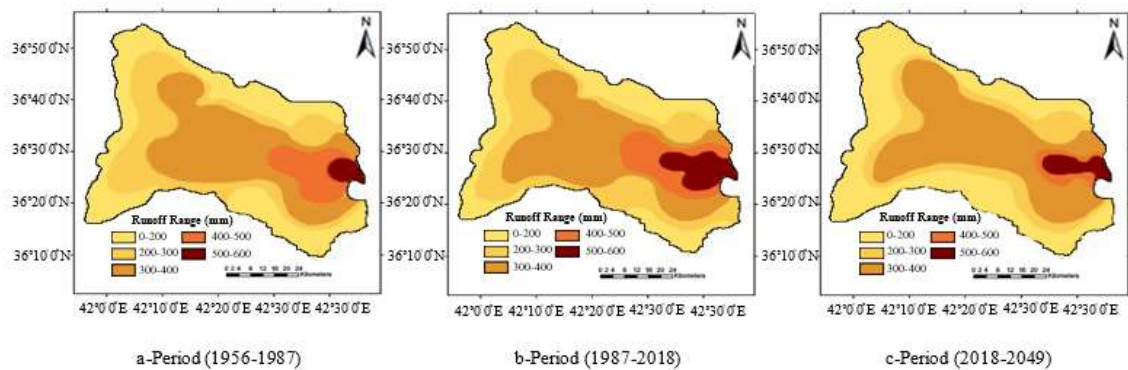


Figure 4.23 : Runoff spatial distribution for the period (1956-2049).

4.3 Artificial Intelligent (AI)

Different neural network approaches, RBF, NARX and FCM, used to develop different neural network sub-models collected together in one model used for local weather

forecasting in the study area where MATLAB platform used to develop these sub-models. The results related to Artificial Intelligent in this study can illustrated as follows.

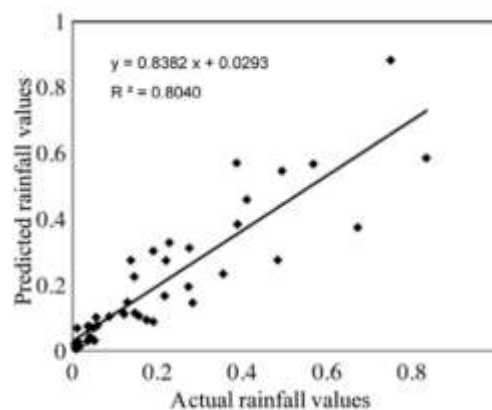
a. Design weather forecasting model as an effective platform for forecasting weather variables for the study area. This model employs three different ANNs trained and gathered in one model works in four stages as a predictor model. This model can used for carrying out related scientific studies like drought assessment as an example. This model has the ability to predict five weather variables for the period from 2018 to 2050 also it was noted that this model has the ability to predict the values of the air variables for the study area for a period limited between 2018 and 2050, after which the model begins to collapse and its results are illogical.

To gain the best performance model, the model structure designed in four stages. All sub- models work separately in the first stage that called training stage then their results were gathered and fed back to working in stage two that called testing stage wherein this stage the performance accuracy of the all designed sub-models were evaluated. Stage three, called predicted stage; in this stage, the data records processed to estimate the predicted data of the selected weather variables. The final stage called the presentation stage where an interface window designed to be an easy facility to work on this model without any difficulty or complexity. A designed window shows several options make it easier for the user to work on this model, where the type of weather variables, method of prediction, data record length, and prediction period in years can chosen. In addition, this window has the ability to show the tested and forecasted results in tables and figures formats as seen in (Figure 3.8.) After checking the operational effectiveness of the model by comparing the percentage of statistical errors criteria. The model has run to predict the rainfall values for the existing year's values for the period (2009-2017) to determine the statistical percentage error as illustrated in (Table 4.5) that shows the statistical percentage error obtained from the comparison between the averages predicted results of the three ANNs and the actual data using the developed model.

Table 4.5 : Comparing rainfall results (actual and predicted).

| Year | Rainfall prediction results | | | | Statistical error | |
|------|-----------------------------|-------|-------|-------------------|-------------------|-----------|
| | RBF | NARX | FCM | predicted average | Actual data | % error |
| 2009 | 223.8 | 224.3 | 224.1 | 224.06 | 218.4 | 2.59 |
| 2010 | 240.6 | 223.5 | 223.9 | 229.33 | 222.1 | 3.25 |
| 2011 | 228.3 | 229.1 | 227.6 | 228.33 | 233.6 | 2.25 |
| 2012 | 232.9 | 233.1 | 232.6 | 232.33 | 251.5 | 7.62 |
| 2013 | 231.2 | 231.6 | 231.0 | 231.26 | 217.2 | 6.47 |
| 2014 | 226.2 | 225.6 | 225.7 | 225.83 | 234.2 | 3.57 |
| 2015 | 200.1 | 195.6 | 197.3 | 197.60 | 213.5 | 7.44 |
| 2016 | 424.5 | 426.9 | 424.5 | 425.3 | 469.4 | 8.96 |
| 2017 | 376.2 | 364.3 | 349.8 | 363.4 | 415.7 | 12.58 |
| 2018 | 331.1 | 351.8 | 331.1 | 338.0 | - | - |
| 2019 | 258.1 | 306.6 | 258.1 | 274.2 | - | - |
| 2020 | 379.5 | 441.3 | 352.9 | 391.2 | - | - |
| 2021 | 250.2 | 332.9 | 250.2 | 277.7 | - | - |
| 2022 | 579.2 | 536.7 | 538.6 | 551.5 | - | Ave. 6.08 |

The average percentage of predicted errors was very small (6.08%). To minimize this percentage error, more types of ANNs should be elected and more other data should be added to the input data set, especially before 1972 and updating, the model database with data variables for 2018 and above. The model run again to predict the rainfall values for the period from 2018 to 2050 were the three predicted time series of the rainfall variable shows marked homogeneity with each other as seen in Figure 4.24 and (Figure 4.25). It is noted that this model gives irrational prediction results until 2050 then its results begin to collapse and its results are irrational. One of the reasons of this collapsing is the increase of percentage predicted errors with time, in any case, this collapsing must be studied carefully taking into account several fundamental points like redesign the ANNs by increasing hidden layers and setting appropriate neurons number.

**Figure 4.24 :** The scatter plot between actual and predicted rainfall.

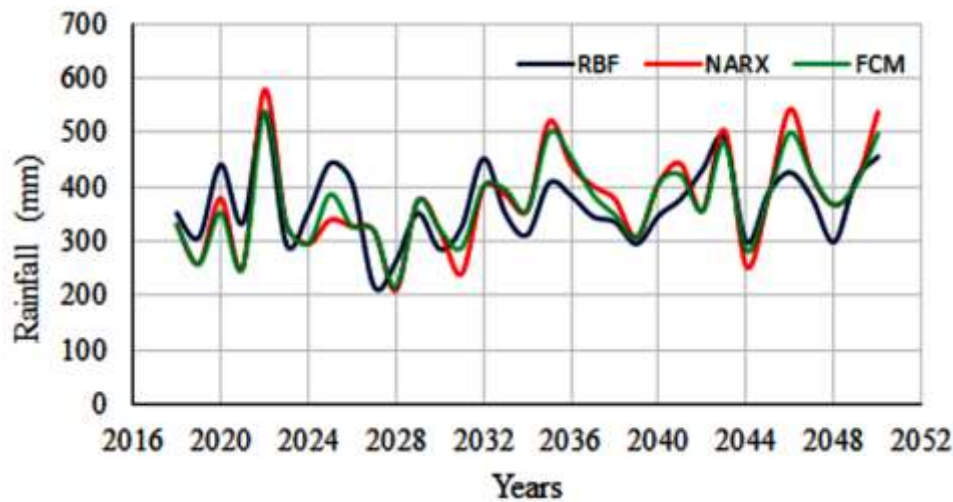


Figure 4.25 : The predicted time series of rainfall from 2018 to 2050.

A kind of empirical comparison made on three adopted artificial neural networks. The results indicate that the NARX sub-models showed a slightly better performance than the other sub-models in terms of testing and training processes that evaluated by four performance metrics as Coefficient of Correlation, Nash-Sutcliffe Efficiency Coefficient, Root Mean Squared Error and Mean Absolute Percentage Error. The comparative average performances accuracy results for all designed sub-models fluctuated from 78.10% to 83.75% where the designed NARX sub-models shows higher average performances accuracy as 83.75%. In addition, this model used as the runoff prediction model in the ungauged basin within the study area.

b. Design drought assessment model consists of Computational Intelligent Model (CIM) based on NARX approach and Adaptive Neuro-Fuzzy Inference System (ANFIS). To ascertain the efficiency performance of ANFIS. The Coefficient of Determination $R^2=0.905$, Root Mean Square Error $RMSE=0.935$, Nash-Sutcliffe coefficient $CE=0.83$ (between 0.75–0.85 the model performance level acceptable or satisfactory is good according to Altunkaynak and Nigussie, 2016), and Mean Absolute Percentage $MAPE=17.39\%$ where the performance accuracy was 82.61%, which makes the system reliable and efficient for SPI prediction for the study area. The value of MAPE statistically compared with the values of actual SPI and predicted SPI. The result shows a good indication of the developed ANFIS reliability. This result could be more effective if MAPE reduced by engaging other meteorological variables that have a strong correlation with actual SPI data or by adding more training data to the model (predicting SPI values for a period before 1970). After testing the system

CIM (NARX and ANFIS) and running it, a significant convergence shown between the predicted SPI values by NARX and predicted SPI values by ANFIS. The average prediction error found to be 27.78% as illustrated in (Figure 3.28).

4.4 Computational Methods

In this study, two computational methods as the Standardized Precipitation Drought Index (SPI) and Soil Conservation Service (SCS-CN) used to analyze the drought and runoff conditions. The results related to these methods can illustrated as follows.

a. The drought assessed in three periods from 1970 to 1992, 1992 through 2017 and for predicted period 2017-2026. The average annual rainfall for the study area is 512.6 mm. The drought assessment results for periods from 1970 to 1992 and from 1992 through 2017 shows that the study area affected by different drought levels where the deficit amount of rainfall ranged from 27% to 34%. The estimated values of drought magnitude (DM), drought duration (DD), average drought intensity (ADI), and drought years in two periods calculated as shown in (Table 4.6). This analysis shows that the drought years increased by 1.8% causing an increase in the drought magnitude by 106.5 mm during the two studied periods. This analysis confirmed the results of the analysis of remote sensing in relation to the decline of vegetation and increased desertification land within the study area.

Table 4.6 : Drought assessment in two studied periods.

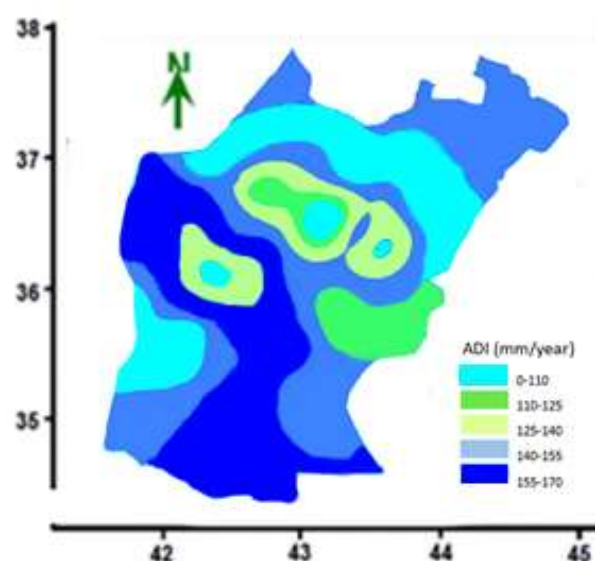
| Drought characteristics | Analysis period (1970-1992) | Analysis period (1992-2017) |
|----------------------------------|-----------------------------|-----------------------------|
| Drought years % | 46.5 | 48.3 |
| DM (mm) | 3433 | 3539.5 |
| DD (year) | 2.3 | 2.4 |
| ADI (mm/year) | 95.74 | 99.67 |
| Increased drought magnitude (mm) | | 106.5 |

b. When the predicted rainfall records from 1970 to 2026 that obtained from developed CIM model were involved in this comparison, and according to (Table 4.7) the highest value of drought magnitude (4655 mm) occurred in Hadher station with an average drought intensity of 148.62 mm/year and a drought duration of 1.9 per year.

Table 4.7 : Drought results according to rainfall records (actual and predicted).

| Stations | Actual rainfall records | | | | Predicted rainfall records | | | | Increased drought magnitude mm |
|----------|-------------------------|-------|---------|-------------|----------------------------|---------|---------|-------------|--------------------------------|
| | Drought years % | DM mm | DD year | ADI mm/year | Drought years % | DM mm | DD year | ADI mm/year | |
| Mosul | 46.5 | 3433 | 2.3 | 95.74 | 48.3 | 3539.5 | 2.4 | 99.67 | 106.5 |
| Sinjar | 52.7 | 3134 | 3.8 | 128.36 | 53.9 | 3368.3 | 3.9 | 137.94 | 234.3 |
| Tel-Afar | 54.0 | 3083 | 3.2 | 131.21 | 56.3 | 3271.7 | 3.6 | 139.24 | 188.7 |
| Rabiaa | 51.4 | 2709 | 2.9 | 101.63 | 52.8 | 2911.8 | 2.4 | 109.24 | 202.8 |
| Bashiqah | 48.7 | 2007 | 2.7 | 85.23 | 49.4 | 2136.7 | 2.9 | 90.47 | 129.7 |
| Hadher | 58.8 | 4655 | 1.9 | 148.62 | 61.5 | 5051.5 | 2.0 | 161.28 | 396.5 |
| Total DM | | 19021 | | | Total DM | 20279.5 | | | 1258.5 |

The percentage of the drought years increased by 10.1% with increasing drought magnitude by 1258.5 mm during the nine years to 2026 in all study area. If this percentage continues to increase every nine years, the study area will suffer from drought affect on the agricultural structure and the vegetation cover in particular and the environment in general. The predicted analysis results shows that, the drought levels in the southern and western regions of the study area (Sinjar, Tel-Afar, and Hadher stations) increased during the predicted period (2017-2026) by 6.2%, as drought year with increased drought magnitude by 819.5 mm compared to the northern and eastern parts (Mosul, Rabiaa, and Bashiqah) where the drought year is 3.9% with an expected increased drought magnitude of 439 mm during this period and this has been clarified when calculating the predicted average drought intensity (ADI) for the period 2017-2026 as shown in (Figure 4.26).

**Figure 4.26 :** Predicted average drought intensity for the period (2017-2026).

The actual SPI from 1970 to 2017 calculated for the six stations using the gamma function that evaluated by Edwards and McKee (1997). All drought conditions were observed that the entire study area affected by different drought levels where the average drought years and average wet years were calculated as 54.4% and 45.6% respectively. In addition, the drought analysis shows that the moderate drought conditions ranging from -1.053 to -1.495, severe drought from -1.521 to -1.862 and extreme drought conditions from -2.107 to -2.865. The SPI charts represent different timescales give an impression about drought characteristics and climate change effects in the study area as illustrated in (Figure 4.27). This figure shows the climate condition over the studied period where the upper part of the x-axis represents the wet years while the bottom part of the x-axis represents the drought years and drought levels.

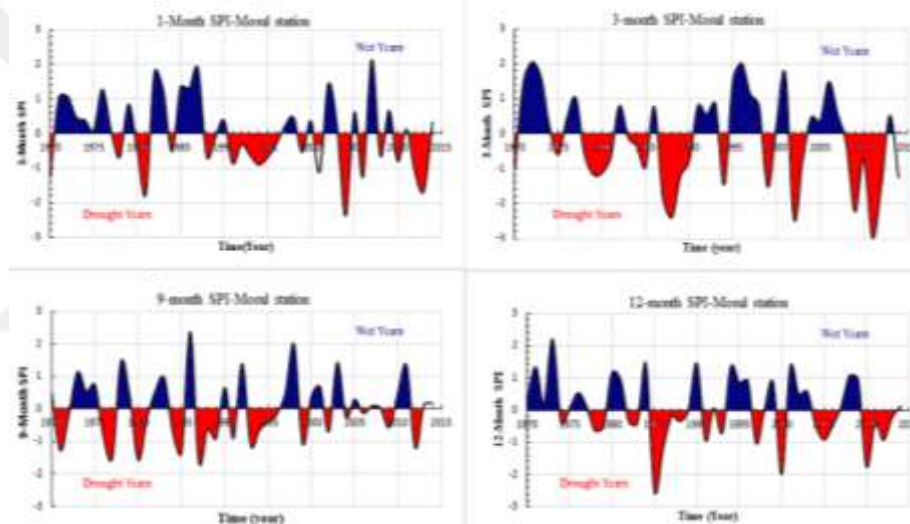


Figure 4.27 : Different timescales SPI charts for Mosul station.

Figure 4.28 can be illustrated the drought levels for different SPI timescales where this figure shows that drought levels increased over time in the study area. All the results obtained from drought analysis indicate that the study area suffers from successive droughts levels.

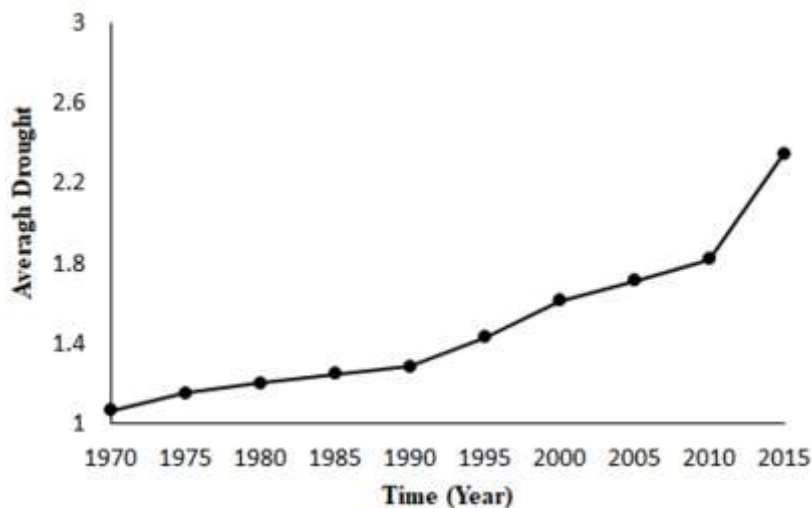


Figure 4.28 : Average drought with different SPI timescales.

Short and long-term meteorological drought (SPI-3 and SPI-12) adopted to assessment meteorological drought in the study area. SPI-3 time-scale as a short-term drought assessment where this index is suitable for agricultural applications as an effective index for moisture conditions analysis for agricultural lands in a growing season dependent on seasonal precipitation (Tian et al, 2018). The study area known as agricultural lands that produce wheat and barley crops, which depend on the rainy season for their growth. These areas found in the northwest and southwest of the study area.

The SPI-3 is therefore very appropriate for analyzing the drought levels in these lands for the next few years. The predicted SPI-3 analysis showed that the land surrounding the stations (Sinjar, Tal Afar, and Hadher) would suffer from increased droughts during the predicted period (2017-2026) where moderate drought will occur in land surrounding Tal Afar station during the period 2017-2020, while extremely drought will occur in 2021-2026. Moderate drought, severe drought, and extreme drought will occur on land surrounding Sinjar station during the periods 2017-2018, 2018-2019, and 2020-2026 respectively. In the lands surrounding Hadher station moderate drought, severe drought, and extreme drought will occur during the period 2017-2019, 2019-2023, and 2023-2026 respectively as shown in (Table 4.8).

Table 4.8 : Predicted SPI-3 classification for the period (1956-2026).

| Station name | SPI-3 classification | | | | | |
|--------------|----------------------|-----------|----------------|-----------|-----------------|-----------|
| | Moderate drought | Year | Severe drought | Year | Extreme drought | Year |
| Tel-Afar | -1.011 | 1951-1952 | -1.728 | 1971-1972 | -2.161 | 2009-2010 |
| | -1.253 | 1958-1959 | -1.756 | 1973-1974 | -2.224 | 2021-2022 |
| | -1.139 | 1962-1963 | | | | |
| | -1.466 | 1977-1978 | | | | |
| | -1.045 | 1984-1985 | | | | |
| | -1.011 | 1987-1988 | | | | |
| | -1.248 | 2000-2001 | | | | |
| | -1.171 | 2007-2008 | | | | |
| | -1.262 | 2008-2009 | | | | |
| | -1.132 | 2017-2018 | | | | |
| Sinjar | -1.262 | 1928-1929 | -1.5024 | 1940-1941 | -2.867 | 1995-1996 |
| | -1.103 | 1957-1958 | -1.892 | 1953-1954 | -2.162 | 1999-2000 |
| | -1.516 | 1964-1965 | -1.661 | 1996-1997 | -2.428 | 2014-2015 |
| | -1.469 | 1979-1980 | -1.516 | 2018-2019 | | |
| | -1.284 | 2006-2007 | | | | |
| | -1.351 | 2016-2017 | | | | |
| Hadher | -1.368 | 1937-1938 | -1.884 | 1929-1930 | -2.262 | 1965-1966 |
| | -1.181 | 1980-1981 | -1.792 | 1949-1950 | -2.267 | 1989-1990 |
| | -1.841 | 1996-1997 | -1.736 | 2007-2008 | -3.276 | 2011-2012 |
| | -1.333 | 2003-2004 | | | -2.573 | 2017-2018 |
| | | | | | -2.761 | 2020-2021 |

For long-term drought assessment, the values of SPI-12 directly related to the state of stream flows, reservoirs levels, and groundwater levels. These values can explain the environmental changes resulting from drought and desertification that can occur in an area over a long period. When analyzing the SPI-12 for the study area using actual and predicted SPI, it found that the region would generally experience extreme drought conditions except for the Sinjar area, where the drought condition predicted to be severely dry as seen in (Table 4.9).

Table 4.9 : Predicted SPI-12 classification for the period (2017-2026).

| Station | SPI-12 classification | | | | | |
|----------|-----------------------|-----------|----------------|-----------|-----------------|-----------|
| | Moderate drought | Year | Severe drought | Year | Extreme drought | Year |
| Mosul | -1.158 | 2018-2019 | -1.862 | 2016-2017 | -2.267 | 2020-2026 |
| Tel-Afar | -1.319 | 2018-2019 | -1.540 | 2016-2017 | -2.820 | 2020-2026 |
| Sinjar | -1.480 | 2015-2016 | -1.685 | | | |
| | -1.073 | 2018-2019 | | 2020-2021 | | |
| Hadher | -1.192 | 2015-2016 | | | -2.267 | |
| | -1.158 | 2017-2018 | | | | 2020-2026 |
| Rabiaa | | | | | -2.107 | 2017-2018 |
| | | | | | -2.865 | 2020-2026 |
| Bashiqah | -1.373 | 2017-2018 | -1.521 | 2014-2015 | -2.380 | 2020-2026 |

This distribution maps as seen in (Figure 4.18) discussed according to drought levels moderate drought, severe drought, and extreme drought that probably accrued in the

study area in the predicted period from 2017 to 2026. Due to the increase in drought years and the decreasing of the average annual rainfall from (512.6 to 396.7) mm. A moderate drought condition was observed which affected the entire study area ranging from (-1.053 to -1.495) as shown in (Figure 4.18-a). Severe drought will also affect the study area where it will range from (-1.521 to -1.862) as shown in (Figure 4.18-b). The eastern part will be negatively affected by extreme drought condition ranging between (-2.107 to -2.865). The study area represents a part of the feeding area of the Tigris River inside Iraq throughout many tributaries, this means lower river water levels in the future; thus the groundwater recharging system will be damaged and impact negatively on the supply of groundwater wells scattered in the study area as shown in (Figure 4.18-c).

b- The Soil Conservation Service (SCS-CN) method adopted to determining annually runoff depth (actual and predicted) values that conducted on Al-Murr basin that located in the north-west of Nineveh province north of Iraq. The comparison and analysis results for runoff depth (actual and predicted) values illustrated below. For a given rainfall data onto 1956-2017, the soil type of the study area is classified under group C (Type: clayey loam) and CN equals 79 for normal condition as illustrated in (Table 4.10) (Sabar and Mohamed 2013).

Table 4.10 : Curve number for three antecedent moisture conditions.

| AMC | I | II | III |
|-------|--------|--------|--------|
| CN | 61.24 | 79 | 89.639 |
| S(mm) | 160.76 | 67.518 | 29.3 |

The runoff depth and the volume of water calculated for each year using the CV method procedures that illustrated in chapter three section 3.4.2 and the obtained runoff results illustrated in (Table 4.11). After testing the performance and prediction accuracy of the model. Average predicted rainfall (2018-2050) estimated. This data was feedback on equation 3.10 to get predicted runoff values as seen in (Table 4.12). The future planning for managing the water quantities in Al Murr basin illustrated in GIS section (c) in this chapter. The relationship between the rainfall-runoff derived from the new time series (actual and predicted) which have accuracy represented by the equation $y=0.9661*x-56.578$ with $R^2=0.9995$ as given in (Figure 4.29).

Table 4.11 : Calculated runoff (mm) and water volume (m³) per year.

| Year | rainfall mm | runoff mm | Water volume *10 ³ m ³ | Year | rainfall mm | runoff mm | Water volume *10 ³ m ³ |
|------|----------------|--------------|--|---|----------------|--------------|--|
| 1956 | 312.5 | 243.882 | 0.599 | 1987 | 280.3 | 212.881 | 0.523 |
| 1957 | 421.5 | 350.028 | 0.861 | 1988 | 760.5 | 685.033 | 1.685 |
| 1958 | 314.7 | 246.007 | 0.605 | 1989 | 267.6 | 200.720 | 0.493 |
| 1959 | 219.5 | 155.115 | 0.381 | 1990 | 295.7 | 227.680 | 0.560 |
| 1960 | 273.7 | 206.556 | 0.508 | 1991 | 321.2 | 252.293 | 0.620 |
| 1961 | 300.3 | 232.110 | 0.570 | 1992 | 411.9 | 340.625 | 0.837 |
| 1962 | 220.7 | 156.242 | 0.384 | 1993 | 476.8 | 404.328 | 0.994 |
| 1963 | 539.2 | 465.823 | 1.145 | 1994 | 387.1 | 316.376 | 0.778 |
| 1964 | 274.7 | 207.513 | 0.510 | 1995 | 494.0 | 421.258 | 1.036 |
| 1965 | 328.5 | 259.361 | 0.638 | 1996 | 348.1 | 278.379 | 0.684 |
| 1966 | 215.6 | 151.456 | 0.372 | 1997 | 382.8 | 312.178 | 0.767 |
| 1967 | 375.8 | 305.348 | 0.751 | 1998 | 343.8 | 274.202 | 0.674 |
| 1968 | 568.5 | 494.761 | 1.217 | 1999 | 148.6 | 90.053 | 0.221 |
| 1969 | 469.3 | 396.951 | 0.976 | 2000 | 184.9 | 122.931 | 0.302 |
| 1970 | 242.9 | 177.200 | 0.435 | 2001 | 402.5 | 331.427 | 0.815 |
| 1971 | 342.5 | 272.940 | 0.671 | 2002 | 335.0 | 265.662 | 0.653 |
| 1972 | 607.5 | 533.329 | 1.311 | 2003 | 315.0 | 215.662 | 0.551 |
| 1973 | 294.5 | 226.525 | 0.557 | 2004 | 302.0 | 233.749 | 0.575 |
| 1974 | 417.0 | 345.619 | 0.850 | 2005 | 284.0 | 216.432 | 0.532 |
| 1975 | 302.2 | 233.942 | 0.575 | 2006 | 232.0 | 166.886 | 0.410 |
| 1976 | 412.0 | 340.723 | 0.838 | 2007 | 36.0 | 5.616 | 0.013 |
| 1977 | 275.5 | 208.280 | 0.512 | 2008 | 236.1 | 170.761 | 0.420 |
| 1978 | 305.5 | 237.124 | 0.583 | 2009 | 357.1 | 287.131 | 0.706 |
| 1979 | 221.7 | 157.182 | 0.386 | 2010 | 289.7 | 221.908 | 0.545 |
| 1980 | 449.8 | 377.788 | 0.929 | 2011 | 64.8 | 22.134 | 0.054 |
| 1981 | 466.1 | 393.805 | 0.968 | 2012 | 181.6 | 119.899 | 0.294 |
| 1982 | 452.9 | 380.833 | 0.936 | 2013 | 244.5 | 178.718 | 0.439 |
| 1983 | 370.6 | 300.278 | 0.738 | 2014 | 221.7 | 157.182 | 0.386 |
| 1984 | 249.2 | 183.181 | 0.450 | 2015 | 215.6 | 151.456 | 0.372 |
| 1985 | 358.7 | 288.688 | 0.710 | 2016 | 302 | 233.749 | 0.575 |
| 1986 | 333.1 | 263.819 | 0.648 | 2017 | 345 | 275.162 | 0.757 |
| | | | | Total water volume: 19.856*103 m ³ | | | |
| | | | | Average runoff : 287.83 mm | | | |

Table 4.12 : Runoff estimated results from predicted rainfall values.

| Year | Rainfall mm | Runoff mm | Water volume *10 ³ m ³ | Year | Rainfall mm | Runoff mm | Water volume *10 ³ m ³ |
|------|----------------|--------------|--|--|----------------|--------------|--|
| 2018 | 377.79 | 310.86 | 0.764 | 2035 | 158.21 | 22.134 | 0.070 |
| 2019 | 393.83 | 321.00 | 0.871 | 2036 | 320.95 | 119.89 | 0.425 |
| 2020 | 110.00 | 276.41 | 0.570 | 2037 | 241.0 | 178.71 | 0.264 |
| 2021 | 219.40 | 385.30 | 0.961 | 2038 | 239.0 | 157.18 | 0.272 |
| 2022 | 222.00 | 384.00 | 0.945 | 2039 | 248.0 | 151.45 | 0.211 |
| 2023 | 242.00 | 250.11 | 0.585 | 2040 | 253.0 | 233.74 | 0.514 |
| 2024 | 250.01 | 246.44 | 0.538 | 2041 | 200.17 | 275.16 | 0.584 |
| 2025 | 327.42 | 305.00 | 0.751 | 2042 | 342.83 | 320.00 | 0.798 |
| 2026 | 308.32 | 295.00 | 0.509 | 2043 | 321.42 | 325.00 | 0.405 |
| 2027 | 201.55 | 304.00 | 0.749 | 2044 | 214.40 | 170.7 | 0.341 |
| 2028 | 172.71 | 240.97 | 0.524 | 2045 | 315.32 | 287.1 | 0.551 |
| 2029 | 300.32 | 216.43 | 0.514 | 2046 | 330.95 | 244.0 | 0.534 |
| 2030 | 230.74 | 166.88 | 0.428 | 2047 | 232.00 | 312.38 | 0.756 |
| 2031 | 261.00 | 40.00 | 0.136 | 2048 | 219.90 | 280.0 | 0.591 |
| 2032 | 285.83 | 170.76 | 0.206 | 2049 | 308.32 | 295.00 | 0.509 |
| 2033 | 259.00 | 210.00 | 0.513 | Total water volume : 12.41 *10 ³ m ³ | | | |
| 2034 | 262.00 | 118.00 | 0.262 | Average runoff : 234.62 mm | | | |

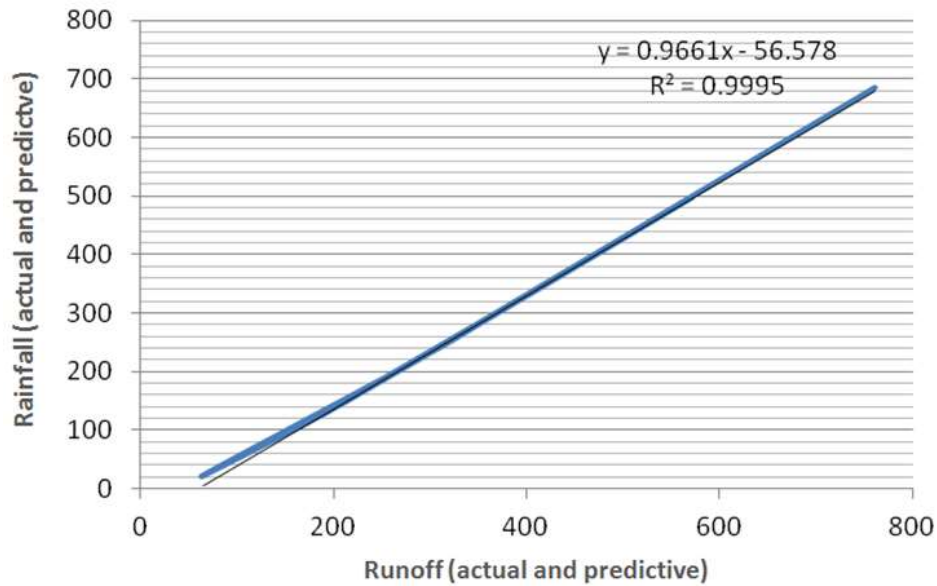


Figure 4.29 : The relationship between the rainfall-runoff in AL Murr basin.

4.5 Statistical Analysis

A kind of statistical analysis done using temporal variations analysis and spearman's rank correlation techniques. The results of these statistical analysis techniques illustrated as follows.

a. Statistically, temporal variations analysis between SPI, runoff, rainfall, temperature, and sandstorm event for the period 1992-2017 the relationships between these variables have been analyzed. Firstly, these data have standardized based on the standard deviation and mean values as been mathematically described as illustrated in equation 4.1 and equation 4.2.

$$z = \frac{X - \mu}{\sigma} \quad (4.1)$$

Where,

X= the observation.

M= the mean.

σ= the standard deviation as illustrated in equation 4.2.

$$\sigma = \sqrt{\frac{\sum |x - \mu|^2}{N}} \quad (4.2)$$

Where,

N= the number of data points in the population

Where, the data is transformed using the mean and standard deviation for the whole set, so it ends up in a standard distribution with a mean of 0 and a variance of 1 as shown in (Table 4.13). Then the correlation analysis has developed. Through this analysis, it is found that from 1992 to 2017 remarkable behavior of the data series are evident. Where a reduction in runoff noticed in this period (only a small amount of runoff in 2016) and drought satiation fluctuated between moderate to extreme drought where all these events accompanied by an abnormal increase in the sandstorms frequency happened in the study area (Figure 4.30). The same remarkable behavior of rain, temperature, and sandstorm events has been monitored where the analysis for the same period from 1992 to 2017 shows increasing in sandstorm events with almost equal temperatures close to the average monthly temperature 28.3° while the rain decreasing as illustrated in (Figure 4.31). Respect to this analysis it seems that there is a relationship of increasing temperature, decreasing rain, drought expansion on the one

hand and reduction in a runoff with increasing dust and sand storms events on the other.

Table 4.13 : Data standardization using excel.

| year | Rain | St. Rain | Temp. | St. Temp. | Storm Event | St. Storm Event |
|------|-------|----------|-------|-----------|-------------|-----------------|
| 1992 | 411.9 | 1.156 | 26.6 | -2.431 | 40 | -0.974 |
| 1993 | 476.8 | 1.769 | 27.8 | -0.751 | 46 | -0.7681 |
| 1994 | 387.1 | 0.921 | 27.8 | -0.739 | 40 | -0.974 |
| 1995 | 494.0 | 1.932 | 28.2 | -0.247 | 20 | -1.660 |
| 1996 | 348.1 | 0.552 | 27.0 | -1.879 | 21 | -1.626 |
| 1997 | 382.8 | 0.880 | 29.2 | 1.299 | 23 | -1.557 |
| 1998 | 343.8 | 0.512 | 29.5 | 1.611 | 60 | -0.287 |
| 1999 | 148.6 | -1.333 | 28.6 | 0.328 | 70 | 0.055 |
| 2000 | 184.9 | -0.990 | 28.8 | 0.616 | 96 | 0.947 |
| 2001 | 402.5 | 1.067 | 28.1 | -0.331 | 61 | -0.253 |
| 2002 | 335.0 | 0.428 | 28.0 | -0.482 | 45 | -0.802 |
| 2003 | 335.0 | 0.428 | 28.2 | -0.180 | 48 | -0.699 |
| 2004 | 302.0 | 0.116 | 28.5 | 0.196 | 41 | -0.939 |
| 2005 | 284.0 | -0.053 | 27.9 | -0.631 | 48 | -0.699 |
| 2006 | 232.0 | -0.544 | 28.6 | 0.436 | 74 | 0.192 |
| 2007 | 98.0 | -1.811 | 29.3 | 1.371 | 100 | 1.084 |
| 2008 | 236.1 | -0.506 | 28.2 | -0.247 | 81 | 0.432 |
| 2009 | 357.1 | 0.637 | 30.1 | 2.511 | 66 | -0.081 |
| 2010 | 289.7 | 0.0006 | 28.2 | -0.139 | 88 | 0.673 |
| 2011 | 64.8 | -2.125 | 28.8 | 0.604 | 105 | 1.256 |
| 2012 | 181.6 | -1.021 | 28.1 | -0.331 | 91 | 0.776 |
| 2013 | 244.5 | -0.426 | 28.6 | 0.316 | 110 | 1.428 |
| 2014 | 233.0 | -0.535 | 28.1 | -0.403 | 95 | 0.913 |
| 2015 | 189.0 | -0.951 | 28.6 | 0.316 | 126 | 1.977 |
| 2016 | 256.0 | -0.317 | 28.3 | -0.115 | 87 | 0.638 |
| 2017 | 312.0 | 0.211 | 27.9 | -0.691 | 96 | 0.947 |
| | Av. | 289.626 | Av. | 28.380 | Av. | 68.384 |
| | St. | 105.769 | St. | 0.694 | St. | 29.140 |

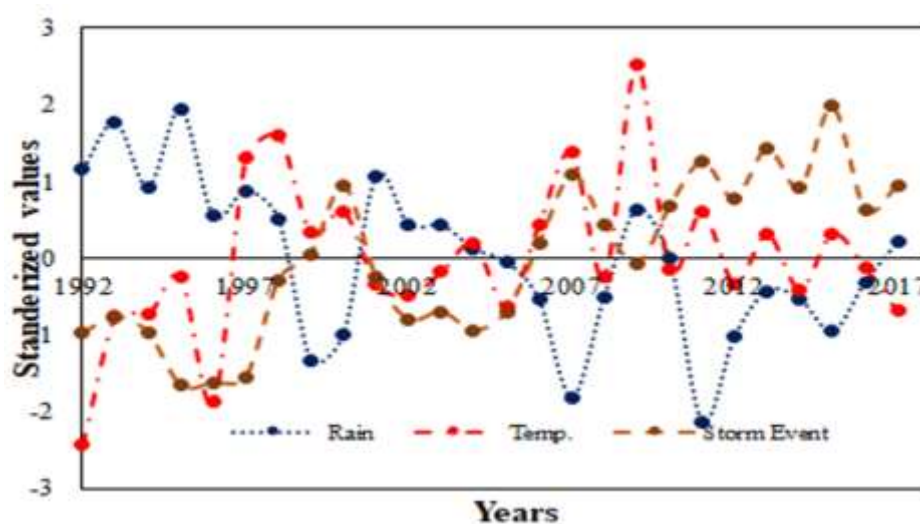


Figure 4.30 : Rainfall, temperature and storms temporal variation analysis.

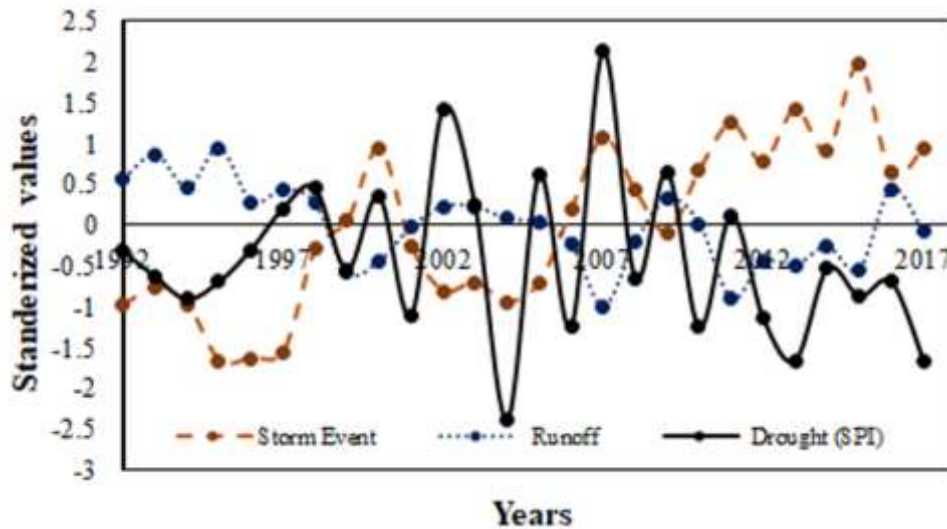


Figure 4.31 : Temporal variation analysis of runoff, drought and storm events.

Spearman's rank correlation technique has applied to summarize the strength (negative or positive) between the sandstorms frequency and rainfall, temperature, runoff and SPI. Also, rank correlation relationship between SPI with each of rainfall and temperature. The rank correlation results show a positive rank correlation between SPI and temperature equal $+0.33$ and a negative rank correlation between SPI and rainfall equal -0.65 where these results seem reasonable. While the rank correlation relationship analysis between sandstorms frequency and each of temperature, rainfall, runoff and SPI shows positive rank correlation equal $+0.45$ and $+0.16$ for temperature and SPI respectively. The value $+0.16$ seems small but this does not prevent a positive relationship between increased sandstorms frequency and increased droughts in the study area. Negative relationships between sandstorms frequency and each of rainfall and runoff equal -0.78 and -0.61 respectively and that seem reasonable.

b. Temporal variation analysis done to examine the behavior of selected weather variables (only for rainfall and temperature) by comparing their status over time in actual stage (1992-2016) and predicted stage (2016-2040). Based on the mean and the standard deviation the variables data set were standardized firstly, then behaviors were clarified where through this analysis remarkable behaviors were discovered. In the actual stage, the behavior of rainfall and temperature can be set as a normal structure time series and make this behavior as a reference to the analysis of the predicted stage. As seen in (Figure 4.32) the temperatures increasing with time followed by a significant decreasing in rainfall especially in the last predicted ten years (2030-2040).

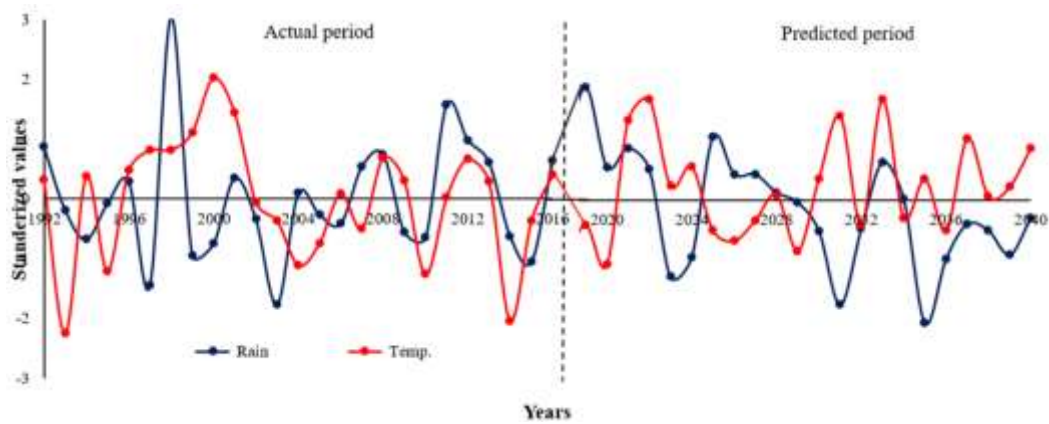


Figure 4.32 : Temporal variation analysis of rainfall and temperature.

To illustrate the strength (negative or positive) correlation between rainfall and temperature in actual and predicted stages, Spearman's rank correlation technique applied to clarify this correlation. The rank correlation results show a positive correlation for the temperature equals + 0.49 and negative rank correlation for rainfall equals - 0.65. These unexpected results carry one meaning that there will be a significant change in the climate of the study area in the coming years.

5. CONCLUSIONS AND RECOMMENDATIONS

As with many aspects of any scientific research, data is a human creation, so it may have some limits on its usability. Here's an overview of some limitations likely encountered. The meteorological data could be incomplete. Missing values, even the lack of a section or a substantial part of the data, could limit its usability. For the meteorological data that used in this study, it was noted that there is a lack of data records for some years for the variables records of the stations in this study. This lack of data is due to a number of reasons, including the study area being held by terrorist organizations, this led to the inability of the operators of these stations to take the climate readings at the time. This lack of data was addressed by taking the average of available data at the beginning and end of the interruption period. Remote sensing is expensive and not cost-effective for collecting details for a small area. In this study in the section of remote sensing applications for detecting and classifying the decreasing in vegetation cover and NDVI analysis the available remote sensing data was only two temporal satellite images from Landsat sensors taken by enhanced thematic mapper (ETM+) sensor board on Landsat7 were used. The resolution of these images (30 m) would make the classification of some pixels unreliable. Which may affect the accuracy of the classification, so for this kind of studies high resolution images must be used like IKONOS or Landsat Enhanced Thematic Mapper Plus (ETM+). Recent advances in Artificial Intelligence procedures hold great potential for converting a deluge of data into weather forecasts that are fast, accurate, and detailed. To adapt these procedures to weather-related applications it's critical to meet certain fundamental needs at multiple spatial and temporal scales for diverse geophysical domains. Artificial Intelligence have some disadvantages in weather studied applications where, technical problems related to used computer and software, Artificial Intelligence still immature and needs significant improvement and Artificial Intelligence models need a massive data set to learn from, before they can predict on their own all these outlines have several limitations of using Artificial Intelligence procedures in weather studies.

The obtained results from this study can be represented by the following views where vegetation cover changes, drought area expansion, increasing dust and sand storm events, changes in temperature and rainfall behaviors with time can be considered as the main cause that increased the desertification phenomenon in the study area. The objective of this study was to adopt scientific procedures that can be used as powerful analysis tools for combating this phenomenon. The study hypothesis was answered by implementing the methodologies that were used for analyzing remote sensing data, creating GIS spatial distribution maps, tracking dust and sandstorm events, designing Artificial Intelligent models for predicting weather variables and using some computational methods with a kind of statistical analysis were prepared. In this context, the used methodology has the following advantages.

1. It is important to evaluate and monitor the vegetation cover using remote sensing techniques to minimize and avoid long-term consequences and any slightest change that possibly happens to this cover with time. Taking into account the possibility of integrating remote sensing with GIS to prepare necessary maps and create databases that consist of different layers of information to manage this cover.
2. Studying the speed and direction of winds is very important to knowing the annual paths of frequent dust and sand storms events and their relationship with the sources of dust and sand grain. However, they need practical application tracking analysis of these storms that occurred in the study area in order to update storms databases with respect to the theoretical paths and the periods of occurrence.
3. Tracking the storm that happened on 24 March 2017 is a good example for analyzing dust and sand storms events in the study area. This kind of storm has a role for increasing the drought areas that were observed through statistical analysis. Using two types of data for analysis and comparison, the first kind of data are “observed data” including all meteorological data and the second type are the “estimated data” that have a close relationship with the drought situation like different drought indices, estimation runoff and evaporation values. The obtained results from this study show that there are many reasons for increasing the local or regional dust and sand storms in the study area where the strongest one is the global climate change.
4. As part of daily life, Artificial Intelligence offers various solutions in various fields, trying to answer questions using different mathematical approaches. In the field of

weather forecasting, Artificial Intelligent showed the ability to provide future data with the lowest possible error depending on the type of the used mathematical approach and the ability of the programmer to deal well with the available data and the structure of the used algorithm. The performances of three effective artificial neural networks, RBF, NARX and FCM investigated for purpose of forecasting four weather variables where twelve sub-models designed to accomplish this matter. Moreover, prediction or forecasting is a powerful ability that Artificial Intelligent characterized by. This ability is effective in serving humanity if it can meet the conditions of realism and accuracy through the obtained results.

5. There are many benefits to assessing the drought conditions of a region using the Standardized Precipitation Index (SPI) because it requires only one type of input in the form of rainfall records and easy mathematical equations. The SPI index characterized by its ability to classify droughts as moderate, severe, or extreme to give a clearer indication of the conditions of any area in terms of the effect of drought. In addition, it is possible to calculate the drought characteristics by calculating its duration, intensity, magnitude, and average. Accurate forecasting of rainfall with long-time response is essential to predict runoff where the methods of Artificial Intelligent have proved by developing models that are capable to simulate the various inputs characteristics of these basins to find the best model that has the ability and possibility to predict the values of runoff with the least possible statistical errors.

In the most general terms, the main steps followed in implementing methodology used in this study should be tacking in to account by developing plans to achieve the following.

- a. Develop a meteorological database that needed in analysis for combating desertification.
- b. Developing a multipurpose flowchart to represent the desertification risk for both government and the public.
- c. Pay attention to the techniques of remote sensing, GIS and Artificial Intelligent and developing models that integrated these techniques in one model if possible.

Indeed, desertification causes must be studied carefully tacking in to account all the factors that range between the climate changes to human activity. Many plans can selected to combating the desertification phenomena expansion in the study area like

establishment water harvesting projects, choosing agricultural activities for the next agricultural season, domestic water supply, and supplemental irrigation and for fish farming depending on availability of water as examples.

Finally, the used procedure in this study can help the decision-makers in proving their plans to avoiding the risk of this phenomenon in the future by analyzing the possible strategies to mitigate the effects of this phenomenon not only for the study area but also for all Iraq's provinces.

As with many aspects of any scientific research, data is a human creation, so it maybe has some limits on its usability. Here's an overview of some limitations likely encounter. The meteorological data could be incomplete. Missing values, even the lack of a section or a substantial part of the data, could limit its usability. For the meteorological data that used in this study, it was noted that there is a lack of data records for some years for the variables records of the stations in this study. This lack of data is due to a number of reasons, including the study area being held by terrorist organizations, this led to the inability of the operators of these stations to take the climate readings at the time. Furthermore, there is uncertainly in spasiel resolution of measuring this data. This lack of data was addressed by taking the average of available data at the beginning and end of the interruption period.

Remote sensing is expensive and not cost-effective for collecting details for a small area.in this study in the section of remote sensing applications for detecting and classified the decreasing in vegetation cover and NDVI analysis the available remote sensing data was only two temporal satellite images from Landsat sensors taken by enhanced thematic mapper (ETM+) sensor board on Landsat7 were used. The resolution of these images (80) m would make the classification of some pixels unreliable Which may affect the accuracy of the classification, so for this kind of studies high resolution images must be used like IKONOS or Landsat Enhanced Thematic Mapper Plus (ETM+). Recent advances in Artificial Inelegant procedures hold great potential for converting a large datsed time series into weather forecasts that are fast, accurate, and detailed. To adapt these procedures to weather-related applications it's critical to meet certain fundamental needs at multiple spatial and temporal scales for diverse geophysical domains. Artificial Inelegant have some disadvantages in weather studied applications where, technical problems related to used computer and software, Artificial Inelegant still immature and needs significant

improvement and Artificial Inelegant models need a massive data set to learn from, before they can predict on their own all these outlines have several limitation of using Artificial Inelegant procedures in weather studies). Reliability of results is how consistently of used methodologies for gaining obtained measuring results, especially when apply the same methods to the same dataset under the same conditions. Many factors can effected the obtained results at different ways, for example, using developed artificial models based on different functions for the same dataset to predicting data time series where the results might be affected by the ability of these functions to respond accurately results so in this case different functions must be tested in the same model to ensure the reliability of results by comparing all gained results as well as comparing these results with previous work might be imported to get more reliability.

Depending on the degree of desertification that gained from the results obtained from this study many recommendations should be taken into account to combating or reverse the effects of this phenomenon in the study area. These recommendations listed below.

1. Establish long-term strategic plans

- a. The complex situation between climate change and desertification must studied with caution. The change in temperature and rain behaviors over time should not underestimated, as this change will lead to largely eliminates or changes the various species composition for the study area.
- b. Cultivation of windbreaks includes planting lines of selected species of fast-growing trees in areas corresponding to prevailing surface winds. Itis hoped that these windbreaks stop the movement of sand dunes and reduce the risk of dust and sandstorms especially in the west and southwest of the study area.
- c. Monitoring and assessment the vegetation cover in the study area periodically with the need to re-cultivate the areas affected by elected plants that fit the current climate situation.
- d. Preserving the rainfall quantity as non-traditional water resources by establishing water-harvesting projects in different areas of the study area where the diversity in geomorphological forms helps to establish several forms of these projects.

- e. Encourage the research centers in Nineveh governorate to update the geo-environmental classification map of the Nineveh governorate and create another kind of maps that can be useful for study desertification.
- f. Encourage farmers to change the usual agricultural plan by growing crops that are more resistant to current climate change conditions and provide free financial and advisory support.
- g. Rationalization water consumption used for agriculture using modern irrigation methods such as drip irrigation.
- h. Prevention of overgrazing, especially at the western and southern part of the study area, to give the natural vegetation cover a chance to spreading normally.

2. Building a knowledge base

Building a knowledge base is an essential step to face the challenges of desertification. This step should be managed by a group of researchers with different specialities where, workshops, seminars, technical meetings and conferences must be held to exchange information to define the baseline of desertification in the study area.

Furthermore, the role of the decision-makers should be activated through various activities such as direct the media in all its forms to raise awareness to the public of the dangers of this phenomenon. In addition, the dangerous effects of this phenomenon must be taken seriously by the Ministry of Education to educate the younger generations in schools and kindergartens by printing simple explanatory texts to explain the dimensions of this phenomenon. As well as the Iraqi government, should be adapting various media sources to focus on the risks of this phenomenon also professional educating activities should be arranged as basic solutions to raise public awareness. This problem must be presented to the international forums and request scientific and financial aid from the UN organization like the United Nations Convention to Combat Desertification UNCCD or United Nations Environment Programme UNEP to combat this phenomenon. Furthermore, a regional network must be established by the Iraqi government for exchanging the information about this phenomenon with surrounding countries where desertification effects began to appear in their territories.

REFERENCES

- Abhishek, K., Kumar, A., Ranjan, R. and Kumar, S.** (2012). A rainfall prediction model using artificial neural network. *Control and System Graduate Research Colloquium (ICSGRC)*, 2012 IEEE, pp. 82–87. IEEE.
- Abrosimov, M., Brovko, A.** (2019). High Generalization Capability Artificial Neural Network Architecture Based on RBF-Network. In *International Conference on Information Technologies* (pp. 67-78). Springer, Cham.
- Ahmad, A., Upadhyay, R., Lal, B. and Singh, D.** (2018). Change Detection of Sodic Land in Raebareli District Using Remote Sensing and GIS Techniques. In *Environmental Pollution* (pp. 487-498). Springer, Singapore.
- AFCC. Air Force Combat Climatology Center** (1995). Operational Climatic Data Summary for Iraq. Iraq: Air Force Combat Climatology Center.
- Ajay, D., Malakiya S. and Suryanarayana, T.** (2016). Assessment of Drought Using Standardized Precipitation Index (SPI) and Reconnaissance Drought Index (RDI). A Case Study of Amreli District, *International Journal of Science and Research (IJSR)*, Volume 5 Issue 8, August 2016, Pp.1995-2001.
- Al-Daghistani, H.** (2007). Geomorphologic Map of Nineveh Governorate, Northwestern Iraq Using Visual Image Interpretation. , *18* (1 E), pp.81-90.
- Al-Daghistani, H.** (2008). Land Use and Land Cover Map of Ninevah Governorate Using Remote Sensing Data. *Iraqi National Journal of Earth Sciences*, 8(2), pp.17-26.
- Al-janabi, S.** (2010). *Climate of Mosul City*. Mosoliya studies, (28), pp.1-16.
- Al-Jiburi, H. and Al-Basrawi, N.** (2015). HYDROGEOLOGICAL MAP OF IRAQ, SCALE 1: 1000 000, 2013. *Iraqi Bulletin of Geology and Mining*, 11(1), pp.17-26.
- Anderson, D. and McNeill, G.** (1992). Artificial neural networks technology. *Kaman Sciences Corporation*, 258(6), pp.1-83.
- Arabeyyat, O., Shatnawi, N. and Matouq, M.** (2018). Nonlinear Multivariate Rainfall Prediction in Jordan Using NARX-ANN Model with GIS Techniques. *JORDAN JOURNAL OF CIVIL ENGINEERING*, 12(3), pp.359-368.
- Astakhova, N., Demidova, L. and Nikulchev, E.** (2015). Forecasting of time series' groups with application of fuzzy c-mean algorithm. *Contemporary Engineering Sciences* 8 (35), Doi:10.12988/ces.2015.510286.

- Azooz, A. and Talal, S.** (2015). Evidence of Climate Change in Iraq, *Journal of Environment Protection and Sustainable Development*, Vol. 1, No. 2, 2015, pp. 66-73.
- Badarinath, K., Kharol, S. and Kaskaoutis, D.** (2010). Long-range transport of dust aerosols over the Arabian Sea and Indian region, A case study using satellite data and ground-based measurements. *Global and Planetary Change* 72(3): 164–181.
- Baddock, M., Bullard, J. and Bryant, R.** (2009). Dust source identification using MODIS: A comparison of techniques applied to the Lake Eyre Basin, Australia. *Remote Sensing of Environment* 113(7), 1511– 1528.
- Basheer, I. A., and Hajmeer, M.** (2000). Artificial neural networks. Fundamentals, computing, design, and application. *Journal of Microbiological Methods* 43 (1), 3–31.
- Bayissa, Y., Maskey, S., Tadesse, T., van Andel, S., Moges, S., van Griensven, A. and Solomatine, D.** (2018). Comparison of the performance of six drought indices in characterizing historical drought for the Upper Blue Nile Basin, Ethiopia. *Arabian Journal of Geosciences*, 8(3), p.81.
- Belal, A., El-Ramady, H., Mohamed, E., and Saleh, A.** (2014). Drought risk assessment using remote sensing and GIS techniques. *Arabian Journal of Geosciences*, 7(1), 35-53.
- Bellman, R.E. and Zadeh, L.A.** (1970). *Decision-making in a fuzzy environment*. *Management science*, 17(4), pp.B-141.
- Bernhardsen, T.** (2002). *Geographic information systems: an introduction*. John Wiley and Sons.
- Buday, T.** (1980). The regional geology of Iraq: tectonism, magmatism and metamorphism (Vol. 2). State Organization for Minerals, *Directorate General for Geological Survey and Mineral Investigations*.
- Cancelliere, A., Di Mauro, G., Bonaccorso, B. and Rossi, G.** (2007). Drought forecasting using the standardized precipitation index. *Water resources management*, 21(5), pp.801-819.
- Caswell, J.** (2014). A nonlinear autoregressive approach to statistical prediction of disturbance storm time geomagnetic fluctuations using solar data. *Journal of Signal and Information Processing* 5 (02), 42.
- Costa, H., Foody, G. and Boyd, D.** (2018). Supervised methods of image segmentation accuracy assessment in land cover mapping. *Remote Sensing of Environment*, 205, 338-351.
- Crochemore, L., Perrin, C., Andréassian, V., Ehret, U., Seibert, S.P., Grimaldi, S., Gupta, H. and Paturel, J.** (2015). Comparing expert judgement and numerical criteria for hydrograph evaluation. *Hydrological Sciences Journal*, 60(3), pp.402-423.
- Daksh, K., Kumari, V., Kumari, A., Mayoore, M., Singh, H. and Mahapatra, S.** (2018). The DROUGHT RISK ASSESSMENT IN VIDARBHA REGION OF MAHARASHTRA, INDIA, USING STANDARDIZED PRECIPITATION INDEX. *International Journal of Innovative Knowledge Concepts*, 6(10), 13-23.

- Deshpande, R.** (2012). On the rainfall time series prediction using multilayer perceptron artificial neural network. *International Journal of Emerging Technology and Advanced Engineering* 2 (1), 2250–459.
- Devi, S., Arulmozhivarman P., Venkatesh, C. and Agarwal, P.** (2016). Performance comparison of artificial neural network models for daily rainfall prediction. *International Journal of Automation and Computing* 13 (5):417–27.
- Diaconescu, E.** (2008). The use of NARX neural networks to predict chaotic time series. *Wseas Transactions on Computer Research* 3 (3):182–91.
- Ding, Y. and Xian, F.** (2016). Kernel-based fuzzy c-means clustering algorithm based on genetic algorithm. *Neurocomputing* 188:233–38.
- Doucoure, B., Agbossou, K. and Cardenas, A.** (2016). Time series prediction using artificial wavelet neural network and multi-resolution analysis: Application to wind speed data. *Renewable Energy* 92:202–21.
- Dymond, C., and Johnson, E.** (2002): Mapping vegetation spatial patterns from modeled water, temperature and solar radiation gradients. *Journal of Photogrammetry and Remote Sensing, Vol. 57*, pp. 69–85.
- Ervin, S.** (1993). Landscape visualization with Emaps. *IEEE Computer Graphics and Applications*, 13(2), 28-33.
- Fan, J., Zhen W. and Xie, W.** (2003). Suppressed fuzzy c-means clustering algorithm. *Pattern Recognition Letters* 24 (9–10):1607–12.
- FAO.** (2003). Towards sustainable agricultural development in Iraq: *The Transition from Relief, Rehabilitation and Reconstruction to Development*. 222 pp.
- FAO.** (2014). GLOBAL INFORMATION AND EARLY WARNING SYSTEM ON FOOD AND AGRICULTURE (GIEWS), Food and Agriculture Organization of the United Nation, COUNTRY: IRAQ, S P E C I A L A L E R T, No. 332. pp11. June 25.
- Farajzadeh, J., Ahmad, F. and Saeed, L.** (2014). Modeling of monthly rainfall and runoff of Urmia Lake Basin using “feed-forward neural network” and “time series analysis” model. *Water Resources and Industry* 7:38–48.
- Faridi, M., Verma, S. and Mukherjee, S.** (2018). Integration of gis, spatial data mining, and fuzzy logic for agricultural Intelligent. *In Soft Computing: Theories and Applications* (pp. 171-183). Springer, Singapore.
- Fathizad, H., Ardakani, M., Mehrjardi, R. and Sodaiezhadeh, H.** (2018). Evaluating desertification using remote sensing technique and object-oriented classification algorithm in the Iranian central desert. *Journal of African Earth Sciences*, 145, pp.115-130.
- Feidas, H., Kontos, T. and Soulakellis, N.** (2007). A GIS tool for the evaluation of the precipitation forecasts of a numerical weather prediction model using satellite data. *Computers and Geosciences* 33(8): 989–1007.
- Foody, G.** (2002). Status of land cover classification accuracy assessment. *Remote Sensing of Environment. Vol. 80*, pp. 185-201.
- Fouad, S.** (2015). Tectonic map of Iraq, scale 1: 1000 000, 2012. Iraqi Bulletin of Geology and Mining, 11(1), pp.1-7.

- Furman H.** (2003). Dust storms in the Middle East: Sources of origin and their temporal characteristics. *Indoor and Built Environment* 12(6): 419–426.
- Ghorbani, M., Deo, R., Kashani, M., Shahabi, M., and Ghorbani, S.** (2019). Artificial Intelligent -based fast and efficient hybrid approach for spatial modelling of soil electrical conductivity. *Soil and Tillage Research*, 186, 152-164.
- Gleason, C., Wada, Y. and Wang, J.** (2018). A hybrid of optical remote sensing and hydrological modeling improves water balance estimation. *Journal of Advances in Modeling Earth Systems*, 10(1), pp.2-17.
- Goudie A and Middleton N.** (1992). The changing frequency of dust storms through time. *Climatic Change* 20: 197–225.
- Gutiérrez, M., Johnson, E., and Mickus, K.** (2004). Watershed assessment along a segment of the Rio Conchos in northern Mexico using satellite images. *Journal of Arid Environments*, 56(3), 395-412.
- Hammond T. and Verbyla D.** (1996). Optimistic bias in classification accuracy assessment. *International Journal of Remote Sensing*, 17(6):1261-66.
- Hekmat S. and Basher M.** (2012). Quantitative Analysis of the Meteorological Data and their Implication for Geo-Environmental Classification Map of the Nineveh Governorate, the first conference of the dust storms and their environmental impacts- Causes and treatments, *Iraqi Journal of Science*, 17-18 Sep. 2012, pp137-145.
- Hellwig, N., Graefe, U., Tatti, D., Sartori, G., Anschlag, K., Beylich, A. and Broll, G.** (2017). Upscaling the spatial distribution of enchytraeids and humus forms in a high mountain environment on the basis of GIS and fuzzy logic. *European journal of soil biology*, 79, 1-13.
- Hoang, N. and Bui, D.** (2018). Spatial prediction of rainfall-induced shallow landslides using gene expression programming integrated with GIS: a case study in Vietnam. *Natural Hazards*, 92(3), 1871-1887.
- Hong, T. and Lee, C.** (1996). Induction of fuzzy rules and membership functions from training examples, *Fuzzy Sets and Systems*, Vol. 84, pp. 33-47, Nov. 1996.
- Hsieh, W. and Tang, B.** (1998). Applying neural network models to prediction and data analysis in meteorology and oceanography. *Bulletin of the American Meteorological Society*, 79(9), 1855-1870.
- Hsu, K., Gupta, H. and Sorooshian, S.** (1995). Artificial neural network modeling of the rainfall-runoff process, *Water Resource. Res.* 31(10), 2517–2530.
- Huang, S., Huang, Q., Leng, G. and Liu, S.** (2016). A nonparametric multivariate standardized drought index for characterizing socioeconomic drought: A case study in the Heihe River Basin. *Journal of Hydrology*, 542, pp.875-883.
- Hung, N., Babel, M., Weesakul, S. and Tripathi, N.** (2009). An artificial neural network model for rainfall forecasting in Bangkok, Thailand. *Hydrology and Earth System Sciences*, 13(8), pp.1413-1425.

- IAU, Inter-Agency Information and Analysis Unit.** (2010). Ninewa Governorate Profile, November.at: https://reliefweb.int/sites/reliefweb.int/files/resources/4859DB127BC8BA3DC12577EB00510F96-Full_Report.pdf.
- IOM, Iraqi Organization for Meteorological Information** (2000). Atlas of climate of Iraq for the years (1981 – 2000), Baghdad, Iraq.
- IAMN, Iraqi Agricultural Meteorological Network** (2019). <http://www.agromet.gov.iq>.
- Iraqi Meteorological Network Data** (2017). Documentation. Available at: <https://www.agromet.gov.iq>.
- Jassas, H. and Merkel, B.** (2015). Assessment of hydro chemical evolution of groundwater and its suitability for drinking and irrigation purposes in Al-Khazir Gomal Basin, Northern Iraq. *Environmental earth sciences*, 74(9), pp.6647-6663.
- Jang, J.** (1993). ANFIS: adaptive-network-based fuzzy inference system. *IEEE transactions on systems, man, and cybernetics*, 23(3), 665-685.
- Jaradat, A.** (2003). Agriculture in Iraq: resources, potentials, constraints, and research needs and priorities. *Food, Agriculture and Environment*, 1(2), pp.160-166.
- Jimoh R., Olagunju M., Folorunso I. and Asiribo, M.** (2013). Modeling Rainfall Prediction using Fuzzy Logic, *International Journal of Innovative Research in Computer and Communication Engineering*, Vol. 1, Issue 4, June 2013, pp1-6.
- Johnson, R., and Kasischke, E.** (1998). Change vector analysis: a technique for the multispectral monitoring of land cover and condition. *International Journal of Remote Sensing*. Vol. 19, pp. 411–26.
- Jung, W., Yun, H., Jeong, M. and Kwon, J.** (2018). Development of a Building Inventory to Link the Damage Prediction Results of Natural and Social Disasters. *Journal of the Korean Society of Hazard Mitigation*, 18(3), pp.117-123.
- Kasabov, N.** (1996). *Foundations of neural networks, fuzzy systems, and knowledge engineering*. Marcel Alencar.
- Kasiviswanathan, K., He, J., Tay, J. and Sudheer, K.** (2019). Enhancement of Model Reliability by Integrating Prediction Interval Optimization into Hydrogeological Modeling. *Water Resources Management*, 33(1), 229-243.
- Keyantash, J. and Dracup, J.** (2002). The quantification of drought: an evaluation of drought indices. *Bulletin of the American Meteorological Society*, 83(8), pp.1167-1180.
- Khattab, M. and Merkel, B.** (2012). Distribution of heterotrophic bacteria and water quality parameters of Mosul Dam Lake, Northern Iraq. *WIT Transactions on Ecology and the Environment*, 164, pp.195-207.
- Kim, S., Lee, J. and Sugisaka, M.** (1993). Inverse kinematics solution based on fuzzy logic for redundant manipulators. In *Proceedings of 1993 IEEE/RSJ*

International Conference on Intelligent Robots and Systems (IROS'93) (Vol. 2, pp. 904-910). IEEE.

- Klir, G., and Yuan, B.** (1995). *Fuzzy Sets and Fuzzy Logic: Theory and Applications*, Prentice Hall Inc., Upper Saddle River, NJ, 1995.
- Klir, G. and Folger, T.** (1988). *Fuzzy sets, uncertainty, and information*, Prentice-Hall International Editions, 1988.
- Kobler M.** (2013). Dust Storms of Iraq, UN Secretary General for Iraq. Nairobi, Kenya: A Ministerial Meeting. Available at: <http://www.term123.com/dust-storms-of-iraq/#mh32BcOB4S6cRkIG.99>.
- Konecny, G.** (2002). *Geoinformation: remote sensing, photogrammetry and geographical information systems*. cRc Press.
- Kosko, B.** (1992). *Neural networks and fuzzy systems: A dynamical systems approach to machine Intelligence/book and disk. Vol. 1* Prentice hall.
- Kuriqi, A. and Ardiçlioğlu, M.** (2018). Investigation of hydraulic regime at middle part of the Loire River in context of floods and low flow events. *Pollack Periodica*, 13(1), pp.145-156.
- Lapedes, A. and Farber, R.** (1987). Nonlinear signal processing using neural networks: *Prediction and system modelling* (No. LA-UR-87-2662; CONF-8706130-4).
- Lee, S., Cho, S. and Wong, P.** (1998). Rainfall prediction using artificial neural networks. *Journal of geographic information and Decision Analysis*, 2(2), pp.233-242.
- Li, S., Cheng, Y. and Lin, S.** (2008). A FCM-based deterministic forecasting model for fuzzytime series. *Computers and Mathematics with Applications* 56(12):3052–63. Doi: 10.1016/j.camwa.2008.07.033.
- Lin, T., Horne, B., Tino, P. and Lee Giles, C.** (1996). Learning long-term dependencies in NARX recurrent neural networks. *IEEE Transactions on Neural Networks* 7 (6):13.
- Liong, S., and Shan, H.** (2010). Raingauge-based rainfall forecasting with artificial neural network. In *Advances in geosciences: Volume 17: Hydrological Science (HS).1 –9*. Singapore: World Scientific Publishing Company.
- Lippmann, R. P.** (1987). An introduction to computing with neural nets,". *IEEE Assp magazine*, 4(2), 4-22.
- Liu, H., and Huete, A.** (1995). A feedback based modification of the NDVI to minimize canopy background and atmospheric noise. *IEEE transactions on geoscience and remote sensing*, 33(2), 457-465.
- Livada, I., and Assimakopoulos, V.** (2007). Spatial and temporal analysis of drought in Greece using the Standardized Precipitation Index (SPI). *Theoretical and applied climatology*, 89(3-4), 143-153.
- Lohani, V., Loganathan, G., and Mostaghimi, S.** (1998). Long-term analysis and short-term forecasting of dry spells by Palmer Drought Severity Index. *Hydrology Research*, 29(1), 21-40.

- Lunetta, R., Knight, J., Ediriwickrema, J., Lyon, J., and Worthy, L.** (2006). Land-cover change detection using multi-temporal MODIS NDVI data. *Remote Sensing of Environment*, 105(2), 142-154.
- Maharaj, E., D'Urso, P., and Caiado, J.** (2019). *Time Series Clustering and Classification*. CRC Press.
- Mamdani, E. and Assilian, S.** (1975). An experiment in linguistic synthesis with a fuzzy logic controller", *International Journal of Man-Machine Studies*, Vol. 7, No. 1, pp. 1-13, 1975.
- Mariano, D., dos Santos, C., Wardlow, B., Anderson, M., Schiltmeyer, A., Tadesse, T. and Svoboda, M.** (2018). Use of remote sensing indicators to assess effects of drought and human-induced land degradation on ecosystem health in Northeastern Brazil. *Remote Sensing of Environment*, 213, 129-143.
- MATLAB R2017a.** (2017). Math works, documentation, neural network toolbox functions. <https://www.mathworks.com/help/fuzzy/functionlist.html>.
- McCulloch, W. and Pitts, W.** (1943). A logical calculus of the ideas immanent in nervous activity. *The bulletin of mathematical biophysics*, 5(4), pp.115-133.
- McKee T., Doeskin N. and Kleist J.** (1993). The relationship of drought frequency and duration to time scales. In: *Proceedings of the 8th conference on applied climatology*, Anaheim, CA, 17–23 January 1993, pp.179–184.
- Michel, C., Andréassian, V. and Perrin, C.** (2005). Soil conservation service curve number method: How to mend a wrong soil moisture accounting procedure? *Water Resources Research*, 41(2).
- Mishra, S. and Singh, V.** (2013). *Soil conservation service curve number (SCS-CN) methodology* (Vol. 42). Springer Science and Business Media.
- Mislan, H., Sigit H. and Sumaryon, M.** (2015). Rainfall Monthly Prediction Based on Artificial Neural Network: A Case Study in Tenggara Station, East Kalimantan –Indonesia, *International Conference on Computer Science and Computational Intelligent (ICCSCI 2015)*, Pp. 142 – 151.
- Mohammad, A., Jung, H., Odeh, T., Bhuiyan, C. and Hussein, H.** (2018). Understanding the impact of droughts in the Yarmouk Basin, Jordan: monitoring droughts through meteorological and hydrological drought indices. *Arabian Journal of Geosciences*, 11(5), p.103.
- Morid, S., Smakhtin, V. and Bagherzadeh, K.** (2007). Drought forecasting using artificial neural networks and time series of drought indices. *International Journal of Climatology*, 27(15), 2103-2111.
- Murshid, A., Loan, S., Abbasi, S., and Alamoud, A.** (2011). VLSI Architecture of Fuzzy Logic Hardware Implementation: a Review. *International Journal of Fuzzy Systems*, 13(2).
- Mustafa, T., Ibrahim, A., Babiker, I. and Abdalla, A.** (2017). Runoff-Rainfall Prediction Formula for West Dar Fur State using Statistical Methods and GIS.

- Naumann, G., Barbosa, P., Carrao, H., Singleton, A. and Vogt, J.** (2012). Monitoring drought conditions and their uncertainties in Africa using TRMM data. *Journal of Applied Meteorology and Climatology*, 51(10), pp.1867-1874.
- Naveen, L., and Mohan, H.** (2019). High-Resolution Weather Prediction Using Modified Neural Network Approach Over the Districts of Karnataka State. In *International Conference on Computer Networks and Communication Technologies* (pp. 125-143). Springer, Singapore.
- NESDIS (2017).** National Environmental Satellite, Data, and Information Service. Available at: <https://www.nesdis.noaa.gov>.
- Nickovic S., Kallos G. and Papadopoulos A.** (2001). A model for prediction of desert dust cycle in the atmosphere. *Journal of Geophysical Research* 106: 18113–18129.
- Nigrin, A.** (1993). *Neural networks for pattern recognition*. MIT press.
- Novara, A., Pisciotta, A., Minacapilli, M., Maltese, A., Capodici, F., Cerdà, A. and Gristina, L.** (2018). The impact of soil erosion on soil fertility and vine vigor. A multidisciplinary approach based on field, laboratory and remote sensing approaches. *Science of the Total Environment*, 622, pp.474-480.
- Omran, E.S.E.,** (2012). A proposed model to assess and map irrigation water well suitability using geospatial analysis. *Water*, 4(3), pp.545-567.
- Ozger, M., Mishra, A.K. and Singh, V.P.** (2011). “Estimating palmer drought severity index using a wavelet fuzzy logic model based on meteorological variables.” *International Journal of Climatology*, 31(13), pp.2021-2032.
- Parry, M., Parry, M., Canziani, O., Palutikof, J., Van der Linden, P., and Hanson, C.** (2007). *Climate change 2007-impacts, adaptation and vulnerability: Working group II contribution to the fourth assessment report of the IPCC.Vol. 4*. Cambridge University Press.
- Pawar, D., Kumar, P. and Kyada, P.** (2004). RAINFALL-RUNOFF MODELING USING FUZZY TECHNIQUE FOR A SMALL WATERSHED IN MAHARASHTRA, INDIA, *International Journal of Engineering and Management Science*, I.J.E.M.S., VOL.4 (3) 2013:388-394
- Pesti, G., Shrestha, B., Duckstein, L. and Bogárdi, I.** (1996). A fuzzy rule-based approach to drought assessment. *Water Resources Research*, 32(6), pp.1741-1747.
- Pike, R. J.** (1999). *A Bibliography of Geomorphometry, the Quantitative Representation of Topography: Supplement 3.0*. US Department of the Interior, US Geological Survey.
- Ponce, V. M., and Hawkins, R. H.** (1996). Runoff curve number: Has it reached maturity? *Journal of hydrologic engineering*, 1(1), 11-19.
- Pongracz, R., Bogardi, I. and Duckstein, L.** (1999). Application of fuzzy rule-based modeling technique to regional drought. *Journal of Hydrology*, 224(3-4), pp.100-114.

- Qi, M. and G. P. Zhang.** (2001). An investigation of model selection criteria for neural network time series forecasting. *European Journal of Operational Research* 132 (3):666–80.
- Rahman, T. and Haque, A. L.** (2014). A Fuzzy-Neuro Based Weather Prediction System for Bangladesh. *Procedia Computer Science*, 36, 606-611.
- Rees, W. G., and Pellika, P.** (2010). *Principles of remote sensing*. Remote Sensing of Glaciers. London.
- Sivakumar, B., Ronny B. and Magnus P.** (2001) Monthly runoff prediction using phase space reconstruction. *Hydrological Sciences Journal* 46, No. 3: 377-387.
- Rohit R.** (2012). On the rainfall time series prediction using multilayer perceptron artificial neural network, *International Journal of emerging technology and advanced engineering*, Vol. 2, No. 1, January 2012, 2250- 2459.
- Ross, T. J.** (2005). *Fuzzy logic with engineering applications* (Vol. 2). New York: Wiley.
- Rouse Jr, J. W., Haas, R. H., Schell, J. A. and Deering, D. W.** (1973). Monitoring the vernal advancement and retrogradation (green wave effect) of natural vegetation.
- Salih, S. A., and Al-Tarif, A. S. M.** (2012). Using of GIS spatial analyses to study the selected location for dam reservoir on Wadi Al-Jirnaf, West of Shirqat Area, Iraq. *Journal of Geographic Information System*, 4(02), 117.
- Shahi, A., Atan, R.B. and SULAIMAN, N.** (2009). AN EFFECTIVE FUZZY C-MEAN AND TYPE-2 FUZZY LOGIC FOR WEATHER FORECASTING. *Journal of Theoretical and Applied Information Technology*, 5(5).
- Shen, H. and Chang, L.** (2013). Online multistep-ahead inundation depth forecasts by recurrent NARX networks. *Hydrology and Earth System Sciences*, 17(3), pp.935-945.
- Sheridan, S. C.** (2002). The redevelopment of a weather-type classification scheme for North America. *International Journal of Climatology: A Journal of the Royal Meteorological Society* 22 (1):51–68. doi:10.1002/joc.709.
- Silveira L, Charbonnier F and Genta J.** (2000). The antecedent soil moisture condition of the curve number procedure. *Hydrological Sciences Journal*, 45(1): 3–12.
- Sonmez, O. and Bizimana, H.** (2018). *Flood hazard risk evaluation using fuzzy logic and weightage based combination methods in Geographic Information System (GIS)*. Scientia Iranica.
- Srinivas, R., Singh, A.P., Dhadse, K., Garg, C. and Deshmukh, A.** (2018). Sustainable management of a river basin by integrating an improved fuzzy based hybridized SWOT model and geo-statistical weighted thematic overlay analysis. *Journal of Hydrology*.
- Stewart, D., Canfield, E., and Hawkins, R.** (2011). Curve number determination methods and uncertainty in hydrologic soil groups from semiarid

- watershed data. *Journal of Hydrologic Engineering*, 17(11), pp. 1180-1187.
- Strahler, A. N.** (1964). Part II. Quantitative geomorphology of drainage basins and channel networks. In *Handbook of Applied Hydrology: McGraw-Hill, New York*, pp.4-39.
- Suganya, R., and Shanthi, R.** (2012). Fuzzy c-means algorithm-a review. *International Journal of Scientific and Research Publications*, 2(11), 1.
- Tabesh, M., Roozbahani, A., Roghani, B., Faghihi, N.R. and Heydarzadeh, R.** (2018). Risk Assessment of Factors Influencing Non-Revenue Water Using Bayesian Networks and Fuzzy Logic. *Water Resources Management*, pp.1-24.
- Thom, H. C. S.** (1958). *A note on the gamma distribution*, Monthly Weather Rev. 86, 117–122.
- Tian, L., Yuan, S. and Quiring, S.M.,** (2018). Evaluation of six indices for monitoring agricultural drought in the south-central United States. *Agricultural and Forest Meteorology*, 249, pp.107-119.
- Tigkas, D., Vangelis, H. and Tsakiris, G.** (2015). DrinC: a software for drought analysis based on drought indices. *Earth Science Informatics*, 8(3), pp.697-709.
- Tiwari, N.K., Sihag, P., Kumar, S. and Ranjan, S.** (2018). Prediction of trapping efficiency of vortex tube ejector. *ISH Journal of Hydraulic Engineering*, pp.1-9.
- Tokar, A.S. and Johnson, P.A.** (1999). Rainfall-runoff modeling using artificial neural networks. *Journal of Hydrologic Engineering*, 4(3), pp.232-239.
- Tsesmelis, D., Karavitis, C., Oikonomou, P., Alexandris, S., and Kosmas, C.** (2019). Assessment of the Vulnerability to Drought and Desertification Characteristics Using the Standardized Drought Vulnerability Index (SDVI) and the Environmentally Sensitive Areas Index (ESAI). *Resources*, 8(1), 6.
- Türkeş, M., and Tatlı, H.** (2009). Use of the standardized precipitation index (SPI) and a modified SPI for shaping the drought probabilities over Turkey. *International Journal of Climatology: A Journal of the Royal Meteorological Society*, 29(15), 2270-2282.
- Tzimopoulos, C., Mpallas, L. and Evangelides, C.** (2008). Fuzzy model comparison to extrapolate rainfall data. *Journal of Environmental Science and Technology*, 1(4), pp.214-224.
- UN** (2013). Sand and Dust Storms Fact Sheet produced by joint analysis and policy unit (JAPU). Available at: <https://reliefweb.int>.
- UNEP.** (2013). *How environmental damage causes food insecurity in IRAQ*. World Environmental Day, Technical Assessment Report, Accessed June 2013.
- UNISDR.** (2009). Drought Risk Reduction Framework and Practices: Contributing to the Implementation of the hydro Framework for Action. Geneva,

Switzerland: United Nations secretariat of the International Strategy for Disaster Reduction (UNISDR).

Url-1. <https://modis.gsfc.nasa.gov/gallery/>

Url-2. www.digitalvidya.com

Url-3. www.star.nesdis.noaa.gov/star/index.php

Url-4. http://www.dma.fi.upm.es/recursos/aplicaciones/logica_borrosa/web/fuzz.

USAID. (2006). Improving Grain Production in Iraq, The Agriculture Reconstruction and Development Program for Iraq (ARDI), fact sheet, U.S. Agency for International Development. June, pp 8. www.usaid.gov/iraq.

USDA, Soil Conservation Service (1972). *Hydrology*. In *National Engineering Handbook*, Section 4. Washington, DC: US Govt. Printing Office.

Vance TC, Mesick S and Cross S. (2009). Integrating particle-tracking models into a GIS for analysis and display of environmental phenomena. In: Proceedings of the 17th ACM SIGSPATIAL, *international conference on advances in geographic information systems*, ACM, USA, 4–6 November 2009, pp.460–463.

Varoujan, K., Al-Ansari, N. and Sven, K. (2013). Sand and dust storm events in Iraq, *Natural Science Journal*. Vol. 5 No. 10, pub date October 10, 2013. Pp. 1084-1094.

Walczak, S. (2019). Artificial neural networks. In *Advanced Methodologies and Technologies in Artificial Intelligent, Computer Simulation, and Human-Computer Interaction*, pp. 40-53. IGI Global.

Wang, B. H. and Vachtsevanos, G. (1992) Learning Fuzzy Logic Control: An Indirect Control Approach, *IEEE International Conference on Fuzzy System~*, San Diego, California, p. 297-304.

Washington, R., Todd, M., Middleton, N. J., and Goudie, A. S. (2003). Dust-storm source areas determined by the total ozone monitoring spectrometer and surface observations. *Annals of the Association of American Geographers*, 93(2), 297-313.

Weerasinghe, H., Schneider, U. A., and Loew, A. (2011). Water harvest-and storage-location assessment model using GIS and remote sensing. *Hydrology and Earth System Sciences Discussions*, 8(2), 3353-3381.

Wei, C.C. (2012). RBF neural networks combined with principal component analysis applied to quantitative precipitation forecast for a reservoir watershed during typhoon periods. *Journal of Hydrometeorology*, 13(2), pp.722-734.

Wilderson WD. (1991) Dust and sand forecasting in Iraq and adjoining countries. No. AWS/TN-91/001. IL: Air Weather Service, Scott Air Force Base.

WMO, World Meteorological Organization (2018). <https://public.wmo.int/en>

Xue, X., and Xiao, M. (2019). Application of adaptive neuro-fuzzy inference system for prediction of internal stability of soils. *European Journal of Environmental and Civil Engineering*, 23(2), 153-171.

- Yahya, B.M. and Seker, D.Z. (2018).** Designing Weather Forecasting Model Using Computational Intelligent Tools. *Applied Artificial Intelligent*, volume 3, pp346-359., pp.1-15.
- Yaseen, K. AL-Timimi, Loay, E. George, and Monim, H. AL-Jiboori. (2012).** Drought Risk Assessment In Iraq Using Remote Sensing And GIS Techniques, *Iraqi Journal of Science*, December 2012, Vol. 53, No. 4, Pp. 1078-1082.
- Zadeh, L. A. (1965).** Fuzzy sets. *Information and Control* 8:3. Doi: 10.1016/S0019-9958(65) 90241-X.
- Zadeh, L. A. (1973).** Outline of a new approach to the analysis of complex systems and decision processes,” *IEEE Transactions on Systems, Man, and Cybernetics*, Vol. 3, No. 1, pp. 28-44, Jan. 1973.
- Zhang, G., Patuwo E., and Hu, M. (1998).** Forecasting with artificial neural networks: The state of the art. *International Journal of Forecasting*. 14 (1):35–62. Doi: 10.1016/S0169-2070 (97)00044-7.
- Zhao, C., Jensen, J., Weng, Q., Currit, N., and Weaver, R. (2019).** Application of airborne remote sensing data on mapping local climate zones: Cases of three metropolitan areas of Texas, US. *Computers, Environment and Urban Systems*, 74, 175-193.

APPENDICES

APPENDIX A: MODIS Imageries

APPENDIX B: Formatted SPI equations in Excel format



APPENDIX A: MODIS Imageries

Forty images used in this study. These images are 500 m resolution version images supplied by MODIS on NASA's Terra satellite taken from 2005 to 2018 as shown in Figures below.

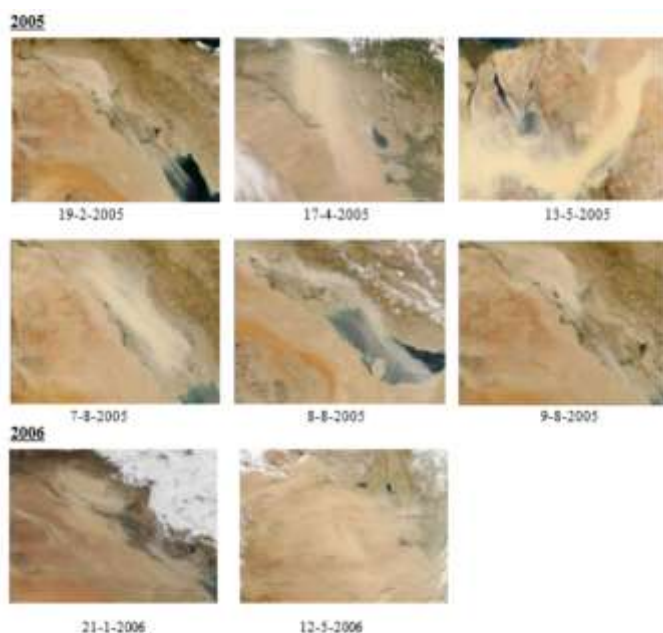


Figure A.1 : MODIS on NASA's Terra satellite taken between 2005 to 2006.

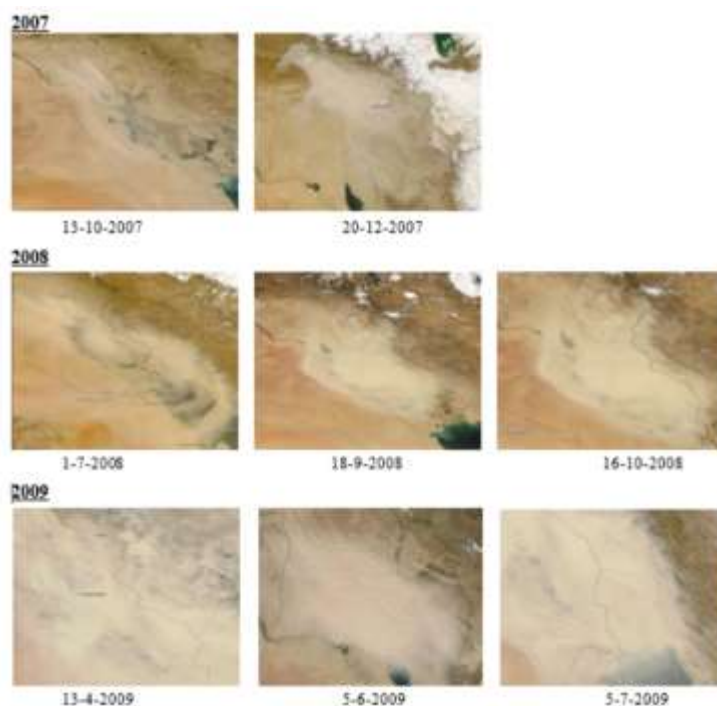


Figure A.2 : MODIS on NASA's Terra satellite taken between 2007 to 2009.

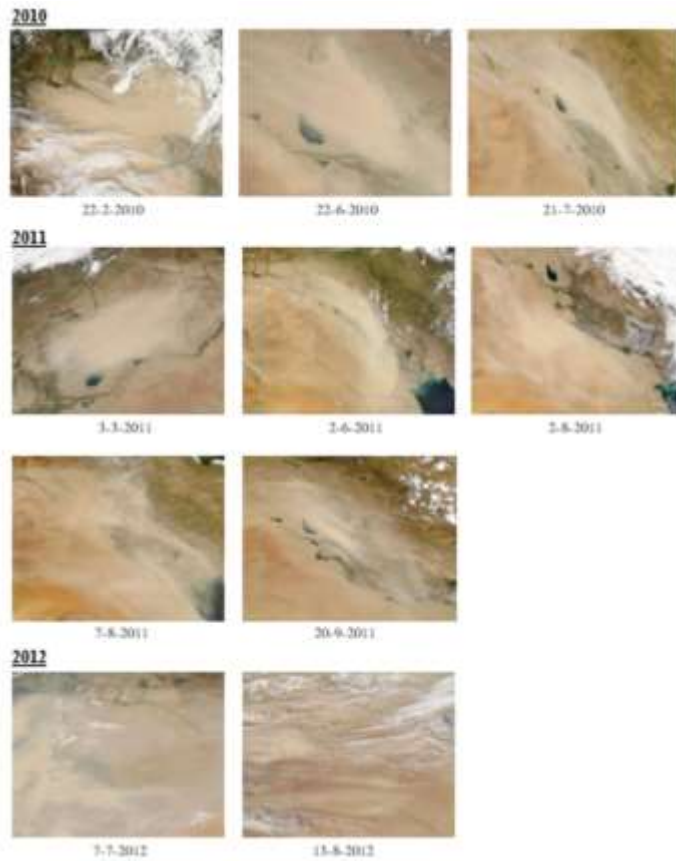


Figure A.3 : MODIS on NASA's Terra satellite taken between 2010 to 2012.

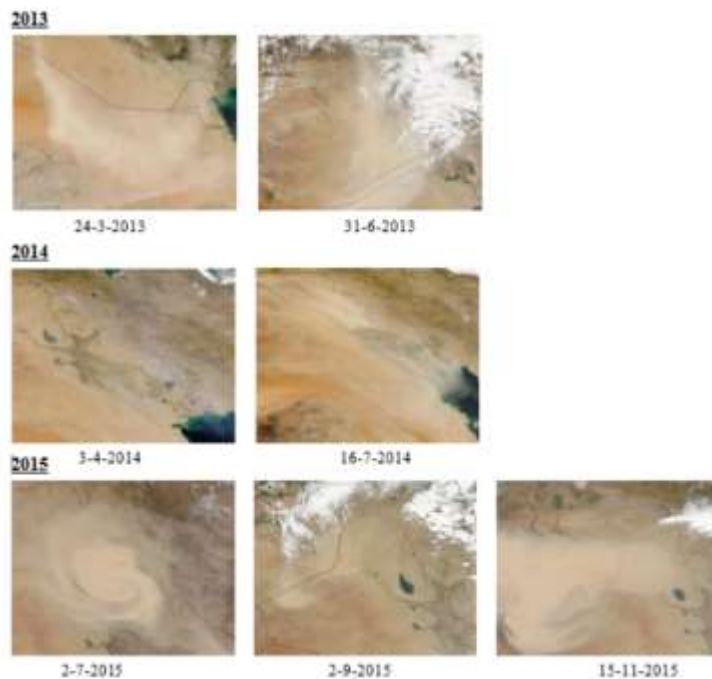


Figure A.4 : MODIS on NASA's Terra satellite taken between 2013 to 2015.

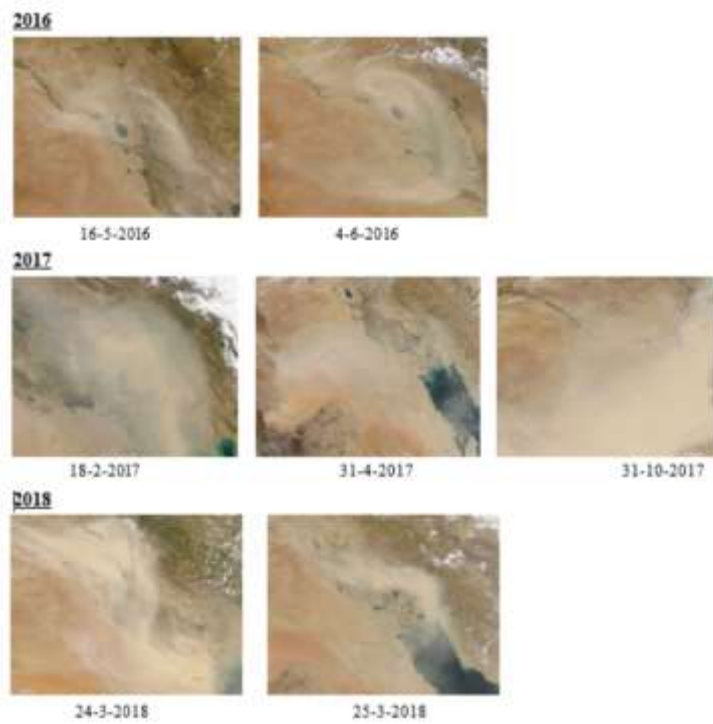


Figure A.5 : MODIS on NASA's Terra satellite taken between 2016 to 2018.

APPENDIX B: Formated SPI equations in Excel format

Samples of SPI calculation for Mosul station. SPI needed equations

$$g(x) = \frac{1}{\beta^\alpha \Gamma(\alpha)} x^{\alpha-1} e^{-x/\beta} \quad \text{for } x > 0 \quad (3.2)$$

Where $\alpha > 0$ is a shape parameter, $\beta > 0$ is a scale parameter, Γ is the gamma function, and $x > 0$ is the precipitation amount.

For complet fitting the distribution, α and β must be calculated using the following equations equation 3.3, equation 3.4 and equation 3.5.

$$\alpha = \frac{1}{4A} \left(1 + \sqrt{1 + \frac{4A}{3}} \right) \quad (3.3)$$

Where,

$$A = \ln(x) - \sum \frac{\ln(x)}{n} \quad (3.4)$$

$$\beta = \frac{x}{\alpha} \quad (3.5)$$

Scnduly, Integrating the probability density function with respect to x and inserting the estimates of a and b yields an expression for the cumulative probability $G(x)$ of an observed amount of precipitation occurring for a given month and time step:

$$G(x) = \int_0^x g(x) dx = \frac{1}{\beta^\alpha \Gamma(\alpha)} \int_0^x x^{\alpha-1} e^{-x/\beta} \quad (3.6)$$

Since the gamma distribution is undefined for $x \leq 0$ and $q = P(x \leq 0) > 0$ where $P(x \leq 0)$ is the probability of zero precipitation, the cumulative probability becomes as follow:

$$H(x) = q + (1-q) G(x) \quad (3.7)$$

Table B.1 : Formated SPI equations in Excel format.

| SPI- 3 | | | | | | | | | |
|--------|-------|----------|---------|--------|-------|-------|-------|--------|--------------------|
| Ln(x) | A | α | β | G(x) | q=m/n | H(x) | t | SPI | |
| 4.683 | 0.073 | 6.960 | 27.677 | 0.104 | | 0.104 | 2.125 | -1.256 | Moderately drought |
| 5.593 | | | | 0.853 | | 0.853 | 1.959 | 1.0511 | Moderately wet |
| 5.601 | | | | 0.859 | | 0.859 | 1.979 | 1.076 | Moderately wet |
| 5.386 | | | | 0.678 | | 0.678 | 1.507 | 0.464 | Mild wet |
| 5.357 | | | | 0.649 | | 0.649 | 1.448 | 0.384 | Mild wet |
| 5.247 | | | | 0.536 | | 0.536 | 1.239 | 0.090 | Mild wet |
| 5.669 | | | | 0.8995 | | 0.899 | 2.144 | 1.279 | Moderately wet |
| 5.248 | | | | 0.5371 | | 0.537 | 1.241 | 0.093 | Mild wet |
| 4.935 | | | | 0.2472 | | 0.247 | 1.671 | -0.682 | Mild drought |
| 5.5220 | | | | 0.800 | | 0.800 | 1.796 | 0.844 | Mild wet |
| 5.040 | | | | 0.333 | | 0.333 | 1.482 | -0.430 | Mild drought |
| 4.450 | | | | 0.0400 | | 0.040 | 2.536 | -1.750 | Severely drought |
| 5.827 | | | | 0.961 | | 0.961 | 2.555 | 1.772 | Severely wet |
| 5.662 | | | | 0.8960 | | 0.896 | 2.127 | 1.259 | Moderately wet |
| 5.205 | | | | 0.492 | | 0.492 | 1.189 | -0.018 | Mild drought |
| 5.688 | | | | 0.909 | | 0.909 | 2.191 | 1.337 | Moderately wet |
| 5.675 | | | | 0.902 | | 0.902 | 2.158 | 1.297 | Moderately wet |
| 5.860 | | | | 0.969 | | 0.969 | 2.645 | 1.878 | Severely wet |
| 4.948 | | | | 0.256 | | 0.256 | 1.649 | -0.654 | Mild drought |
| 5.163 | | | | 0.450 | | 0.450 | 1.262 | -0.124 | Mild drought |
| 5.357 | | | | 0.649 | | 0.649 | 1.447 | 0.383 | Mild wet |
| 4.858 | | | | 0.193 | | 0.193 | 1.812 | -0.864 | Mild drought |
| 5.086 | | | | 0.374 | | 0.374 | 1.400 | -0.318 | Mild drought |
| 4.961 | | | | 0.266 | | 0.266 | 1.625 | -0.622 | Mild drought |
| 4.841 | | | | 0.183 | | 0.183 | 1.841 | -0.902 | Mild drought |
| 4.933 | | | | 0.245 | | 0.245 | 1.677 | -0.689 | Mild drought |
| 5.093 | | | | 0.381 | | 0.381 | 1.387 | -0.299 | Mild drought |
| 5.291 | | | | 0.582 | | 0.582 | 1.321 | 0.208 | Mild wet |
| 5.386 | | | | 0.678 | | 0.678 | 1.506 | 0.463 | Mild wet |
| 4.995 | | | | 0.293 | | 0.293 | 1.564 | -0.541 | Mild drought |
| 5.349 | | | | 0.641 | | 0.641 | 1.432 | 0.362 | Mild wet |
| 4.751 | | | | 0.133 | | 0.133 | 2.005 | -1.108 | Moderately drought |

CURRICULUM VITAE



Name Surname : Bashar Muneer Yahya
Place and Date of Birth : Republic of Iraq- Mosul- 28/05/1974
E-Mail : basharyahya222@gmail.com

EDUCATION

:

- **B.Sc.** : 1998, Mosul University, Engineering , Water Recorses
- **M.Sc.** : 2000, Mosul University, Science, Geology (remote Sensing center)

PUBLICATIONS, PRESENTATIONS AND PATENTS ON THE THESIS:

- Hekmat S. AL-Daghastani, Taha H. AL-Salim and **Bashar M. Yahya**. (2004) Hydrologic System Observation and Rainwater Harvesting in Sinjar Remote Sensing Data Alluvial Fans in the North of Jabel Using Remote. *Iraqi National Journal of Earth Science*, Volume: 4 Issue: 1 Pages: 15-28.
- **Bashar M. Yahya**. (2008). A Theoretical Study Using Geographic Information Systems to Harvest Rain Water in Kand Structure Area Northern Iraq. *Iraqi National Journal of Earth Science*, Volume: 8 Issue: 1 Pages: 14-24.
- Basman Y. Hameed and **Bashar M. Yahya**. (2012). The Preparation of an Electronic Map for the Development of Wadi AL-shour Basin Valley North Eastern Mosul City Using Geographic Information System (GIS). *Iraqi National Journal of Earth Science*, Volume: 12 Issue: 3 Pages: 1-16.

- Hekmat S. AL_Daghastani and **Bashar M. yahya** (2012). Quantitative Analysis of the Meteorological Data and their Implication for Geo-Environmental Classification Map of the Nineveh Governorate, the first conference of the dust storms and their environmental impacts- Causes and treatments, *Iraqi Journal of Science*, 17-18 Sep. 2012, pp137-145.
- **Bashar M. Yahya** and Khansaa A. Ahmed. (2013). landuse landcover Change Detection near Mosul Dam Lake using Digital Image Processing. *Iraqi National Journal of Earth Science*, Volume: 13 Issue: 2 Pages: 11-22.
- **Bashar M. Yahya**. (2013) Using Spatial Expert Support System to Select Suitable Sites for Rain Water Harvesting. *AL Rafdain Engineering Journal*. Volume: 21 Issue: 4 Pages: 46-54.
- **Bashar M. Yahya** and Dursun Zafer Seker. (2019). The Impact of Dust and Sandstorms in Increasing Drought Areas in Nineveh Province, Northwestern Iraq. *Journal of Asian and African Studies*, volume 3, pp346-359.
- **Bashar M. Yahya** and Dursun Zafer Seker. (2019). Designing Weather Forecasting Model Using Computational Intelligent Tools. *Applied Artificial Intelligent* 33, no. 2 (2019): 137-151.
- **Bashar M. Yahya** and Dursun Zafer Seker. (2019). Integrated Fuzzy Logic for Long- Term Drought Prediction Northwestern of Iraq. *International Journal of Computational Intelligent Systems*. Recived 5/10/2019, Acepted 18/9/2019. In press.